TRAIT-BASED VARIATION IN HOST CONTRIBUTION TO PATHOGEN TRANSMISSION

Miranda E. Welsh

A dissertation submitted to the faculty at the University of North Carolina at Chapel Hill in partial fulfillment of the requirements for the degree of Doctor of Philosophy in the Curriculum for the Environment and Ecology.

Chapel Hill
2016

Approved by:

Charles E. Mitchell

John F. Bruno

William A. Hoffmann

Aaron Moody

James Umbanhowar

ABSTRACT

Miranda E. Welsh: Trait-based variation in host contribution to pathogen transmission
(Under the direction of Charles E. Mitchell)

Host competence defines a host's potential to transmit disease, and, from the perspective of a pathogen, a good host is a competent one. Highly competent hosts boost transmission, increase the size of epidemics, and promote emergence in new host populations. From a host's perspective, competent hosts increase disease risk, and control efforts are more successful when competent hosts can be rapidly identified and targeted. Competence varies widely both within and among host species, and this variation is generally quantified observationally, on a case-by-case basis. While locally effective, this approach limits our ability to successfully control pathogens that emerge in new hosts or novel conditions.

To this end, I tested whether the functional traits of hosts can predict host competence. These traits include host physiological, morphological, and life-history characteristics. I focused on functional traits for two reasons: 1) several functional traits have demonstrated effects on host-pathogen or host-vector interactions, and 2) functional traits have provided a useful framework for developing general, predictive models of ecological processes in both simple and complex systems (e.g., competition, community assembly). In developing and testing trait-based models of host competence, my overarching goal was to contribute to a mechanistic understanding of disease processes and to promote synthesis across models of disease and community dynamics.

Across 23 hosts of a generalist, vector-borne pathogen, hosts functional traits covaried along a single, general axis of ecological strategy. This axis ran from traits associated with slow growth and resource conservation to traits associated with fast growth and resource acquisition. As hosts became more fast-growing along this axis, they became more likely to acquire and transmit pathogen infection, but they were also more impacted by infection. This suggests that fast-growing hosts contribute disproportionately to transmission, but slow-growing hosts may encourage pathogen persistence. Trait-based models of competence could become less accurate in two cases: 1) when applied at the individual instead of the species level, and 2) when hosts were exposed to novel environments. Combined, my results demonstrate the potential for trait-based approaches to improve forecasts of pathogen transmission and emergence, and also illustrate two important caveats to their application.

To my gracious and greathearted guides, the Doctors Welsh and Mitchell.

ACKNOWLEDGEMENTS

The author would like to thank Marty Dekkers for his assistance in performing the experiments and for being awesome, Dr. Alison Power, for providing vector and virus stock, and Dr. Eric Seabloom and Dr. Elizabeth Borer, for providing host plant seeds. Funding provided by the National Science Foundation (DEB-0923671), and the NSF/NIH joint program in the Ecology and Evolution of Infectious Diseases (DEB-1015909). Support for J.P.C. was also provided by the USGS Ecosystems Program.

TABLE OF CONTENTS

LIST OF TABLES

LIST OF FIGURES

LIST OF ABBREVIATIONS

AIC	Akaike information criterion
ANOVA	Analysis of variance
BYDV	Barley yellow dwarf virus
CFA	Confirmatory factor analysis
CFI	Comparative fit index
C:N	Carbon:nitrogen ratio
CBO	Coast Black Oat (*Avena sativa* var.)
ELISA	Enzyme-linked immunosorbent assay
GDTs	Growth-defense tradeoffs
GRM	Growth rate model
HDT	Host developmental tempo
HREC	Hopland Research and Extension Center (University of California)
Lf. Elong	Leaf elongation rate
Lf. Emerge	Leaf emergence rate
LMA	Leaf mass per area
LES	Leaf economics spectrum
LRH	Limiting resource hypothesis
%N	Percent tissue nitrogen
PCA	Principal component analysis
PC1	Principal component one
PGLS	Phylogenetic generalized least squares
Photo	Maximum photosynthetic rate

RMF	Root mass fraction
RGR	Relative growth rate
RVI	Relative variable importance
SEM	Structural equation model
TLI	Tucker-Lewis index
UNNRS	University of California Natural Reserve System

CHAPTER 1: HOST LIFE HISTORY AND DEFENSE AGAINST PATHOGENS AND PARASITES

Introduction

Several disciplines have proposed that host lifespan is a strong driver and correlate of defense evolution. Evolutionary biology, epidemiology, and ecology have all considered the effects of host lifespan on the costs, benefits, and resulting evolution of host defense against pathogens. Yet a cross-disciplinary consensus as to the direction of these effects has yet to emerge. Host defense against pathogens can take three primary forms: resistance, tolerance, and acquired immunity (Box1). Three main theoretical frameworks have developed formal predictions for relationships between host lifespan and defense: life history, plant defense, and epidemiology. Previous syntheses have either focused on a single theoretical framework (Michalakis and Hochberg 1994, Agnew et al. 2000, Stamp 2003, Nunez-Farfan et al. 2007) or a single form of defense (Rosenthal and Kotanen 1994, Strauss and Agrawal 1999, Lochmiller and Deerenberg 2000, Stowe et al. 2000). Here, we synthesize theoretical expectations and empirical evidence for correlated evolution in host lifespan and defense against pathogens. To develop general patterns and test fundamental principles, we synthesize across theoretical frameworks and across forms of defense. For each form of defense, we review predictions from the three theoretical frameworks and weigh the empirical evidence for each predicted relationship between host lifespan and defense investment. For each defense, we conclude with suggestions for future work. Our over-arching goals are to clarify the current state of progress, and to highlight the most productive routes forward.

Box 1. Definitions

Correlated evolution: positively or negatively correlated evolutionary change in two traits within a single host population due to direct or indirect causal mechanisms

Parasite/pathogen: a natural enemy that attacks a single host per life history stage (Lafferty and Kuris 2002). Terms are used interchangeably here.

Defense: any or all of resistance, tolerance, and acquired immunity

Resistance: any host defense that reduces host probability of pathogen or parasite infection

Tolerance: any host defense that reduces the fitness effects of parasitism. Also, the reaction norm of fitness across a parasite load gradient (Stowe 1998)

Acquired immunity: also, 'adaptive immunity', a defense that reduces hosts' probability of pathogen/parasite reinfection via immunological memory.

Defense via resistance

Life History theory

In life history theory, the evolution of lifespan is determined by a balance between two opposing selection forces: 1) selection for shorter lifespans as exposure to natural enemies and the probability of mortality increases with age, and 2) selection for longer lifespans to allow for greater reproductive output. Predicted relationships between lifespan and resistance investment are contingent upon the ontogenetic expression of resistance. If resistance investment remains constant or increases with age, it slows the accumulation of sources of mortality. Relative to juveniles, this serves to decrease the mean or variance of adult mortality and increase the reproductive value of adults, which selects for longer lifespans. Conversely, if resistance investment decreases with age, the mean or variance of adult mortality increases relative to juveniles, which selects for shorter lifespans (Roff 1992, Stearns 1992, Agnew et al. 2000). At any lifespan, selection for resistance should be minimal when parasites attack older hosts preferentially, post reproduction (Thompson 1982). Thus, beyond the presence and level of resistance, the ontogeny of resistance expression and parasite attack may influence the direction

of selection acting on lifespan, and thus the predicted correlation between lifespan and resistance investment.

The evolution of shorter lifespans can also be considered an alternative to costly or constrained resistance evolution (Minchella 1985, Hochberg et al. 1992), as shorter lifespans minimize the accumulating fitness costs of parasitism (Minchella 1985, Adamo 1999). If resistance is comparatively costly or there is little variation for resistance, the introduction of new parasites or increases in parasite virulence may select for earlier host reproduction and shorter lifespans (Minchella 1985). In this scenario, decreased lifespan and increased resistance investment are redundant strategies of maintaining fitness, and positive correlations between lifespan and resistance investment are expected.

Epidemiological theory

In epidemiological theory, there are conceptual arguments for both high and low levels of resistance in long-lived hosts. Correlated evolution of lifespan and resistance is expected via both direct and indirect, or pathogen-mediated, mechanisms. Directly, resistance may have costs in terms of growth rate, such that increasing resistance necessitates a longer lifespan to maintain reproductive effort (Boots and Bowers 2004, Miller et al. 2007). Long-lived hosts that suffer repeated pathogen attack may invest more in resistance due to a greater potential benefit (van der Meijden et al. 1988, Hochberg et al. 1992), or resistance may increase fitness more in short-lived organisms with only one chance at reproduction and a greater potential cost of parasitism (van der Meijden et al. 1988). As in life-history theory, increased resistance and decreased lifespan could be redundant in terms of pathogen evasion (Hochberg et al. 1992). Indirectly, changes in resistance investment or lifespan can alter pathogen dynamics, which then feedback to alter selection regimes (Kirchner and Roy 1999). On the one hand, selection for resistance may be

stronger in populations of long-lived hosts where the threshold transmission rate for pathogen establishment is lower, which increases the probability of pathogen introduction (Anderson and May 1982). On the other hand, selection for resistance may be weaker in long-lived hosts with low intrinsic birth rates, which can reduce pathogen persistence because susceptible hosts are replaced at a lower rate. Epidemiological theory has used dynamic host-pathogen models to predict which of the above outcomes is most likely, and under what conditions.

In the simplest model, with single, homogenous host and pathogen populations and no host recovery, the equilibrium fraction of infected hosts, and thus the risk of infection, increased with host lifespan. Increased host longevity increased the infection rate of susceptible hosts relative to the loss of susceptibles from natural mortality (Kirchner and Roy 1999). Because infection risk is higher in long-lived populations, selection for resistance should be stronger. Note, however, that the above model did not explicitly deal with resistance evolution, but with the effect of host lifespan on disease dynamics. Predictions are largely the same, however, in a model with a heterogeneous, recovering host population that explicitly considered the fitness of host genotypes varying in resistance. Again, resistant genotypes were increasingly favored as host lifespan increased due to higher equilibrium pathogen prevalence, except when pathogen virulence was very low. When it was, resistance investment decreased with host lifespan because the costs of resistance outweighed the mild fitness consequences of attack (Miller et al. 2007).

In addition to parasite virulence, host population structure is predicted to influence the evolution of lifespan and resistance. Carlsson-Graner and Thrall (2006) examined the evolution of resistance in a spatially explicit metapopulation model of three host strains (no, intermediate, and high resistance) infected by a genetically uniform, sterilizing pathogen. In very short-lived hosts, the frequency of resistance, at any level, was always at or near zero at equilibrium,

regardless of habitat patchiness, host dispersal, or disease prevalence. In longer-lived hosts, the equilibrium frequency of resistance increased with increasing host dispersal and pathogen transmission. They suggest that, in a metapopulation context, a cost of resistance in terms of decreased reproduction may be greater for short-lived hosts, where high reproduction and dispersal can be essential for regional persistence. This creates a resistance-colonization tradeoff, whereby short-lived or isolated hosts experience higher costs of resistance. When hosts are long-lived or populations are more connected, the costs of resistance are lower because local and regional dynamics depend less on dispersal, and resistance is predicted to evolve to higher levels (Carlsson-Graner and Thrall 2006).

Plant defense theory

Predictions of correlated lifespan-defense evolution from plant defense theory are based mostly on some form of growth-defense tradeoff. Mass-specific growth rates generally scale allometrically with lifespan across both plant and animal taxa (Lindstedt and Calder 1976, Garnier 1992, West et al. 1997, Brown et al. 2004, Savage et al. 2004, Atanasov 2005, Speakman 2005, Atanasov 2007, MarbÃ et al. 2007, Lovegrove 2009), and here we will assume that, all else being equal, increases in growth rate correspond to decreases in lifespan. In addition, we confine our discussion to theories of plant resistance evolution and do not consider theories of plastic resistance expression. Theories of plant resistance evolution include the Optimal Defense (Rhoades 1979), Growth Rate (Coley et al. 1985), and Growth-Differentiation Balance (Herms and Mattson 1992) hypotheses, but exclude the Carbon:Nutrient Balance and similar hypotheses (Bryant et al. 1983, Stamp 2003).

Relative to life history theory, plant defense theory is more explicit about sources of variation in the costs and benefits of resistance: costs are predicted to vary with resource supply

and benefits are predicted to vary with pathogen pressure (Herms and Mattson 1992, Stamp 2003). At a given resource supply rate, the Optimal Defense hypothesis predicts that resistance investment will increase with pathogen pressure, which increases with the temporal apparency of hosts and therefore lifespan. This positive correlation between lifespan and resistance investment may be further reinforced by a cost of resistance in terms of growth rate (Rhoades and Cates 1976, Rhoades 1979). Across resource supply rates, resistance is predicted to be more costly in low-resource environments, and resistance investment is expected to decrease, regardless of lifespan (Rhoades 1979, Herms and Mattson 1992, Stamp 2003). In contrast, the Growth Rate hypothesis predicts high levels of resistance in low-resource environments. When growth is resource-limited, the turnover of plant tissue is slow and regrowth of tissue lost to pathogens is costly. Thus, the benefits of resistance and therefore resistance investment are predicted to be greater in low-resource environments (Coley et al. 1985, Stamp 2003). At a given resource supply rate, the costs of resistance are predicted to increase with growth rate when the proportion of photosynthate allocated to resistance is constant across hosts (Gulmon and Mooney 1986). Thus, the Optimal Defense and Growth Rate hypotheses both predict a negative relationship between growth rate and resistance investment and thus a positive relationship between lifespan and resistance within resource environments. They make opposite predictions regarding resistance investment along resource gradients.

The Growth-Differentiation Balance hypothesis includes arguments from both the Optimal Defense and Growth Rate hypotheses, and considers resource competition and enemy pressure to be the main selective forces driving defense evolution. In this hypothesis, defense investment is determined by a carbon allocation tradeoff between growth and differentiation (i.e., chemical/structural resistance and storage). The costs and benefits of allocation are

environmentally contingent, as the environment dictates the relative importance of competition and enemy pressure as selective forces. At very low resource availability, growth and photosynthesis are both limited, neither competition nor enemy pressure are very intense, and plants are predicted to invest preferentially in storage and maintenance structures over resistance. At intermediate resource availability, growth is more limited than photosynthesis, competition is less of a selective force than enemy pressure, and plants are expected to allocate excess carbon to resistance. At high resource availability, neither growth nor photosynthesis are limited, the selective force of competition is strong relative to enemy pressure, and plants are expected to invest in resource pre-emption over storage or resistance (Herms and Mattson 1992, Stamp 2003). Thus, the Growth-Differentiation Balance hypothesis predicts a hump-shaped relationship between growth rate or lifespan and resistance investment across resource environments. Because it assumes that variation in inherent growth rate across species is due to adaptation to different resource environments (Stamp 2003), it also implicitly predicts a hump-shaped relationship between growth rate or lifespan and resistance investment when species with varying growth rates occupy a common resource environment.

Evolution of resistance in hosts with acquired immunity

Thus far, we have considered correlated evolution in lifespan and innate resistance in organisms that do not also possess acquired immunity. The evolution of resistance when organisms do possess acquired immunity has only been considered in epidemiological theory. Predictions of correlated lifespan-resistance evolution tend to be qualitatively similar whether hosts possess immunity or not, especially if immunity can be lost over time. When immunity wanes, equilibrium pathogen prevalence, and thus selection for resistance, is still expected to increase with host lifespan (Boots and Bowers 2004, Miller et al. 2007). In a susceptible-

infected-immune model in which hosts varied in innate resistance, Anderson and May (1982) predicted that equilibrium pathogen prevalence and the fitness of resistant individuals would increase with generation time relative to lifespan. Thus, populations that delayed reproduction were expected to invest more in resistance, even if they were completely immune upon recovery. Some models predict more complicated patterns of resistance investment with lifespan when immunity is permanent or near permanent. In one, equilibrium pathogen prevalence and selection for resistance initially increased with lifespan, but did not continue to increase beyond intermediate lifespans. At intermediate lifespans, a large proportion of the population had been infected and developed immunity, even when resistance was high. At this point, the fitness benefits of investing in reproduction started to outweigh those of investing in resistance, and the relationship between lifespan and resistance investment was parabolic (Miller et al. 2007).

Theoretical summary

In life-history theory, the benefits of resistance are in terms of changes to the ontogeny of mortality, which drive lifespan evolution. If resistance evolution is comparatively costly or constrained, the evolution of decreased lifespan is expected in response to increasing parasite pressure. Investment in resistance, or lack thereof, therefore determines the direction of selection acting on lifespan. In both cases, pathogen pressure is the ultimate driver of both direct and indirect (via resistance evolution) selection on lifespan. Epidemiological models confirm that pathogen pressure, and thus the benefits of resistance, will generally be greater in long-lived hosts. Long-lived hosts are therefore predicted to invest more in resistance, with some exceptions due to pathogen virulence, host population structure, and acquired immunity. Plant defense theory explicitly considers both the costs and benefits of resistance, and argues that both of these are at least partially determined by a hosts' resource environment. With few exceptions, life-

history and epidemiological theory both predict positive lifespan-resistance relationships across species or populations. Within resource environments, plant defense theory predicts either a positive or hump-shaped relationship between lifespan and resistance investment, but predictions are more varied across resource environments.

E*mpirical tests*

Empirical evidence for correlated evolution in lifespan and resistance comes from comparative studies and artificial or natural selection experiments. Comparative studies are the most numerous, and suggest patterns of correlated evolution, but selection experiments are stronger tests of a causal relationship. Reviewing invertebrate life history evolution in response to parasitism, Michalakis and Hochberg (1994) showed that, in the absence of resistance, parasitism can select for either increased or decreased lifespan depending on the ontogeny of attack, as predicted by life-history theory. Comparative common garden experiments have demonstrated negative relationships between host growth or maturation rates and resistance in lettuce cultivars differing only in the presence of a resistance gene (Bergelson 1994); radish cultivars varying in resistance expression (Hoffland et al. 1996); populations of *Urtica dioica* with different histories of parasitism by a parasitic plant (Koskela 2002); and in snail populations with varying trematode parasite prevalence (Lafferty 1993, Fredensborg and Poulin 2006). Because growth rate and lifespan generally scale allometrically, these results support a positive correlation between lifespan and resistance investment. Across *Daphnia* populations, however, there was no correlation between resistance to a sterilizing bacterial pathogen and host maturation rate (Little et al. 2002). In addition, a phylogenetically controlled analysis of milkweed species found no evidence for a relationship between host growth rate and resistance (Agrawal and Fishbein 2008).

In some cases, resistance and longevity may be linked on the molecular level. In nematodes, increased expression of the transcription factor DAF-2 increased growth but decreased resistance expression (van den Berg et al. 2006). Increased expression of the Accelerated Cell Death-6 allele in *Arabidopsis thaliana* increases resistance to a range of bacterial and fungal pathogens but decreases growth rate (Todesco et al. 2010). In all of the aforementioned experiments, resource availability was the same for all individuals or statistically controlled for. Thus, within a given resource environment, there is moderate support for a positive relationship between lifespan and resistance investment. Even across resource environments, growth rate was negatively correlated with the proportion of net plant production allocated to resistance chemicals in three species of tropical trees (Kurokawa et al. 2004). When belowground resource availability was experimentally varied, differences in growth rate between resistant and susceptible lettuce cultivars were greatest at low resource availability (Bergelson 1994). This supports resource allocation tradeoffs as a mechanism of lifespan-resistance relationships (Bergelson 1994), contingent on the resource environment, as plant defense theory posits.

Artificial and natural selection experiments offer equivocal support for correlated evolution in host lifespan and resistance. Both moth and bacterial hosts evolved increased resistance when reared in the presence of pathogens for several generations, and resistant lines developed or grew more slowly than unexposed lines (Boots and Begon 1993, Lohse et al. 2006). Comparing unselected lines of the herbaceous plant host *Brassica rapa* to lines selected for resistance to two fungal pathogens, growth rate decreased with increased resistance to one pathogen but not the other (Mitchell-Olds and Bradley 1996). When lines of *Drosophila nigrospiracula* were selected for behavioral resistance to an ectoparasite, there was no difference

in lifespan between selected and unselected lines, though resistant females produced fewer eggs (Luong and Polak 2007). In yellow dung flies (*Scathophaga stercoraria*), lines selected for chemical resistance to intercellular parasites had shorter lifespans, but only in low resource conditions (Schwarzenbach and Ward 2006). These results suggest that correlations between lifespan and resistance investment may depend on pathogen and environmental characteristics. In addition to artificial selection experiments, observations of natural selection have also been used to test for a correlations between lifespan and resistance. Because invasive species often have fewer pathogens in their introduced range, invasions offer a convenient but uncontrolled means of testing whether lifespan or growth rate responds when the strength of selection for defense declines. Two introduced plants, a naturalized herb and an invasive tree, allocated less to resistance and more to growth when compared to native genotypes in a common garden (Siemann and Rogers 2001, Blair and Wolfe 2004). As with the evidence from comparative studies, the results of artificial and natural selection experiments tend to support a positive relationship between lifespan and resistance. Those that don't find a relationship between lifespan and resistance suggest that resistance investment may tradeoff with other host life-history characteristics, like reproduction, or that the strength of resistance tradeoffs is environmentally contingent.

Combined, there is empirical support for the general prediction of positively correlated evolution in host lifespan and resistance investment from life history, epidemiological, and plant defense theories. There are exceptions, however, and theory suggests that these may arise when factors such as pathogen virulence, environmental resource availability, and host immunity are uncontrolled for. Future investigations of host lifespan and resistance investment should control for, and, if possible, quantify the effects of such factors. Comparisons of lifespan and resistance

investment across species adapted to varying resource environments, or selection experiments in which resource availability is factorially manipulated, could test the hypotheses of plant defense theory that resource availability interacts as a driver of lifespan and resistance evolution. To test the epidemiological and life history theory hypotheses regarding the contingency of lifespan-resistance relationships on pathogen virulence or the ontogeny of attack, studies could investigate lifespan-resistance relationships in reference to parasites varying in these characteristics.

Defense via tolerance

Life History Theory

Life history theory predicts both positive and negative correlations between host lifespan and tolerance. On the one hand, tolerance mechanisms don't slow the accumulation of pathogens and other sources of mortality with age. As such, they may be more effective at increasing survival in young age classes, which is expected to select for shorter lifespans (Stearns 1992). On the other hand, tolerance may be one of three strategies (tolerance, resistance, and life-history change) for reducing the fitness effects of pathogens. If tolerance is costly or there is little variation for it in a population, hosts are predicted to evolve either shorter lifespans or greater resistance in order to maintain fitness (Minchella 1985, Adamo 1999). When shorter lifespans are an alternative to tolerance, life history theory predicts a positive correlation between host lifespan and tolerance.

Epidemiological theory

In epidemiological models, resistance acts to decrease a host's probability of infection and pathogen transmission, whereas tolerance acts to decrease the negative effects of infection on host fitness. The costs and benefits of tolerance and resistance are modeled similarly, and

model predictions of tolerance investment with varying host lifespan mirror those of resistance. Again, because long-lived hosts are expected to encounter a larger number and diversity of pathogens, and incur a larger cost of parasitism, the optimal investment in tolerance is predicted to increase with host lifespan (Anderson and May 1982, Miller et al. 2007). While resistance genes are often predicted to be polymorphic, tolerance is expected to evolve only to fixation. As a resistance gene spreads through a population, pathogen transmission decreases. This decreases selection for resistance and prevents resistance genes from becoming fixed. Tolerance decreases the fitness consequences of infection but does not affect the probability of becoming infected. Tolerant hosts may even harbor greater pathogen populations or survive longer while infected. As a result, pathogen transmission increases as a tolerance genes spread through a population, which increases selection for tolerance and drives tolerance genes to fixation (Roy and Kirchner 2000, Miller et al. 2007). While investment in tolerance is expected to increase with lifespan, observed levels of tolerance are expected to be nonexistent for short-lived organisms, high for long-lived organisms, and either high or nonexistent for organisms of intermediate lifespan (Miller et al. 2007).

Virulence is generally thought of as a characteristic of parasites, but the effect of infection on host fitness is also determined by tolerance. Theoretical investigations of parasite virulence and host life-history coevolution model changes in parasite virulence by varying the fecundity or survival of infected hosts, but this variation could also originate from differences in host tolerance. Because the theoretical treatment of virulence actually involves two different biological mechanisms, models of variation in host lifespan with pathogen virulence can also be interpreted as variation in lifespan with tolerance. For directly transmitted pathogens, moderate increases in virulence or decreases in tolerance are expected to select for increased allocation to

early reproduction and decreased lifespan (Hochberg et al. 1992, Restif et al. 2001, Gandon et al. 2002). When epidemiological feedbacks are considered, large decreases in tolerance can also select for longer lifespans. When tolerance is very low and the effects of infection are severe, pathogens have short effective transmission periods and epidemics cause severe mortality but die out quickly. Thus, an equally fit host strategy at very low tolerance is to mature slowly, allowing for increased reproductive output in individuals that survive short epidemics (Koella and Restif 2001, Restif et al. 2001). For pathogens with free-living environmental stages, decreased tolerance is only expected to select for shorter lifespans because epidemics do not fade out quickly (Restif et al. 2001). With few exceptions, then, models of pathogen virulence also predict that tolerance will increase with host lifespan.

Plant defense theory

Components of tolerance are associated with plant growth rate (Strauss and Agrawal 1999, Stowe et al. 2000, Tiffin 2000), and selective factors other than natural enemies may be acting on growth rate (Coley et al. 1985, Rosenthal and Kotanen 1994, Nunez-Farfan et al. 2007). According to the Growth Rate hypothesis, increased resource availability will select for increased growth rate, which decreases the proportional cost of replacing lost or damaged tissue. If lifespan decreases with growth rate, the costs of tolerance are lower in short-lived hosts. In other words, short-lived hosts may be getting many tolerance traits virtually cost free, as a byproduct of being fast-growing (Coley et al. 1985, Stamp 2003). With the same logic, the Growth-Differentiation balance hypothesis predicts that fast-growing plants will have little resistance to, but be more tolerant of, enemy damage (Herms and Mattson 1992). This hypothesis assumes that relative growth rate increases asymptotically with environmental resource availability and with the relative strength of competition as a selective force (Herms and

Mattson 1992, Stamp 2003). Because lifespan and growth rate scale allometrically, a negative correlation between lifespan and tolerance is predicted. Thus, these two hypotheses expect tolerance to be greatest in fast-growing, short-lived individuals, but as a byproduct of lifespan evolution in response to resources and competition, not a direct consequence of it.

The Optimal Defense hypothesis largely pertains to the evolution of resistance and does not make explicit predictions concerning the evolution of tolerance. However, if tolerance is considered a defense, with associated tradeoff costs, then, as with resistance, the Optimal Defense hypothesis would predict a negative relationship between growth rate and tolerance (Rhoades 1979, Stamp 2003). If lifespan and temporal apparency decrease with growth rate, tolerance investment is expected to increase with lifespan. As with lifespan in life-history theory, plant growth rate can also be considered an evolutionarily labile trait, increasing in response to high enemy damage in order to reproduce early and limit pathogen-induced fitness loss. If there is little variation for tolerance in a population, growth is expected to increase with increasing enemy pressure (Kirkwood 1981, Belsky et al. 1993). As with resistance, this scenario would produce a positive relationship between host lifespan and tolerance, because tolerance and increased growth rate are redundant strategies.

Evolution of tolerance in hosts with acquired immunity

As with resistance, only epidemiological theory has considered the evolution of tolerance when hosts can also become immune to reinfection. Again, the predictions of correlated tolerance-lifespan evolution are qualitatively similar for hosts that lack immunity and hosts in which immunity wanes over time (van Boven and Weissing 2004, Miller et al. 2007). Tolerance investment is expected to increase with lifespan, and tolerance genes are expected to become fixed in long-lived host populations and go extinct in short-lived host populations (van Boven

and Weissing 2004, Miller et al. 2007). If immunity is very long lasting or permanent, hosts with intermediate lifespans are expected to evolve complete tolerance more often than hosts with long or short lifespans. In this case, pathogen prevalence initially increases with host lifespan, which increases selection for tolerance. As host lifespan increases further, the increasing proportion of immune individuals eventually causes disease prevalence to decrease, which decreases selection for tolerance (Miller et al. 2007).

Theoretical summary

Both within and among theories, predictions for the evolution of host tolerance with lifespan are not as consistent as those of resistance with lifespan. Both life-history and plant defense theory present rationale for either positive or negative relationships between host tolerance and lifespan. Epidemiological theory also predicts both positive and negative relationships between tolerance and lifespan, but it makes explicit predictions about when each relationship will be observed. If there is little potential for tolerance evolution or parasite virulence is high, one of two equally fit host strategies is for hosts that survive short epidemics to mature slowly and invest in later reproduction. In this case, hosts with little tolerance are expected to have shorter lifespans. In all other cases, epidemiological theory predicts that long-lived hosts will evolve tolerance more often than short-lived hosts.

Empirical tests

Though the evidence is sparse, correlated evolution of host lifespan and tolerance is suggested by comparative studies and laboratory selection experiments. Comparing populations of *Urtica dioica* with varying histories of parasitism by a parasitic plant, parasitized populations flowered significantly later and were less tolerant of, but more resistant to, infection (Koskela 2002). Similarly, two studies of mosquito host tolerance to microspsoridian parasites support a

negative relationship between lifespan and tolerance. In this system, rapidly developing mosquitoes were more tolerant of infection, became smaller adults, and had shorter lifespans (Koella et al. 2009). When mosquito lines were selected for early or late pupation, parasite induced mortality increased with age at pupation and later pupating individuals lived longer. This increase in mortality was attributed to a decrease in host tolerance, as there was no effect of host selection on pathogen load (Koella and Agnew 1999). These results suggest that components of tolerance are associated with growth rate, as plant defense theory posits. In mosquitoes, tolerance and shorter lifespans do not seem to be redundant strategies of mitigating the fitness effects of parasitism. Rather, increased growth rate is a potential mechanism of tolerance, which suggests a reassessment the assumption that tolerance has a cost in terms of growth rate, which is common in theoretical models. While a few studies support a role of host growth rate and lifespan in the evolution of tolerance, tolerance is not consistently associated with growth rate across studies: among 36 species of milkweed, Agrawal and Fishbein (2008) found no support for a relationship between host growth rate and tolerance after controlling for the phylogenetic relatedness of hosts.

When compared to resistance, the evolution of tolerance is understudied. Current evidence weakly supports a negative relationship between tolerance and lifespan and a positive relationship between tolerance and growth rate. As with resistance, empirical work lags behind the theoretical, especially in terms of testing the specific predictions of epidemiological and plant defense theory. If tolerance and growth rate evolution are both influenced by environmental resource availability, as plant defense theory predicts, then comparative studies across hosts adapted to varying resource conditions should find positive correlations between resource availability, growth rate, and pathogen tolerance. Comparative studies of tolerance evolution in

response to pathogens with varying virulence, or lifespan evolution when there is little variation for tolerance, could test the prediction from epidemiological theory that virulent pathogens can select for long-lived, intolerant hosts. In contrast to resistance, the strategy of host tolerance is not expected to create a coevolutionary arms race between hosts and pathogens (Roy and Kirchner 2000). Because of its potential evolutionary stability, selection for tolerance in domestic animal hosts, and therapies to increase human tolerance, are just beginning to be investigated (Schneider and Ayres 2008). To understand the consequences of these applications, empirical tests of the theoretically proposed mechanisms and consequences of tolerance evolution are essential.

Defense via acquired immunity

Epidemiological theory

Only epidemiological theory explicitly considers correlated evolution in host lifespan and acquired immunity. Rationale exists for both higher and lower immune investment in long-lived hosts. On the one hand, long-lived hosts are more likely to encounter specific parasites several times (Medzhitov and Janeway 1997, Boots and Bowers 2004, Miller et al. 2007), and acquired immunity may be less costly than innate resistance or tolerance. While the costs of maintaining an immune system can be considerable, the costs of immune function are only fully realized when parasites are encountered. Innate mechanisms of defense may be more costly in long-lived hosts because they generally have larger body sizes, and the costs of maintaining defense in the absence of infection scale exponentially with body size (Rolff and Siva-Jothy 2003). Acquired immunity may have evolved to ameliorate these costs (Medzhitov and Janeway 1997, Rolff and Siva-Jothy 2003). Alternatively, the rate at which new susceptibles enter a population is higher in short-lived hosts, which could lead to increased transmission and probability of reinfection,

selecting for increased investment in acquired immunity in short-lived hosts (van Boven and Weissing 2004).

In a dynamic host pathogen model, Miller et al. (2007) investigated evolutionarily stable levels of immune investment in hosts of varying lifespan, and resulting predictions were contingent upon whether immunity could be lost. If it could be lost, investment in immunity was predicted to increase with host lifespan. If immunity was permanent, immune investment was predicted to increase with lifespan up to a point, after which equilibrium parasite prevalence became so low that selection for immunity was weak. At extremely long lifespans, the optimal investment in permanent immunity was eventually none (Miller et al. 2007). This model dealt with the evolution of acquired immunity in response to a single parasite. As host lifespan increases, hosts may encounter a larger diversity of parasites, increasing the benefit of innate and nonspecific defenses. Thus, high investment in acquired immunity in long lived hosts may not necessarily correspond to low investment in innate mechanisms of defense when parasite diversity is high (Miller et al. 2007). Using a similar approach, Boots and Bowers (2004) predicted that selection for acquired immunity would also depend on pathogen characteristics. In their model, acquired immunity was most likely to evolve in response to pathogens with high transmission rates and intermediate virulence. Under these conditions, hosts often recovered from an initial infection and the probability of reinfection was high, so there was a strong fitness benefit of acquired immunity (Boots and Bowers 2004). In sum, epidemiological theory predicts increasing investment in acquired immunity with host lifespan, contingent upon immunity loss rate and pathogen characteristics.

Empirical tests

One comparative study support the prediction of increasing investment in acquired immunity with host lifespan. Across bird species, adult cell-mediated immunocompetence was positively correlated with a life history axis representing decreasing developmental rate and increasing longevity, body size, survival rate, after controlling for ecological and environmental correlates (Tella et al. 2002). There is also some support for a tradeoff between growth and immunity, which is one mechanism for a positive relationship between lifespan and immunity. Several studies have observed declining immunocompetence with starvation and metabolic upregulation in response to an immune challenge, which suggests that immunity is energetically costly (Lochmiller and Deerenberg 2000). Accordingly, immune activation resulted in reduced growth rate among great tit nestlings (Tschirren and Richner 2006). Compared to mice with normal immune function, engineered mice lacking B and T cells had higher metabolic rates, which suggests that the upregulation of innate defenses may be even more costly than the maintenance of acquired immunity (Raberg et al. 2002). Whether these short-term phenotypic costs actually manifest in correlated evolution of lifespan and immune investment has yet to be demonstrated. Immune activation is clearly costly, but a cost of immune system maintenance has yet to be demonstrated, as does a consequence of these costs in terms of correlated evolution. There is some support for the hypothesis that acquired immunity mitigates what would be a greater cost of innate immunity, but whether this cost increases with lifespan is unknown. Further knockout experiments in longer-lived vertebrates, where the relative degree of metabolic up regulation is compared, could assess these costs. Artificial selection experiments in which the response of immunocompetence to selection on host lifespan is observed could also be used to test for correlated evolution in lifespan and acquired immunity.

The prediction that relationships between lifespan and immune investment will vary with the loss rate of immunity would be difficult to test, especially considering that immune duration can vary both within hosts, in response to different pathogens, and between hosts. Comparative studies in a system where hosts vary in lifespan and immune duration to a shared pathogen would be a good first step. Epidemiological theory also predicts that immune investment will vary with pathogen transmission rate, and therefore transmission rate should be controlled for, as much as is possible, in comparative and experimental tests of relationships between lifespan and immune investment. Observed decreases in immunocompetence with decreasing resource availability suggest that the costs of immune system maintenance may be environmentally contingent, and resource availability may influence the costs of acquired immunity (Lochmiller and Deerenberg 2000, Ricklefs and Wikelski 2002). To test the relative effects of lifespan and resource availability on immune investment, phylogenetic studies could use a generalist pathogen to compare the variation in immune response explained by host life history vs. environmental characteristics.

Summary

The evolution of defense, in any form, will be driven by several factors, one of them being host lifespan. Reciprocally, the evolution of lifespan can be driven by the evolution, loss or gain, of defense against pathogens. Life-history theory predicts that the direction of correlated lifespan-defense evolution will depend on how defenses affect the ontogeny of pathogen attack (Roff 1992, Stearns 1992), and the relative costs, benefits, and potential for defense versus lifespan evolution in response to parasitism (Minchella 1985, Hochberg et al. 1992). Epidemiological theory adds additional contingencies to these predictions, in the form of parasite characteristics (Koella and Restif 2001, Restif et al. 2001, Miller et al. 2007), host population

structure (Carlsson-Graner and Thrall 2006), and the duration of immunity in hosts that also possess acquired immunity (Miller et al. 2007). Plant defense theory adds resource availability as yet another interacting driver of correlated growth rate, lifespan, and defense evolution (Rhoades 1979, Herms and Mattson 1992, Stamp 2003). Regardless of what they consider to be the cause, all three bodies of theory predict that resistance investment will generally be positively correlated with lifespan, and negatively correlated with growth rate. Predictions of correlated evolution in lifespan and tolerance are less consistent across theories. In life history and epidemiological theory, arguments exist for both positive and negative relationships between lifespan and tolerance. Opposing predictions arise from differences in the assumed cost function of tolerance with lifespan, and also from differences in the treatment of epidemiological feedbacks across models. In epidemiological theory, investment in acquired immunity is generally expected to increase with host lifespan. Empirical evidence tends to support the predicted, positive correlation between host lifespan and resistance investment. More speculatively, the limited available evidence also supports the predicted, negative correlation between host lifespan and investment in tolerance, and the predicted positive correlation between lifespan and investment in acquired immunity. Whether these relationships are indeed contingent on pathogen characteristics and resource availability has not been investigated empirically. We suggest several strategies for more extensively testing theoretical predictions, as well as investigating interacting drivers and contingencies in defense evolution.

Implications

The evolution of host defense against pathogens is often correlated with host lifespan. Lifespan and defense investment can exert reciprocal selection pressures, either directly via host tradeoffs or indirectly via pathogen population dynamics. As such, artificial selection for longer

lifespans has the potential to result in correlated changes in defense, and selection for increased defense may also alter host lifespan. In addition, disease eradication, disease emergence, and any other change to the selection regime driving defense evolution could result in correlated life-history evolution. Environmental resource availability and the characteristics of specific pathogens may interact with host lifespan to drive defense evolution, and predictions of correlated lifespan-defense evolution are often contingent on these factors. Without a more thorough understanding of evolutionarily correlated traits and the mechanisms behind these correlations, the outcomes of artificial selection and anthropogenic changes to natural selection regimes, for either lifespan or defense, may surprise us. One thing to note is that many of the theoretical models described here deal with the evolution of defense in response to specialist pathogens in a single host population. In host populations where generalist pathogen transmission is maintained by reservoir hosts, the predictions of single-host, single-pathogen models may not hold. This situation would be similar to the evolution of tolerance to pathogens with an environmental reservoir. Because host lifespan is disconnected from pathogen persistence, correlated evolution may not be observed (Restif et al. 2001), or it may occur in directions opposite those predicted by single-host, single-pathogen models. The evolution of defense in response to generalist pathogens in complex host communities deserves further theoretical and empirical investigation.

REFERENCES

Adamo, S. A. 1999. Evidence for adaptive changes in egg laying in crickets exposed to bacteria and parasites. Animal Behavior **57**:117-124.

Agnew, P., J. C. Koella, and Y. Michalakis. 2000. Host life history responses to parasitism. Microbes and Infection **2**:891-896.

Agrawal, A. A., and M. Fishbein. 2008. Phylogenetic escalation and decline of plant defense strategies. Proceedings of the National Academy of Sciences **105**:10057-10060.

Anderson, R. M., and R. M. May. 1982. Infectious Diseases of Humans: Dynamisc and Control. Oxford University Press, Oxford.

Atanasov, A. T. 2005. The linear alometric relationship between total metabolic energy per life span and body mass of poikilothermic animals. Biosystems **82**:137-142.

Atanasov, A. T. 2007. The linear allometric relationship between total metabolic energy per life span and body mass of mammals. Biosystems **90**:224-233.

Belsky, A. J., W. P. Carson, C. L. Jensen, and G. A. Fox. 1993. Overcompensation by plants: herbivore optimization or red herring? Evolutionary Ecology **7**:109-121.

Bergelson, J. 1994. The effects of genotype and the environment on costs of resistance in lettuce. American Naturalist **143**:349-359.

Blair, A. C., and L. M. Wolfe. 2004. The evolution of an invasive plant: an experimental study with *Silene latifolia*. Ecology **85**:3035-3042.

Boots, M., and M. Begon. 1993. Trade-offs with resistance to a granulosis virus in the Indian meal moth, examined by a laboratory evolution experiment. Functional Ecology **7**:528-534.

Boots, M., and R. G. Bowers. 2004. The evolution of resistance through costly acquired immunity. Proceedings: Biological Sciences **271**:715-723.

Brown, J. H., J. F. Gillooly, A. P. Allen, V. M. Savage, and G. B. West. 2004. Toward a Metabolic Theory of Ecology. Ecology **85**:1771-1789.

Bryant, J. P., F. S. Chapin, and D. R. Klein. 1983. Carbon/nutrient balance of boreal plants in relation to vertebrate herbivory. Oikos **40**:357-368.

Carlsson-Graner, U., and P. H. Thrall. 2006. The impact of host longevity on disease transmission: host-pathogen dynamics and the evolution of resistance. Evolutionary Ecology Research **8**:659-675.

Coley, P. D., J. P. Bryant, and F. S. Chapin. 1985. Resource availability and plant antiherbivore defense. Science **230**:895-899.

Fredensborg, B. L., and R. Poulin. 2006. Parasitism shaping host life-history evolution: adaptive responses in a marine gastropod to infection by trematodes. Journal of Animal Ecology **75**:44-53.

Gandon, S., P. Agnew, and Y. Michalakis. 2002. Coevolution between parasite virulence and host life-history traits. American Naturalist **160**:374-388.

Garnier, E. 1992. Growth analysis of congeneric annual and perennial grass species. Journal of Ecology **80**:665-675.

Gulmon, S. L., and H. A. Mooney. 1986. Costs of defense and their effects on plant productivity.*in* T. J. Givnish, editor. On the Economy of Plant Form and Function. Cambridge University Press, London.

Herms, D. A., and W. J. Mattson. 1992. The dilemma of plants: to grow or defend. The Quarterly Review of Biology **67**:283-335.

Hochberg, M. E., Y. Michalakis, and T. d. Meeus. 1992. Parasitism as a constraint on the rate of life-history evolution. Journal of Evolutionary Biology **5**:491-504.

Hoffland, E., G. J. Niemann, J. A. Van Pelt, J. B. M. Pureveen, G. B. Eijkel, J. J. Boon, and H. Lambers. 1996. Relative growth rate correlates negatively with pathogen resistance in radish: the role of plant chemistry. Plant, Cell, and Environment **19**:1281-1290.

Kirchner, J. W., and B. A. Roy. 1999. The evolutionary advantages of dying young: epidemiological implications of longevity in metapopulations. The American Naturalist **154**:140-159.

Kirkwood, T. B. L. 1981. Repair and its evolution: survival versus reproduction. Pages 165-189 *in* C. R. Townsend and P. Caplow, editors. Physiological Ecology: An Evolutionary Approach to Resource Use. Sinauer and Associates, Inc., Sunderland, MA.

Koella, J. C., and P. Agnew. 1999. A correlated response of a parasites virulence and life cycle to selection on its host's life history. Journal of Evolutionary Biology **12**:70-79.

Koella, J. C., L. Lorenz, and I. Bargielowski. 2009. Microsporidians as evolution-proof agents of malaria control? Advances in Parisitology **68**:315-327.

Koella, J. C., and O. Restif. 2001. Coevolution of parasite virulence and host life history. Ecology Letters **4**:207-214.

Koskela, T. 2002. Variation in life-history traits among *Urtica dioica* populations with different history in parasitism by the holoparasitic plant *Cuscuta europaea*. Evolutionary Ecology **16**:433-454.

Kurokawa, H., Y. Kitahashi, T. Koike, J. Lai, and T. Nakashizuka. 2004. Allocation to defense or growth in dipterocarp forest seedlings in Borneo. Oecologia **140**:261-270.

Lafferty, K. D. 1993. The marine snail, *Cerithidea californica*, matures at smaller sizes where parasitism is high. Oikos **68**:3-11.

Lafferty, K. D., and A. M. Kuris. 2002. Trophic strategies, animal diversity and body size. Trends in Ecology and Evolution **17**:507-513.

Lindstedt, S. L., and W. A. Calder. 1976. Body Size and Longevity in Birds. The Condor **78**:91-94.

Little, T. J., H. J. Carius, O. Sakwinska, and D. Ebert. 2002. Competitiveness and life-history characteristics of *Daphnia* with respect to susceptibility to a bacterial pathogen. Journal of Evolutionary Biology **15**:796-802.

Lochmiller, R. L., and C. Deerenberg. 2000. Trade-offs in evolutionary immunology: just what is the cost of immunity? Oikos **88**:87-98.

Lohse, K., A. Gutierrez, and O. Kaltz. 2006. Experimental evolution of resistance in *Paramecium caudatum* against the bacterial parasite *Holospora undulata*. Evolution **60**:1177-1186.

Lovegrove, B. G. 2009. Age at first reproduction and growth rate are independent of basal metabolic rate in mammals. Journal of Comparative Physiology B: Biochemical, Systemic, and Environmental Physiology **179**.

Luong, L. T., and M. Polak. 2007. Costs of resistance in the *Drosophila-Macrocheles* system: a negative genetic correlation between ectoparasite resistance and reproduction. Evolution **61**:1391-1402.

MarbÃ , N. r., C. M. Duarte, and S. AgustÃ-. 2007. Allometric Scaling of Plant Life History. Proceedings of the National Academy of Sciences of the United States of America **104**:15777-15780.

Medzhitov, R., and C. A. Janeway. 1997. Innate immunity: the virtues of a nonclonal system of recognition. Cell **91**:295-298.

Michalakis, Y., and M. E. Hochberg. 1994. Parasitic effects on life-history traits: a review of recent studies. Parasite **1**:291-294.

Miller, M. R., A. White, and M. Boots. 2007. Host life span and the evolution of resistance characteristics. Evolution **61**:2-14.

Minchella, D. J. 1985. Host life-history variation in response to parasitism. Parasitology **90**:205-216.

Mitchell-Olds, T., and D. Bradley. 1996. Genetics of *Brassica rapa*. 3. Costs of disease resistance to three fungal pathogens. Evolution **50**:1859-1865.

Nunez-Farfan, J., J. Fornoni, and P. L. Valverde. 2007. The evolution of resistance and tolerance to herbivores. Annual Review of Ecology, Evolution, and Systematics **38**:541-566.

Raberg, L., M. Vestberg, D. Hasselquist, R. Holmdahl, E. Svensson, and J. Nilsson. 2002. Basal metabolic rate and the evolution of the adaptive immune system. Proceedings: Biological Sciences **269**:817-821.

Restif, O., M. E. Hochberg, and J. C. Koella. 2001. Virulence and age at reproduction: new insights into host-parasite coevolution. Journal of Evolutionary Biology **14**:967-979.

Rhoades, D. F. 1979. Evolution of plant chemical defense against herbivores *in* G. A. Rosenthal and D. H. Janzen, editors. Herbivores: Their Interactions with Secondary Plant Metabolites. Academic Press, New York.

Rhoades, D. F., and R. G. Cates. 1976. Toward a general theory of plant antiherbivore chemistry. Recent Advances in Phytochemistry **10**:168-213.

Ricklefs, R. E., and M. Wikelski. 2002. The physiology/life-history nexus. Trends in Ecology & Evolution **17**:462-468.

Roff, D. A. 1992. The Evolution of Life Histories: Theory and Analysis. Chapman and Hall, New York.

Rolff, J., and M. T. Siva-Jothy. 2003. Invertebrate ecological immunology. Science **301**:472-475.

Rosenthal, J. P., and P. M. Kotanen. 1994. Terrestrial plant tolerance to herbivory. Trends in Ecology and Evolution **9**:145-148.

Roy, B. A., and J. W. Kirchner. 2000. Evolutionary dynamics of pathogen resistance and tolerance. Evolution **54**:51-63.

Savage, V. M., J. F. Gillooly, J. H. Brown, G. B. West, and E. L. Charnov. 2004. Effects of Body Size and Temperature on Population Growth. The American Naturalist **163**:429-441.

Schneider, D. S., and J. S. Ayres. 2008. Two ways to survive infection: what resistance and tolerance can teach us about treating infectious diseases. Nature Reviews: Immunology **8**:889-895.

Schwarzenbach, G. A., and P. I. Ward. 2006. Responses to selection on phenoloxidase activity in yellow dung flies. Evolution **60**:1612-1621.

Siemann, E., and W. E. Rogers. 2001. Genetic differences in growth of an invasive tree species. Ecology Letters **4**:514-518.

Speakman, J. R. 2005. Body size, energy metabolism and lifespan. J Exp Biol **208**:1717-1730.

Stamp, N. 2003. Out of the quagmire of plant defense hypotheses. Quarterly Review of Biology **78**:23-55.

Stearns, S. C. 1992. The Evolution of Life Histories. Oxford University Press, Oxford.

Stowe, K. A. 1998. Experimental evolution of resistance in *Brassica rapa*: correlated responses of tolerance in lines selected for glucosinolate content. Evolution **52**:703-712.

Stowe, K. A., R. J. Marquis, C. G. Hochwender, and E. L. Simms. 2000. The evolutionary ecology of tolerance to consumer damage. Annual Review of Ecology and Systematics **31**:565-595.

Strauss, S. Y., and A. A. Agrawal. 1999. The ecology and evolution of plant tolerance to herbivory. Trends in Ecology and Evolution **14**:179-185.

Tella, J. L., A. Scheuerlein, and R. E. Ricklefs. 2002. Is cell-mediated immunity related to the evolution of life-history strategies in birds? Proceedings: Biological Sciences **269**:1059-1066.

Thompson, J. N. 1982. Interaction and Coevolution. John Wiley and Sons, New York.

Tiffin, P. 2000. Mechanisms of tolerance to herbivore damage: What do we know? Evolutionary Ecology **14**:523-536.

Todesco, M., S. Balasubramanian, T. T. Hu, M. B. Traw, M. Horton, P. Epple, C. Kuhns, S. Sureshkumar, C. Schwartz, C. Lanz, R. A. E. Laitinen, Y. Huang, J. Chory, V. Lipka, J. O. Borevitz, J. L. Dangl, J. Bergelson, M. Nordborg, and D. Weigel. 2010. Natural allelic variation underlying a major fitness trade-off in Arabidopsis thaliana. Nature **465**:632-636.

Tschirren, B., and H. Richner. 2006. Parasites shape the optimal investment in immunity. Proc. R. Soc. B **273**:1773-1777.

van Boven, M., and F. J. Weissing. 2004. The evolutionary economics of immunity. The American Naturalist **163**:277-294.

van den Berg, M. C. W., J. Z. Woerlee, H. Ma, and R. C. May. 2006. Sex-dependent resistance to the pathogenic fungus *Cryptococcus neoformans*. Genetics **173**:677-683.

van der Meijden, E., M. Wijn, and H. J. Verkaar. 1988. Defense and regrowth, alternate plant strategies in the struggle against herbivores. Oikos **51**:355-363.

West, G. B., J. H. Brown, and B. J. Enquist. 1997. A General Model for the Origin of Allometric Scaling Laws in Biology. Science **276**:122-126.

CHAPTER 2: THE ROLE OF HABITAT FILTERING IN THE LEAF ECONOMICS SPECTRUM AND PLANT SUSCEPTIBILITY TO PATHOGN INFECTION[1]

Introduction

The Leaf Economics Spectrum (LES) is a global axis of leaf trait covariation that is thought to arise from biophysical constraints, selection against unfit trait combinations, and gradients in abiotic conditions, which together produce a fundamental tradeoff between two ecological strategies (Wright et al. 2004; Reich 2014; Donovan et al. 2011). One end of the LES corresponds to a strategy of resource conservation and longevity, and the other end corresponds to a strategy of resource acquisition and growth. At the conservative end, 'slow-return' phenotypes are slow growing with low photosynthetic rates and tissue nutrient concentrations, but high leaf mass per area (LMA); at the acquisitive end, 'quick-return' phenotypes display the opposite combination of traits (Leishman et al. 2007; Wright et al. 2004). Globally, 74% of the log-log covariation in leaf physiological traits can be captured by the single multivariate axis of the LES (Wright et al. 2004), and the LES has been documented repeatedly across systems and scales (Wright et al. 2004; Leishman et al. 2007; Diaz et al. 2004; Reich et al. 1999).

The covariation among leaf traits that defines the LES can weaken in at least three situations. First, at small spatial scales (e.g., within neighborhoods), a lack of diversity can limit the variation in each trait, which in turn limits covariation among traits (Funk and Cornwell

[1] This chapter is soon to appear as an article in the Journal of Ecology. The original citation is as follows: Welsh, M. E., Cronin, J. P. and Mitchell, C. E. (2016). The role of habitat filtering in the leaf economics spectrum and plant susceptibility to pathogen infection. J Ecol. Accepted Author Manuscript. doi:10.1111/1365-2745.12632

2013; Messier et al. 2010). Second, in highly homogeneous environments, the narrow range of environmental conditions can limit trait variation (Funk and Cornwell 2013; Webb et al. 2010), as a result of habitat filtering (ecological selection against individuals with traits less suited to tolerate or compete in a given set of environmental conditions; Maire et al. 2012; Kraft et al. 2014). Third, when communities in heterogeneous environments have not been subjected to habitat filtering, individuals with traits that will eventually be filtered out can temporarily persist, overwhelming the trait covariation that, among fit individuals, would comprise the LES (Wright and Sutton-Grier 2012; Donovan et al. 2014).

Ecological selection takes time, and there may be a lag between a change in environmental conditions and the filtering of traits in communities. One circumstance in which communities may not yet be filtered to the current environment is in the wake of abiotic environmental change. While the specifics will vary depending on rates of environmental change, demographic processes, and colonization, three possible chronological stages of habitat filtering following environmental change may be: 1) unfiltered, in which environmental change has just occurred, colonization and filtering have yet to occur, and individuals temporarily persist in conditions they will eventually be filtered out of, 2) semi-filtered, in which some colonization and filtering have occurred but the process is still ongoing, so some individuals still persist in conditions they will eventually be filtered out of, and 3) completely filtered, in which all filtering has occurred and the community is no longer changing in response to the environment (Jackson and Sax 2010; Smith et al. 2009). By selecting against functional strategies that deviate from the LES, habitat filtering may strengthen the trait covariation that comprises the LES (Reich 2014; Fig. 2.1). Comparative studies have suggested a strong role of ecological selection via habitat filtering in generating the LES (Donovan et al. 2011), but this role has not been tested

experimentally.

The traits that comprise the LES modulate plant interactions with the abiotic and biotic environment, and are commonly used to inform general models of community and ecosystem processes (e.g., Lavorel and Grigulis 2012; Scheiter et al. 2013). By focusing on the mechanisms through which organisms respond to and affect their environment, these trait-based models offer a means of moving beyond system- and species-specific approaches to ecology (Suding and Goldstein 2008; Lavorel and Garnier 2002). Ecological processes are often mediated by multiple traits (Cronin et al. 2010; Johnson et al. 2012; Cronin et al. 2014; Baraloto et al. 2012; Laliberte et al. 2012), and several authors have suggested that trait-based models use position along axes of trait covariation, like the LES, to predict function, as it captures the effects of several traits simultaneously (Cronin et al. 2010; Johnson et al. 2012; Baraloto et al. 2012), and could be used to synthesize across multiple ecological processes when different processes are mediated by different but correlated traits.

In disease ecology, position along the LES or similar axes of trait covariation is increasingly being used to predict host competence (i.e., the ability to acquire and spread pathogen infection) across a diversity of host species (Cronin et al. 2010; Johnson et al. 2012; Han et al. 2015). The ability to acquire infection is a critical component of host competence, and we will refer to this component as host susceptibility to infection. Plant susceptibility to infection by vector-borne pathogens has been hypothesized to increase from slow- to quick-return hosts along the LES via four non-exclusive mechanisms (Cronin et al. 2010). First, vectors may prefer to feed on more nutritious hosts, those with greater tissue nutrient concentrations (Kursar and Coley 2003; Mattson 1980; Wright et al. 2010). Second, vector feeding may be mechanically limited by greater host tissue density and LMA (Kursar and Coley 2003). Third, quick-return

phenotypes may invest less in non-nitrogenous chemical defenses, such as phenolics and terpenoids (Mattson 1980). Finally, quick-return phenotypes may also have a weaker non-specific hypersensitive response to pathogens and vectors (Todesco et al. 2010). All of the traits involved in these hypothesized mechanisms covary along the LES, implying that plant host position along the LES may capture the joint influence of multiple traits on susceptibility. In the one direct test of this hypothesis to date, an experiment with six hosts of a vector-borne virus, susceptibility increased among the six host species from slow- to quick-return along the LES (Cronin et al. 2010).

The potential role of habitat filtering in generating the LES, combined with the role of the LES in governing host-pathogen interactions and other ecological processes (Lavorel 2013; Cronin et al. 2010; Baraloto et al. 2012), suggests that to understand and predict the effects of environmental change on many plant-based ecological processes will require integrative studies that simultaneously investigate both the causes and consequences of the LES (Webb et al. 2010; Suding et al. 2008). Furthermore, a rigorous understanding of causes and consequences will be facilitated by an experimental approach. Yet, few studies have taken such an integrative experimental approach (Suding and Goldstein 2008), and we are aware of no studies that have applied such an approach to disease ecology.

In developing such an approach, one challenge is to incorporate heterogeneities both within and among species (Johnson et al. 2015). While our understanding of the LES and other functional strategies has been built primarily on variation among species, there can be considerable overlap in LES traits among species, to the degree that individuals cannot be reliably assigned to species based solely on their traits (Albert et al. 2010). Furthermore, recent studies have shown that explicit consideration of variation within species—including variation

resulting from plastic responses to environmental conditions—can be necessary to accurately predict the ecological consequences of trait variation (Donovan et al. 2014; Messier et al. 2010; Violle et al. 2012; Clark 2010). This general challenge applies to disease ecology because host-pathogen interactions can vary considerably both within and among host species (Hersh et al. 2012), and both sources of heterogeneity can affect transmission (Lloyd-Smith et al. 2005). As such, host-pathogen interactions might provide a crucible for testing the performance of individual-level, trait-based models under environmental change.

To test the linkages between a major environmental gradient, host traits, and host susceptibility to pathogen infection, we experimentally simulated the above three stages of habitat filtering: from unfiltered, to semi-filtered, to completely filtered communities. In each scenario of filtering, we quantified the strength of the LES and the accuracy of individual-level, trait-based models of host susceptibility to pathogen infection. We predicted that the strength of the LES would increase with the completeness of habitat filtering and in consequence so would the accuracy of trait-based models of plant susceptibility to pathogen infection.

Materials and Methods

Study System

To experimentally test the effect of habitat filtering on the LES, and the resulting consequences for predicting the susceptibility of host individuals to pathogen infection, we used 23 annual and perennial grass species from the Mediterranean grasslands of California and Oregon (Table 2.1). These species share a generalist, vector-borne pathogen, *Barley yellow dwarf virus PAV* (BYDV-PAV, family *Luteoviridae*), a phloem-infecting RNA virus that is obligately and persistently transmitted by certain species of aphids. Focal host species were selected from over 90 grass species present at the University of California's Hopland Research

and Extension Center (HREC) in Hopland, CA, USA to represent a range of several ecological attributes: local abundance at HREC (including all dominant species in a set of observational plots), frequency across 11 sites spanning 15° latitude (Borer et al. 2010; Borer et al. 2014: CA and OR, US sites), life history (annual vs. perennial), and geographic provenance (native vs. exotic). In this system, annual grasses are poorer competitors for soil nitrate than perennials, perennials mainly persist in resource-poor habitats, and dominance by annuals increases with nitrogen supply (Seabloom et al. 2003; Harpole et al. 2007; Weiss 2006; Zavaleta et al. 2003; Huenneke et al. 1990), indicating that nitrogen supply is an important environmental filter. Specifically, these studies together indicate that, in California grasslands, perennials typically occur in low-nitrogen environments and annuals typically occur in high-nitrogen environments as a result of habitat filtering. Across annuals and perennials, increased nitrogen supply can also cause plastic, quick-return shifts in LES traits (Cronin et al. 2010).

Experimental design and protocol

The experiment was conducted in a greenhouse at the University of North Carolina, Chapel Hill, NC, USA, and ran from August-November, 2010. In a randomized block design (6 blocks), we factorially manipulated host species (23 species; Table 2.1) and nitrogen supply (low/high; Table 2.2), for a total of 276 individuals. We used three combinations of nitrogen supply treatment and host life history (annual vs. perennial) to simulate three chronological scenarios of habitat filtering: from unfiltered, to semi-filtered, to completely filtered communities. Specifically, the unfiltered scenario included only perennials at high nitrogen and annuals at low nitrogen, such that each life history was growing the nitrogen environment it would typically be filtered out of in the field, as if all filtering had yet to occur. The semi-filtered scenario included perennials and annuals at both low and high nitrogen, so half of each life

history was growing in the environment it would typically be filtered out of, while half was growing in the environment it would typically be filtered to, as if some filtering had occurred but the process was still ongoing. Lastly, the completely filtered scenario included only perennials at low nitrogen and annuals at high nitrogen, so all individuals of both life histories were growing in the environments they are typically filtered to in the field, as if all filtering had occurred (Fig. 2.1, left). While there are few cases of rapid decreases in nitrogen supply, especially outside of an experimental context, we employed nitrogen supply as a model abiotic filter representing many other filters for which conditions can change in opposite directions in different communities. For example, the patchy effects of climate change may increase temperature or water availability in some areas but decrease it in others. Unfortunately, these abiotic filters are difficult to experimentally mimic. Our experimental manipulation of nitrogen is both tractable and captures a key general feature of environmental change: ecological turnover often lags behind abiotic change, and thus many individuals live in conditions that they will eventually be filtered out of.

Hosts were grown in a 50:50 mix of sterilized soil and sand, with ample phosphorus, potassium, and micronutrients (Borer et al. 2014; Table 2.2) in 1L Conetainer pots (Stuewe and Sons, Inc., OR, US). Planting was timed to minimize differences in grass host phenology, such that all hosts reached the two-leaf stage within a week of each other. Beginning at the two-leaf stage, we quantified three leaf traits and two metrics of growth rate on all individuals (Table 2.3a). Photosynthetic capacity was quantified with an infrared gas analyzer, the CIRAS-2 Portable Photosynthesis System V2.01 (PP Systems). Measurements of photosynthetic capacity, tissue nitrogen, and LMA were stratified across blocks (two individuals per treatment combination per block per day over three days), while leaf growth and leaf emergence

measurements began at the two-leaf stage on each individual, regardless of block. Two individuals, a perennial at high nitrogen and an annual at low nitrogen, were later excluded from the data set due to missing trait data.

One month after germination, all 276 hosts were exposed to infection with BYDV-PAV by caging five *Rhopalosiphum padi* L. aphid vectors carrying BYDV-PAV on each host. Infected vectors were produced by feeding aphids on lab-maintained, infected host tissue of the highly competent agricultural host *Avena sativa* var. Coast Black Oat (CBO) for 48 hours. Aphids were propagated from field-collected populations in New York, USA, and the BYDV-PAV strain was isolated from a wild *Bromus vulgaris* (Hook.) Shear individual in Oregon, USA. To verify that aphids were uninfected prior to feeding on infected CBO (and all inoculated hosts were therefore exposed to newly infected aphids), we also simultaneously 'mock inoculated' healthy, highly susceptible CBO individuals (two CBO individuals/nitrogen treatment/block) with aphids that were fed on uninfected CBO tissue (Cronin et al. 2010). After three days, all aphids were removed with horticultural oil. Inoculations occurred over three days, two blocks per day, and there was no effect of inoculation day on susceptibility (χ^2=0.86, df=2, p=0.65). Five weeks after exposure to infected vectors, the infection status of all hosts was determined via Enzyme-Linked Immunosorbent Assays (ELISAs; Agdia Inc., IN, USA). All mock inoculated individuals were confirmed uninfected.

Statistical Analyses

To compare support for the LES across habitat filtering scenarios, we used principal components analysis (PCA) to assess the proportion of trait variation explained by the first, multivariate axis (PC1) in each scenario, and Pearson product-moment correlation coefficients to assess the strength and direction of individual trait correlations with that axis. To test for effects

of habitat filtering on trait-based models of susceptibility, we used logistic regression in each filtering scenario to test for significant effects of (1) host position along PC1 (i.e., each individual's PC1 score), and (2) all five "raw" traits of each host on the probability of successful infection. Across filtering scenarios, we compared model accuracy by assessing the proportions of true or false positives and true or false negatives predicted by each model. To investigate biological mechanisms underlying variation in host susceptibility to pathogen infection, we used an information theoretic approach to calculate the relative variable importance (RVI) of each raw trait in logistic models of susceptibility, and repeated this analysis across filtering scenarios. RVI is the proportional influence of each trait on AICc across a global model and nested models (Burnham and Anderson 2002). All analyses were run in R ver. 3.0.2 (R Core Team 2015). PCA ordinations used the 'prcomp' function, logistic regressions the 'glm' function, and RVI analyses the 'dredge' and 'importance' functions in the 'MuMIn' package (Barton 2015).

To test whether trait-susceptibility relationships were driven by shared evolutionary history, we tested for phylogenetic signal in the residuals of the two most accurate models of susceptibility: the PC1 model and the AIC-best raw traits model in the scenario of complete habitat filtering (Ives et al. 2007; Pearse and Purvis 2013; Bouchenak-Khelladi et al. 2008; Blomberg et al. 2003; Fig. 2.2). Using model residuals allowed us to include intraspecific variation in tests of phylogenetic signal, as there are currently no tests of phylogenetic signal that can incorporate intraspecific variation in a binomial trait like susceptibility. Tests for phylogenetic signal used the 'phylosig' function in the 'phytools' package (v 0.4-60; randomizations=1,000; Revell 2012).

Life history and geographic provenance are highly correlated in the Mediterranean grasslands of California, with most perennial grasses being native and most annual grasses being

exotic (D'Antonio et al. 2007; Table 2.1), so, in these grasslands, nitrogen supply acts as an important filter not only for perennials vs. annuals, but also for natives vs. exotics. Like annuals, exotic grasses have been shown to be worse competitors for soil resources, and their populations can benefit from increased resource availability (Seabloom et al. 2003; Corbin and D'Antonio 2004). Thus, experimental simulation of habitat filtering by nitrogen supply could filter on host provenance instead of host life history. To test whether our conclusions were robust to alternate filtering criteria, we re-ran all analyses using provenance instead of life history to partition the dataset into completely filtered (exotics at high nitrogen and natives at low nitrogen), or unfiltered (exotics at low nitrogen and natives at high nitrogen) scenarios (Welsh et al. 2016).

Results

The strength of the LES increased with the completeness of habitat filtering. In the unfiltered scenario (perennials at high nitrogen and annuals at low nitrogen), the first axis in a principal components analysis of host traits (PC1) explained only 39.5% of the trait variation, and two traits, LMA and leaf emergence rate, were correlated with PC1 in directions opposite the LES (Table 2.4). The strength of the LES increased in the semi-filtered scenario, where PC1 explained more (45.9%) of the variation and all traits were correlated with PC1 in the directions of the LES (Table 2.4). The LES was strongest in the completely filtered scenario (perennials at low nitrogen and annuals at high nitrogen): PC1 captured 59.4% of the variation in traits across individuals, and trait correlations with PC1 strengthened and remained in the directions of the LES (Table 2.4). All traits were significantly plastic in response to nitrogen supply, and the effects of nitrogen on traits did not differ by host life history (annual/perennial). Except for LMA, traits responded to increased nitrogen supply by becoming more quick-return (Table 2.3b).

Trait-based models of host susceptibility to pathogen infection were most accurate when the LES was most strongly supported, in the completely filtered scenario. Under complete filtering, PC1 predicted host susceptibility with 77.5% accuracy (Table 2.5), and host susceptibility increased from slow to quick return along the LES (Fig. 2.3; Table 2.6). Specifically, the odds of infection increased 248-fold along the range of PC1, reflecting an increase in the probability of infection from 0.05 at the slow-return extreme of the LES to 0.93 at the quick-return extreme (Fig. 2.3; Table 2.6). In the semi-filtered and unfiltered scenarios, PC1 was a worse predictor of susceptibility and model accuracy decreased by 10.6-11.4% (Table 2.5), though the effect of PC1 was still significant in both cases (Table 2.6). Similarly, when all five host traits were used as independent variables, model accuracy decreased from 80.4% to 74.5% to 69.8% across the completely filtered, semi-filtered, and unfiltered scenarios (Table 2.5). The null accuracy of a binomial model is 50%, with a maximum of 100%, so these differences in model accuracy among filtering scenarios span 39% of the possible range in accuracy.

To mechanistically explore how filtering scenario influenced model performance, we calculated the relative variable importance of individual traits when raw trait values were used as predictors. Relative variable importance quantifies the influence of each trait on susceptibility by comparing the effect of each trait on Akaike weights across all possible models. The most influential traits varied by filtering scenario. In the completely filtered scenario, positive effects of tissue nitrogen concentration and leaf emergence rate were most important in explaining variation in susceptibility (Fig. 2.4a; Table 2.7a). In the semi-filtered scenario, a negative effect of LMA and a positive effect of leaf emergence rate were most important (Fig. 2.4b; Table 2.7b). In the unfiltered scenario, negative effects of LMA and tissue nitrogen concentration were most important (Fig. 2.4c; Table 2.7c). In all filtering scenarios, several models competed for lowest

AICc (best model) when raw trait values were used as predictors, and a single best model of susceptibility could not be unambiguously identified (Table 2.7).

Because shared evolutionary history can confound analyses including multiple species, we tested for a phylogenetic signal in the residuals of the two most accurate trait-based models of susceptibility: the LES-based model and the AIC-best raw traits model in the completely filtered scenario. In both cases, we found no indication of phylogenetic signal (LES-based model: Blomberg's K= 0.267, P= 0.799; raw traits model: K=0.242, P=0.820; Fig. 2.2; Pearse and Purvis 2013), indicating that the strongest observed relationships between susceptibility and traits were not driven by phylogeny.

In California grasslands, life history (annual/perennial) and provenance (exotic/native) are strongly associated (Table 2.1; D'Antonio et al. 2007). To examine the robustness of our results, we re-ran our analyses using provenance instead of life history as the filtering criterion in the unfiltered and completely filtered scenarios (the semi-filtered scenario is the same for provenance and life history). All results were qualitatively similar (Tables 2.8-2.10).

Discussion

Our results suggest that habitat filtering is one of the primary processes responsible for leaf trait covariation along the LES. The LES was strongest and captured both inter- and intraspecific variation in traits when individuals were grown in a completely filtered scenario, in the resource conditions they typically inhabit in the field. The strength of the LES decreased as individuals were grown in increasingly unfiltered scenarios, in increasingly dissimilar resource environments to that which they inhabit. This suggests that the LES breaks down as habitat filtering weakens, and that a lack of filtering or semi-filtering can reveal the potential for trait variation that is rarely observed in the field. In our data, plasticity in response to novel nitrogen

environments contributed to the weakening of the LES in less-filtered scenarios, and the magnitude of this plasticity was similar in annuals and perennials (Table 2.3b). As such, trait plasticity in both life histories, and not an idiosyncratic response of either one, caused the strength of the LES to decline in the unfiltered and semi-filtered scenarios. Communities may be essentially unfiltered by the current environment following rapid environmental change (Smith et al. 2009; Jackson and Sax 2010), and communities may be semi-filtered in the absence of biotic interactions, particularly resource competition, or when there is little variation in environmental conditions or traits (Funk and Cornwell 2013; Harpole et al. 2006). Since our observed trait data spanned 28% of the global range in trait values (vs. Wright et al. 2004), and our experimental conditions spanned most of the global range in nitrogen supply, our semi-filtered scenario may chiefly represent a lack of competitive interactions.

In the completely filtered scenario, grass host position along the LES predicted susceptibility to pathogen infection across 138 individuals of 23 host species with 77.5% accuracy, and individuals that were more quick-return were more susceptible. When the axis of trait covariation was less representative of the LES, in the semi-filtered and unfiltered scenarios, the trait axis was a less accurate predictor of host susceptibility. Models became increasingly inaccurate as filtering weakened regardless of whether a trait axis or raw trait values were used to predict infection. While the trait axes captured less trait variation in the semi-filtered and unfiltered scenarios, models using all traits and trait information also became less accurate. As such, the decreased power of trait-based models in increasingly unfiltered scenarios is likely due to a decoupling of the traits that effect host-pathogen and host-vector interactions.

Specifically, variation in host susceptibility along the LES may be influenced primarily by variation in host tissue nitrogen, leaf emergence rate, and photosynthetic rate. In the

completely filtered scenario, when the trait axis represented the LES and best predicted susceptibility, positive effects of these three traits were most important in explaining variation in susceptibility. The direction and identity of these effects is in accordance with the mechanisms through which host position along the LES was expected to influence host-vector and host-pathogen interactions: vectors may prefer more nutritious hosts, and fast-growing hosts may invest less in defense against vectors and pathogens (Kursar and Coley 2003; Mattson 1980; Wright et al. 2010; Todesco et al. 2010). Moving from the filtered to the semi-filtered or unfiltered scenarios, trait axes became increasingly misrepresentative of the LES and worse predictors of susceptibility. Accordingly, the directions of specific trait effects on susceptibility became increasingly misaligned with potential mechanisms. In the unfiltered scenario, a negative effect of LMA on susceptibility is in agreement with one mechanism, that vector feeding could be mechanically limited on high LMA leaves, but other trait effects contradict potential mechanisms. Negative effects of tissue nitrogen and photosynthetic capacity go against the expectation of vector preference for nutritious hosts, and greater vector and viral colonization of fast-growing, poorly defended hosts. This suggests that host susceptibility responds to variation in multiple host traits, which is further supported by the fact that several models competed for the AIC-best model of susceptibility when specific traits were used as predictors. In many plant pathogen systems, variation in susceptibility can be driven by multiple traits (e.g., Poland et al. 2009); our results further indicate that the directions of such effects are most aligned with potential mechanisms when traits covary along the LES.

By altering trait covariance structure, the history and extent of habitat filtering in a system can affect the predictive capacity of trait-based models of community or ecosystem processes. While this is a caveat to their application, the LES has been repeatedly observed in the

field, at scales from communities to the globe (Wright et al. 2004; Leishman et al. 2007; Reich et al. 1999; Diaz et al. 2004), consistent with the ideas that semi-filtered or unfiltered states are typically limited to smaller spatial scales, or are ephemeral. In this respect, our results strongly support increased exploration of trait-based approaches to ecological epidemiology, particularly those that utilize broad axes of trait covariation. The conditions in which the LES is supported encompass many of the settings in which there is great interest in predicting pathogen dynamics. Trait-based estimates of host susceptibility, a chief component of host competence (Cronin et al. 2010; Johnson et al. 2012), could be powerful and efficient replacements of estimates from laboratory inoculations, which are often laborious and sometimes infeasible. Host position along the LES could also be used to predict and target the communities, species, populations, or individuals most likely to harbor disease. Trait data are accumulating much more rapidly than epidemiological data: traits are often easier to measure, and several current models of ecosystem function are informed by traits, so there is continued motivation to expand existing trait data sets.

In addition to being a key component of host competence, host susceptibility is a crucial parameter in dynamic models of pathogen transmission, emergence, and persistence (Keeling and Rohani 2008). If broad axes of host trait covariation can inform such models, we may be able to move beyond post-hoc understandings of outbreaks and epidemics, using these axes to predict increases or decreases in pathogen transmission in response to variation in host community composition and diversity. Towards predicting the directional response of pathogen transmission to environmental change, the LES offers a means of synthesizing disease models with models of plant community turnover along abiotic gradients. At community to biome scales, where the LES is strongly supported, productive areas tend to be dominated by quick-return strategies (Diaz et al. 2004; Poorter and Bongers 2006; Leishman et al. 2007). In trait-

based models of resource competition, quick-returns are relatively poor competitors for below-ground resources (Craine et al. 2002; Harpole et al. 2006), and their relative abundance increases with both experimental addition of nitrogen or phosphorus (Laliberte et al. 2012; Lan and Bai 2012), and increasing rates of atmospheric nitrogen deposition (Stevens et al. 2004). Increased resource availability is a primary driver of global change. Our results predict that as communities become increasingly quick-return dominated they will also become increasingly susceptible, and may therefore be more likely to experience epidemics or harbor pathogens.

Similar to the LES, variation in the functional strategy of animals can be represented by the pace-of-life continuum, an axis of physiological and life-history trait covariation that runs from slow- to fast-living strategies (Dobson and Oli 2007). Parallel to our results, recent studies have demonstrated that fast-living animal hosts may be more susceptible and more likely to harbor pathogens (Han et al. 2015; Johnson et al. 2012). As in plants, pace-of-life traits can respond plastically to variation in nutrition (Taborsky 2006) and influence extinction risk along abiotic gradients (Olden et al. 2008). In this respect, plant systems offer an experimentally tractable model for testing the robustness of axes of functional strategy, and whether genetic and plastic variation along these axes determines variation in competence among individuals and transmission among communities. In the context of laboratory or mesocosm studies of trait-driven variation in competence, our results also highlight the importance of considering the environments in which traits are expressed. If experimental conditions differ from the field, hosts may display rarely-seen trait combinations and observed effects on host-pathogen interactions could be of limited applicability.

In summary, our results suggest that 1) habitat filtering plays a key role in generating the LES, a global axis of plant trait covariation, 2) a lack of filtering decreases the performance of

trait-based models, specifically the ability of the LES to predict susceptibility to pathogen infection. This information might be used, in combination with trait-based models of community turnover, to understand pathogen response to environmental change. Specifically, when filtering has already occurred, individual position along the LES can predict host susceptibility to generalist pathogen infection. When the environment changes, individuals and species will be filtered by their traits, but this process takes time. During the process, trait-based models of community or ecosystem function could be less accurate. Given time for filtering to occur, there is mounting evidence that similar environments harbor similar traits and functional compositions (Laliberte et al. 2012; Baraloto et al. 2012; Diaz et al. 2004; Leishman et al. 2007; Poorter and Bongers 2006), but not necessarily similar species (Laliberte et al. 2012). Predicting the identity of host species that will increase in response to environmental change may require species-specific knowledge, but predicting the traits of host communities and resulting pathogen transmission may not.

Data Accessibility

Data deposited in the Dryad repository: http://datadryad.org/resource/doi:10.5061/dryad.356v3

Table 2.1. Host identities, life history (A=annual, P=perennial), provenance (E=exotic, N=native), and seed source.

Host Species	Life History	Provenance	Seed Source
Aegilops triuncialis L.	A	E	Field collected: Basket Butte, OR, USA
Aira caryophyllea L.	A	E	Field collected: Basket Butte, OR, USA
Arrhenatherum elatius (L.) P. Beauv. ex J. Presl & C. Presl	P	E	Field collected: Basket Butte, OR, USA
Avena barbata Pott ex Link	A	E	Field collected: Hopland, CA, USA
Avena fatua L.	A	E	Azlin Seed Service, Leland, MS, USA
Briza maxima L.	A	E	Field collected: Basket Butte, OR, USA
Bromus carinatus Hook. & Arn.	P	N	Field collected: Basket Butte, OR, USA
Bromus diandrus Roth	A	E	Field collected: Basket Butte, OR, USA
Bromus hordeaceus L.	A	E	Field collected: Basket Butte, OR, USA
Cynosurus echinatus L.	A	E	Field collected: Basket Butte, OR, USA
Elymus glaucus Buckley	P	N	Field collected: Basket Butte, OR, USA
Elymus multisetus M.E. Jones	P	N	Field collected: Basket Butte, OR, USA
Koeleria macrantha (Ledeb.) Schult.	P	N	Field collected: Basket Butte, OR, USA
Lolium multiflorum Lam.	A	E	Field collected: Basket Butte, OR, USA
Melica californica Scribn.	P	N	Hedgerow Farms, Winters, CA, USA
Nassella lepida (Hitchc.) Barkworth	P	N	Field collected: Basket Butte, OR, USA
Nassella pulchra (Hitchc.) Barkworth	P	N	Field collected: Basket Butte, OR, USA
Poa secunda J. Presl	P	N	Field collected: Basket Butte, OR, USA
Schedonorus arundinaceus (Schreb.) Dumort., nom. cons.	P	E	Field collected: Basket Butte, OR, USA
Taeniatherum caput-medusae (L.) Nevski	A	E	Field collected: Basket Butte, OR, USA
Vulpia microstachys (Nutt.) Munro	A	N	Field collected: Basket Butte, OR, USA
Vulpia myuros (L.) C.C. Gmel.	A	E	Field collected: Basket Butte, OR, USA
Avena sativa L. 'Coast Black'	A	E	National Small Grains Collection, Aberdeen, ID, USA

Table 2.2. Potting medium and nitrogen treatment. On a per area basis, nutrient and high nitrogen addition rates reflect those of the Nutrient Network, a world-wide fertilization experiment in grasslands (Borer et al., 2014).

Soil Component	Description	Ammount per Individual
Sand	Pasturized	0.5 L
LC1 Soil	Low-nutrient soil, SunGro Horticulture, Agawam, MA, USA	0.5 L
Phosphorous	Triple Phosphate, 45% P_2O_5, Espoma, NJ, USA	0.196 g
Potassium	Potash, 50% K_2O, Winston Weaver Co., Inc., NC, USA	0.093 g
Micronutrients	Micromax, Scotts, OH, USA	0.385 g
Nitrogen	>98% NH_4NO_3, Fisher Scientific, NY, USA	low N: 0.005 g *
		high N: 0.110 g *

* Applied in equal parts over 5 weeks and dissolved in 10mL H_20 per week

Table 2.3. (a) List of host traits, abbreviations, units, and measurement methods. Traits included three leaf traits and two metrics of growth rate. (b) The mean effect of nitrogen (N) supply on host trait values (N=274). N effect β and p-values are for linear regression coefficients and the Wald tests of those coefficients. Life history: N effect p-values are Wald tests of the life-history by nitrogen treatment interaction term. Except for LMA, traits were more quick-return at high nitrogen. The positive response of leaf emergence rate to nitrogen was marginally greater in annuals, but otherwise life histories responded similarly to the nitrogen supply treatment.

(a)					**(b)**	
Host Trait	Abbr	Units	Timing of Measurement(s)	Method	N Effect	Life History: N Effect
Maximum Photo-synthetic Capacity	Photo.	μmol/mg/s	~4 wks post-germination on youngest, fully expanded leaf	Maximum CO_2 flux: CIRAS-2 infrared gas analyzer, PP Systems, MA, US	β=1.106, p<0.001	p=0.767
Leaf Mass per Area	LMA	mg/cm^2	~4 wks post-germination on youngest, fully expanded leaf	Dry mass/scanned leaf section area: WinFOLIA, Regent Instruments, QC, CA	β=0.173, p=0.005	p=0.543
% Tissue Nitrogen	%N	100*mg/mg	~4 wks post-germination on youngest, fully expanded leaf	Combustion analysis: Duke Environmental Stable Isotope Laboratory, NC, US	β=1.572, p<0.001	p=0.340
Growth: leaf elongation rate	Lf. Elong	cm/day	~2 wks post-germination on 3rd-4th emergent leaf	length increase over 4 days	β=0.340, p=0.012	p=0.068
Growth: leaf emergence rate	Lf. Emerge	leaves/ day	~2 wks post-germination, beginning with 3rd-4th emergent leaf	Number of new leaves over 10 days	β=0.119, p<0.001	p=0.914

Table 2.4. Principal Components Analyses of host traits in three scenarios of habitat filtering by life history and nitrogen (N) supply. Trait abbreviations are as in Table 2.3. Loadings are for each trait onto principal component 1 (PC1). 'Corr.' is the correlation coefficient between each trait and PC1, -1 and 1 being perfect negative and positive correlations, respectively. The LES was most strongly supported in the completely filtered scenario.

Scenario	Variance Captured by PC1	Trait	Loading	Corr.
Completely Filtered: Annuals +N, Perennials -N (N=138)	59.4%	LMA	-0.438	-0.755
		Photo	0.523	0.901
		%N	0.524	0.903
		Lf. Elong	0.293	0.505
		Lf. Emerge	0.417	0.719
Semi-filtered: Annuals and Perennials, -N and +N (N=274)	45.9%	LMA	-0.378	-0.572
		Photo	0.584	0.884
		%N	0.515	0.781
		Lf. Elong	0.310	0.470
		Lf. Emerge	0.394	0.596
Unfiltered: Annuals -N, Perennials +N: (N=136)	35.9%	LMA	0.374	0.501
		Photo	0.453	0.607
		%N	0.667	0.887
		Lf. Elong	0.219	0.293
		Lf. Emerge	-0.412	-0.551

Table 2.5. Performance of logistic models of susceptibility with (a) PC1 or (b) all five traits in three scenarios of habitat filtering. PC1 is the first principal component axis in a principal components analysis of host traits. Sensitivity (True Negative Rate) and Specificity (True Positive Rate) give the proportion of correct model predictions of uninfected or infected hosts, respectively. Predictive Positive and Negative values give the proportion of predicted infections that were true infections, and the proportion of predicted healthy hosts that were actually uninfected. Average accuracy is the average across the four percentages of correct model predictions.

	Predictor (s)	Scenario	N	N Parameters	Sensitivity (TNR)	Specificity (TPR)	Predictive Value Positive	Predictive Value Negative	Average Accuracy
(a)	PC1	Completely Filtered	138	2	78.1%	76.9%	75.8%	79.2%	77.5%
	PC1	Semi-filtered	274	2	66.4%	65.7%	67.2%	65.0%	66.1%
	PC1	Unfiltered	136	2	67.2%	66.7%	71.4%	62.2%	66.9%
(b)	Traits	Completely Filtered	138	6	80.8%	80.0%	78.8%	81.9%	80.4%
	Traits	Semi-filtered	274	6	74.6%	74.3%	75.4%	73.5%	74.5%
	Traits	Unfiltered	136	6	70.5%	69.3%	74.3%	65.2%	69.8%

Table 2.6. Logistic regressions of host susceptibility on PC1, the first principal component axis in a principal components analysis of host traits, in the unfiltered (a), semi-filtered (b), and completely filtered (c) scenarios of habitat filtering by host life history and nitrogen supply. The binomial response is host infection upon exposure. In all cases, the likelihood ratio test indicated a significant improvement over a null modal. The Hosmer-Lemeshow tests indicated a significant lack of fit to the data in scenarios (a) and (c), but no lack of fit in scenario (b).

(a) *Unfiltered (N=136)*						
Predictor	β	SE β	Wald's X^2	*df*	*p*	e^{β} (odds ratio)
Constant	0.259	0.188	1.9	1	0.170	NA
PC1	-0.640	0.155	17.1	1	<0.001	0.527
Test			X^2	*df*	*p*	
Model Evaluation						
Liklihood ratio			20.3	1	<0.001	
Goodness-of-fit						
Hosmer and Lemeshow			17.0	4	0.002	
(b) Semi-filtered *(N=274)*						
Predictor	β	SE β	Wald's X^2	*df*	*p*	e^{β} (odds ratio)
Constant	0.052	0.129	0.2	1	0.680	NA
PC1	0.510	0.093	30.1	1	<0.001	1.665
Test			X^2	*df*	*p*	
Model Evaluation						
Liklihood ratio			34.9	1	<0.001	
Goodness-of-fit						
Hosmer and Lemeshow			8.7	7	0.274	
(c) Completely filtered (N=138)						
Predictor	β	SE β	Wald's X^2	*df*	*p*	e^{β} (odds ratio)
Constant	-0.19	0.205	0.9	1	0.35	NA
PC1	0.783	0.139	32	1	<0.001	2.189
Test			X2	df	p	
Model Evaluation						
Liklihood ratio			44.3	1	<0.001	
Goodness-of-fit						
Hosmer and Lemeshow			10.2	4	0.037	

Table 2.7. AICc model selection tables used to calculate the relative variable importance of specific host traits in (a) the completely filtered scenario, (b) the semi-filtered scenario, and (c) the unfiltered scenario, using host life history as a filtering criteria. Host traits are: leaf emergence rate (Lf. Emerge), leaf elongation rate (Lf. Long), leaf mass per area (LMA), mass-based photosynthetic capacity (Photo), and percent tissue nitrogen (%N). In all scenarios, the global model was a significant improvement over a null model (filtered: Likelihood ratio χ^2=47.9, df=5, p<0.001; semi-filtered: χ^2=59.6, df=5, p<0.001; unfiltered: χ^2=37.7, df=5, p<0.001). A Hosmer and Lemeshow test suggested a marginal lack of fit to the data in the filtered scenario (χ^2=7.4, df=4, p=0.061), a significant lack of fit in the semi-filtered scenario (χ^2=10.3, df=4, p=0.036), and no lack of fit in the unfiltered scenario (χ^2=2.7, df=4, p=0.61).

(a) Intercept	Lf. Emerge	Lf. Elong	LMA	Photo	%N	df	logLik	AICc	delta	weight
-4.376	1.302	NA	NA	NA	0.858	3	-72.490	151.158	0.000	0.161
-4.991	1.254	NA	NA	0.275	0.597	4	-71.684	151.668	0.510	0.125
-4.268	NA	NA	NA	NA	1.028	2	-74.089	152.266	1.108	0.092
-4.921	NA	NA	NA	0.293	0.742	3	-73.152	152.484	1.325	0.083
-2.799	1.241	NA	-0.444	NA	0.773	4	-72.172	152.645	1.487	0.076
-4.273	1.398	-0.098	NA	NA	0.881	4	-72.346	152.992	1.834	0.064
-2.334	NA	NA	-0.548	NA	0.914	3	-73.584	153.348	2.190	0.054
-4.893	1.345	-0.107	NA	0.283	0.615	5	-71.508	153.470	2.312	0.051
-4.282	1.235	NA	-0.180	0.246	0.589	5	-71.641	153.736	2.578	0.044
-4.883	1.719	NA	NA	0.608	NA	3	-73.958	154.094	2.936	0.037
-4.238	NA	-0.025	NA	NA	1.037	3	-74.078	154.336	3.177	0.033
-3.821	NA	NA	-0.281	0.246	0.729	4	-73.045	154.391	3.233	0.032
-4.878	NA	-0.047	NA	0.298	0.753	4	-73.117	154.535	3.377	0.030
-2.894	1.312	-0.070	-0.395	NA	0.798	5	-72.103	154.660	3.501	0.028
-2.331	NA	0.003	-0.550	NA	0.913	4	-73.584	155.469	4.311	0.019
-4.533	1.328	-0.100	-0.093	0.267	0.610	6	-71.497	155.635	4.477	0.017
-3.670	1.680	NA	-0.312	0.551	NA	4	-73.824	155.949	4.791	0.015
-4.828	1.772	-0.063	NA	0.621	NA	4	-73.892	156.085	4.927	0.014
-3.884	NA	-0.031	-0.257	0.253	0.737	5	-73.031	156.517	5.358	0.011
-3.776	1.721	-0.044	-0.274	0.567	NA	5	-73.794	158.043	6.885	0.005
-4.759	NA	NA	NA	0.759	NA	2	-77.041	158.171	7.013	0.005
-2.980	NA	NA	-0.456	0.670	NA	3	-76.744	159.667	8.509	0.002
-4.790	NA	0.031	NA	0.751	NA	3	-77.025	160.228	9.070	0.002
-2.891	NA	0.056	-0.494	0.647	NA	4	-76.691	161.684	10.525	0.001
2.302	2.271	NA	-1.404	NA	NA	3	-78.635	163.449	12.291	0.000
2.147	2.097	0.137	-1.440	NA	NA	4	-78.303	164.906	13.748	0.000
-1.862	2.947	NA	NA	NA	NA	2	-83.060	170.210	19.051	0.000
-2.063	2.818	0.108	NA	NA	NA	3	-82.849	171.876	20.718	0.000
4.365	NA	0.293	-1.945	NA	NA	3	-83.009	172.196	21.038	0.000
5.161	NA	NA	-1.957	NA	NA	2	-84.777	173.644	22.485	0.000
-0.947	NA	0.322	NA	NA	NA	2	-92.975	190.038	38.880	0.000
-0.116	NA	NA	NA	NA	NA	1	-95.422	192.874	41.716	0.000

(b)

Intercept	Lf. Emerge	Lf. Elong	LMA	Photo	%N	df	logLik	AICc	delta	weight
3.808	1.212	NA	-1.654	NA	NA	3	-161.037	328.163	0.000	0.218
3.560	1.108	0.143	-1.678	NA	NA	4	-160.340	328.829	0.666	0.156
2.893	1.150	NA	-1.535	0.104	NA	4	-160.587	329.323	1.160	0.122
3.402	1.102	NA	-1.645	NA	0.115	4	-160.603	329.356	1.193	0.120
3.281	1.036	0.125	-1.669	NA	0.089	5	-160.095	330.413	2.250	0.071
2.954	1.083	0.120	-1.590	0.073	NA	5	-160.134	330.493	2.330	0.068
3.044	1.117	NA	-1.578	0.063	0.061	5	-160.538	331.300	3.137	0.045
4.704	NA	0.189	-1.916	NA	NA	3	-162.864	331.818	3.655	0.035
4.371	NA	NA	-1.866	NA	0.178	3	-163.046	332.180	4.017	0.029
5.196	NA	NA	-1.917	NA	NA	2	-164.160	332.365	4.202	0.027
3.115	1.046	0.121	-1.636	0.030	0.064	6	-160.081	332.476	4.313	0.025
4.145	NA	0.157	-1.878	NA	0.140	4	-162.216	332.581	4.418	0.024
3.900	NA	NA	-1.741	0.136	NA	3	-163.363	332.815	4.652	0.021
3.910	NA	0.159	-1.797	0.092	NA	4	-162.537	333.223	5.060	0.017
4.203	NA	NA	-1.834	0.030	0.152	4	-163.030	334.208	6.045	0.011
4.214	NA	0.158	-1.892	-0.013	0.151	5	-162.214	334.651	6.488	0.009
-2.736	1.872	NA	NA	0.475	-0.289	4	-171.384	350.916	22.753	0.000
-2.756	1.786	NA	NA	0.301	NA	3	-172.821	351.731	23.568	0.000
-2.771	1.861	0.034	NA	0.470	-0.293	5	-171.344	352.912	24.749	0.000
-2.775	1.780	0.018	NA	0.297	NA	4	-172.810	353.770	25.607	0.000
-1.149	2.162	NA	NA	NA	NA	2	-177.584	359.213	31.050	0.000
-1.548	2.035	NA	NA	NA	0.121	3	-177.041	360.171	32.008	0.000
-1.375	2.092	0.104	NA	NA	NA	3	-177.187	360.463	32.300	0.000
-1.659	2.000	0.080	NA	NA	0.103	4	-176.821	361.790	33.627	0.000
-2.334	NA	NA	NA	0.395	NA	2	-180.514	365.072	36.909	0.000
-2.306	NA	NA	NA	0.530	-0.218	3	-179.635	365.359	37.196	0.000
-2.409	NA	0.066	NA	0.380	NA	3	-180.353	366.795	38.632	0.000
-2.397	NA	0.081	NA	0.518	-0.229	4	-179.398	366.944	38.781	0.000
-0.914	NA	NA	NA	NA	0.249	2	-187.210	378.464	50.301	0.000
-1.126	NA	0.138	NA	NA	0.214	3	-186.479	379.047	50.884	0.000
-0.448	NA	0.193	NA	NA	NA	2	-188.279	380.603	52.440	0.000
0.044	NA	NA	NA	NA	NA	1	-189.857	381.728	53.565	0.000

(c)

Intercept	Lf. Emerge	Lf. Elong	LMA	Photo	%N	df	logLik	AICc	delta	weight
6.703	NA	NA	-1.605	NA	-0.580	3	-75.140	156.462	0.000	0.273
8.595	NA	NA	-2.200	-0.410	NA	3	-76.041	158.264	1.802	0.111
7.261	-0.441	NA	-1.696	NA	-0.601	4	-75.002	158.309	1.847	0.108
6.465	NA	0.096	-1.591	NA	-0.592	4	-75.008	158.322	1.860	0.108
7.366	NA	NA	-1.743	-0.115	-0.472	4	-75.053	158.412	1.950	0.103
8.413	NA	0.136	-2.211	-0.433	NA	4	-75.782	159.869	3.408	0.050
9.354	-0.497	NA	-2.332	-0.432	NA	4	-75.866	160.037	3.575	0.046
7.262	NA	0.115	-1.765	-0.146	-0.456	5	-74.872	160.205	3.743	0.042
7.016	-0.432	0.094	-1.681	NA	-0.612	5	-74.874	160.210	3.748	0.042
8.151	-0.507	NA	-1.879	-0.139	-0.473	5	-74.876	160.214	3.752	0.042
5.271	NA	NA	-1.886	NA	NA	2	-78.742	161.575	5.113	0.021
9.187	-0.507	0.138	-2.346	-0.456	NA	5	-75.599	161.660	5.198	0.020
8.058	-0.513	0.117	-1.903	-0.172	-0.456	6	-74.689	162.029	5.567	0.017
5.132	NA	0.053	-1.886	NA	NA	3	-78.699	163.579	7.117	0.008
5.340	-0.063	NA	-1.899	NA	NA	3	-78.739	163.660	7.199	0.007
5.195	-0.056	0.053	-1.897	NA	NA	4	-78.696	165.697	9.236	0.003
1.821	NA	NA	NA	0.489	-1.216	3	-81.332	168.846	12.384	0.001
1.386	0.634	NA	NA	0.470	-1.157	4	-80.968	170.242	13.780	0.000
1.741	NA	0.064	NA	0.476	-1.216	4	-81.274	170.853	14.392	0.000
1.300	0.635	0.066	NA	0.457	-1.157	5	-80.906	172.274	15.812	0.000
3.403	NA	NA	NA	NA	-0.853	2	-84.190	172.471	16.009	0.000
2.759	0.855	NA	NA	NA	-0.799	3	-83.515	173.211	16.749	0.000
3.148	NA	0.140	NA	NA	-0.877	3	-83.895	173.972	17.510	0.000
2.519	0.837	0.136	NA	NA	-0.823	4	-83.240	174.786	18.324	0.000
-0.532	1.423	NA	NA	NA	NA	2	-91.332	186.754	30.292	0.000
-0.001	1.417	NA	NA	-0.088	NA	3	-91.169	188.520	32.058	0.000
-0.636	1.424	0.041	NA	NA	NA	3	-91.303	188.787	32.325	0.000
0.207	NA	NA	NA	NA	NA	1	-93.546	189.122	32.660	0.000
-0.094	1.415	0.061	NA	-0.098	NA	4	-91.108	190.521	34.060	0.000
0.781	NA	NA	NA	-0.096	NA	2	-93.342	190.775	34.313	0.000
0.116	NA	0.036	NA	NA	NA	2	-93.523	191.136	34.675	0.000
0.695	NA	0.059	NA	-0.106	NA	3	-93.283	192.749	36.287	0.000

Table 2.8. Principal components analyses of host traits in two scenarios of habitat filtering by provenance and nitrogen (N) supply. Loadings are for each trait onto principal component 1 (PC1), and the last column gives the bivariate correlations of each trait with PC1. The LES was most strongly supported in the filtered scenario. Note that the semi-filtered scenario would be the same as that of Table 2.4.

Scenario	Variance Captured by PC1	Trait	Loading	Corr.
Completely Filtered: Exotics +N, Natives -N: (N=138)	56.4%	LMA	-0.436	0.732
		Photo	0.530	0.889
		%N	0.512	0.859
		Lf. Elong	0.303	0.510
		Lf. Emerge	0.419	0.703
Unfiltered: Exotics -N, Natives +N: (N=136)	35.5%	LMA	-0.077	0.105
		Photo	0.698	0.931
		%N	0.654	0.872
		Lf. Elong	0.279	0.371
		Lf. Emerge	0.024	0.032

Table 2.9. Logistic regressions of host susceptibility on PC1, the first principal component axis in a principal components analysis of host traits, in two scenarios of habitat filtering by host provenance and nitrogen supply: (a) completely filtered, and (b) unfiltered. In both cases, the likelihood ratio test indicated a significant improvement over a null modal, but the Hosmer-Lemeshow test indicated a significant lack of fit to the data. Note that the semi-filtered scenario would be the same as that of Table 2.6.

(a) Completely Filtered (N=138)

Predictor	β	SE β	Wald's X^2	*df*	*p*	e^{β} (odds ratio)
Constant	-0.174	0.197	0.78	1	*0.380*	NA
PC1	0.711	0.137	26.8	1	<0.001	2.036
Test			X^2	*df*	*p*	
Model Evaluation						
Liklihood ratio			35.8	1	<0.001	
Goodness-of-fit						
Hosmer and Lemeshow			10.2	4	0.037	

(b) Unfiltered (N=136)

Predictor	β	SE β	Wald's X^2	*df*	*p*	e^{β} (odds ratio)
Constant	0.207	0.172	1.4	1	*0.230*	NA
PC1	0.041	0.13	0.098	1	0.75	NA
Test			X^2	*df*	*p*	
Model Evaluation						
Liklihood ratio			0.1	1	0.754	
Goodness-of-fit						
Hosmer and Lemeshow			11.7	5	0.039	

Table 2.10. Performance of trait-based models of susceptibility with (a) PC1 or (b) specific traits in two scenarios of habitat filtering by host provenance and nitrogen supply. PC1 is the first principal component axis in a principal components analysis of host traits. Sensitivity (True Negative Rate) and Specificity (True Positive Rate) give the proportion of correct model predictions of uninfected or infected hosts, respectfully. Predictive Positive and Negative values give the proportion of predicted infections that were true infections, and the proportion of predicted healthy hosts that were actually uninfected. Average accuracy is the average across the four percentages of correct model predictions. Note that the semi-filtered scenario would be the same as that of Table 2.5.

	Predictor (s)	Scenario	N	N Parameters	Sensitivity (TNR)	Specificity (TPR)	Predictive Value Positive	Predictive Value Negative	Average Accuracy
(a)	PC1	Completely Filtered	138	2	76.7%	75.4%	74.2%	77.8%	76.0%
	PC1	Unfiltered	136	2	50.8%	49.3%	55.2%	44.9%	50.1%
(b)	Traits	Completely Filtered	138	6	78.1%	76.9%	75.8%	79.2%	77.5%
	Traits	Unfiltered	136	6	70.5%	69.3%	74.3%	65.2%	69.8%

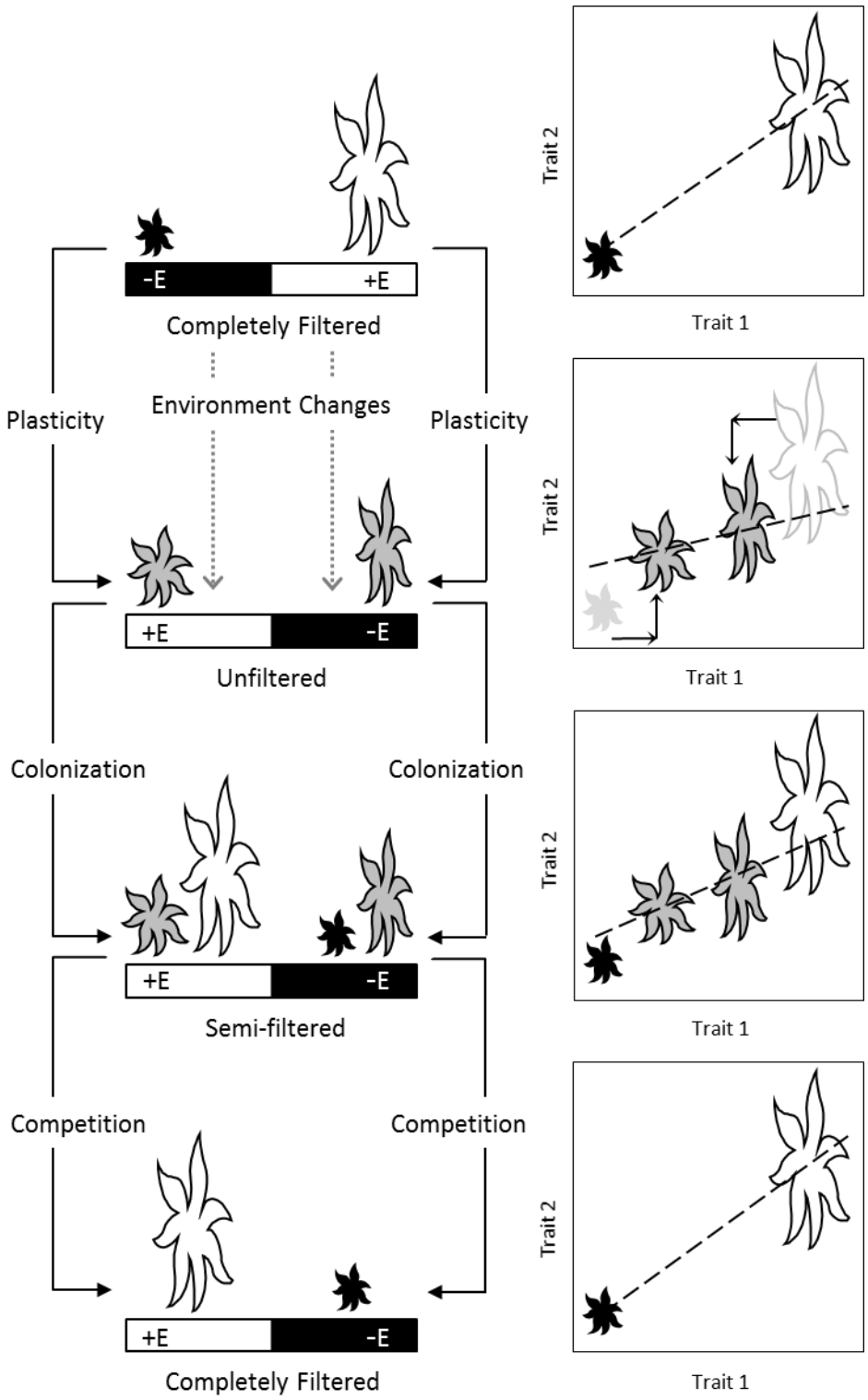

Figure 2.1. Hypothesized effects of habitat filtering on the strength of the Leaf Economics Spectrum (LES). Following changes in the abiotic environment (from –E to +E and vice versa), filtering may proceed from an original state to an unfiltered, semi-filtered, and then completely filtered community (left column from top to bottom). Initially, the original communities respond plastically to novel environmental conditions. The communities become semi-filtered as species

colonize the environments in which they are most fit, and completely filtered as competitive exclusion removes unfit species. More complete habitat filtering is hypothesized to strengthen the trait covariation that comprises the LES (right column, illustrated in two dimensions for simplicity).

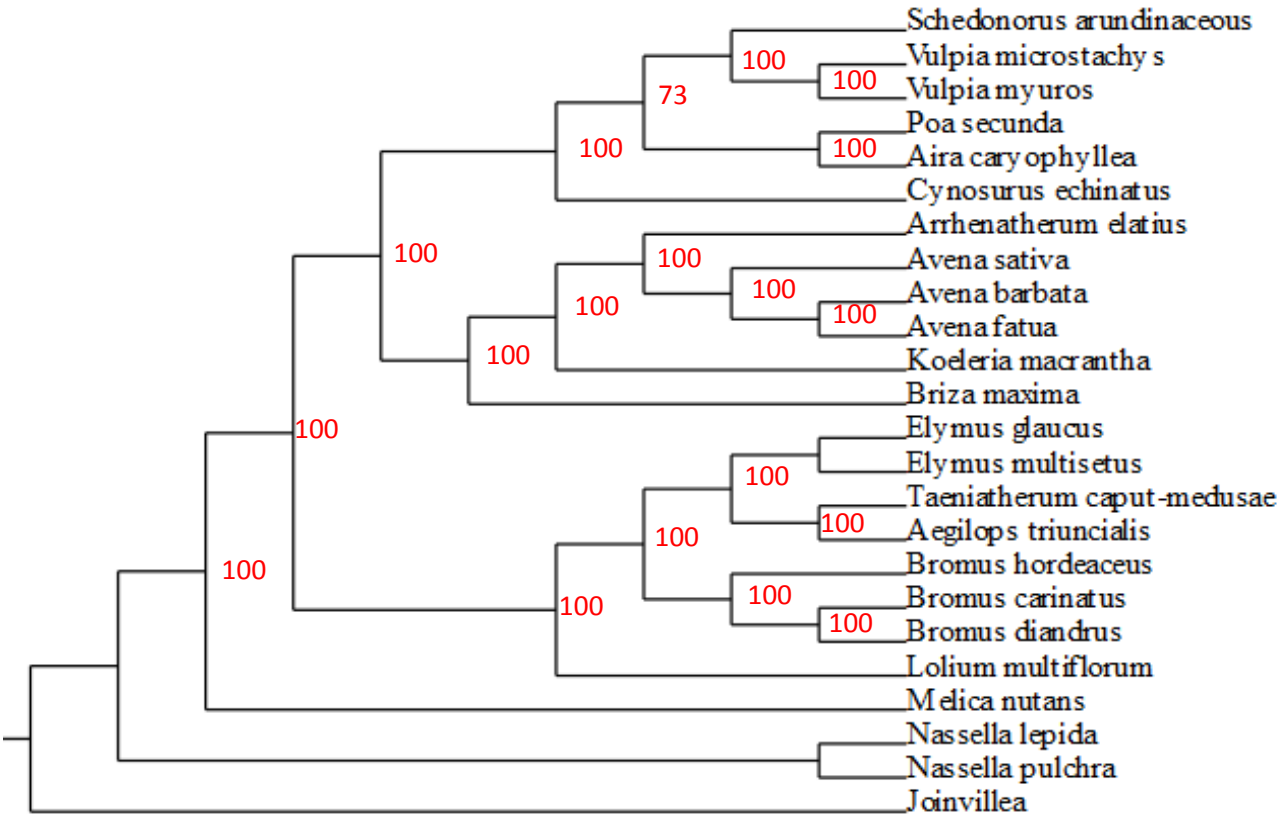

Figure 2.2. Phylogeny used in the phylogenetic analyses. Node labels indicate bootstrap support. Created using phyloGenerator (Pearse and Purvis, 2013) with options '-gene *rbcL*, *matK* –alignment muscle –phylogen RAxML –integrated Bootstrap 1000', and constraint tree topology following Bouchenak-Khelladi et al. (2008). Sequence data was not available for *Elymus multisetus*, *Nassella pulchra*, and *Melica californica*, so polytomies were created for *Elymus* and *Nassella*, and *Melica californica* was replaced with the congener *Melica nutans*. Joinvillea (monocot, Joinvilleaceae) was used as an outgroup.

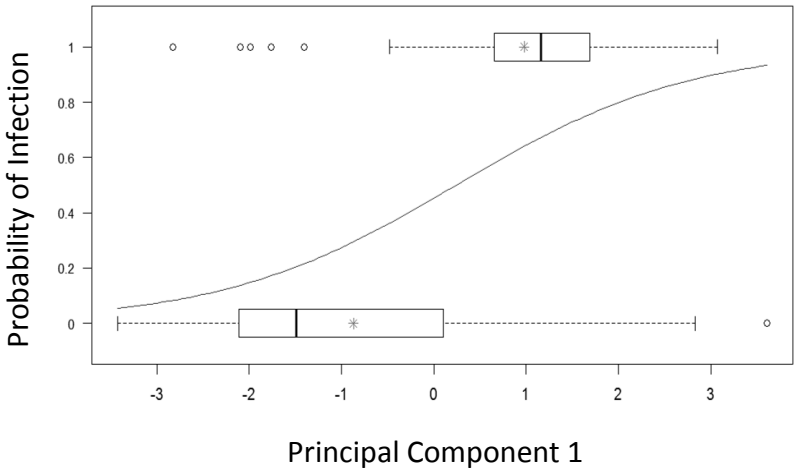

Figure 2.3. In the completely filtered scenario, the predicted probability of host infection (curved gray line) increased with host principal component 1 (PC1) score, which gives host position along the LES and increases from slow- to quick-return (β=0.783, $p<0.001$, N=138; Table 2.6). Box and whisker diagrams represent the observed distribution of PC1 scores in each infection category (0=uninfected, 1=infected): means (black bars), medians (gray asterisks), first quartiles (box edges), and third quartiles (whisker edges).

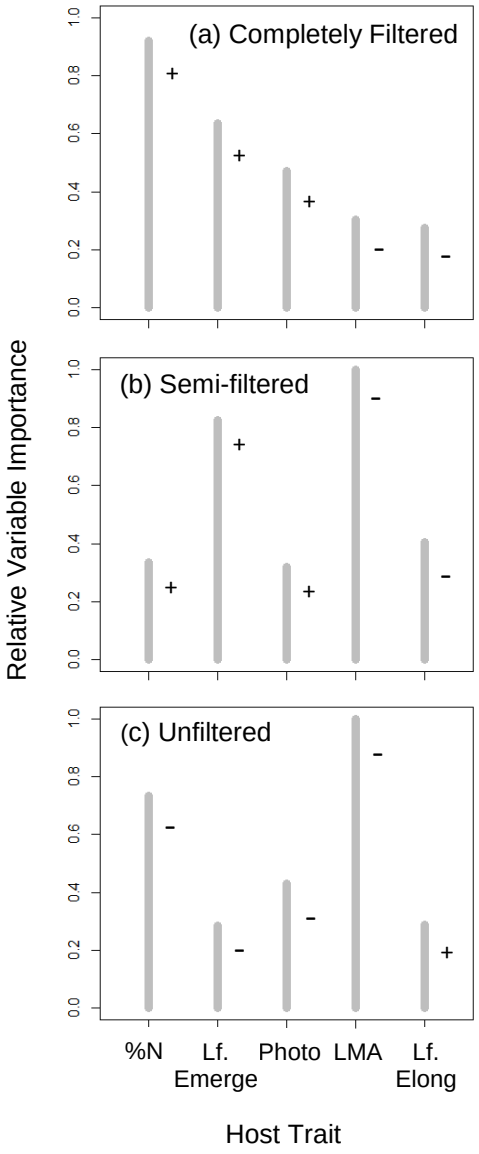

Figure 2.4. Relative Variable Importance of each host trait in models of host susceptibility across three scenarios of habitat filtering by host life history and nitrogen supply. Symbols indicate the direction of trait effects in the global model. Trait abbreviations are as in Table 2.3.

REFERENCES

Albert, C. H., Thuiller, W., Yoccoz, N. G., Douzet, R., Aubert, S. & Lavorel, S. (2010) A multi-trait approach reveals the structure and the relative importance of intra- vs. interspecific variability in plant traits. *Functional Ecology,* **24,** 1192-1201.

Baraloto, C., Hardy, O. J., Paine, C. E. T., Dexter, K. G., Cruaud, C., Dunning, L. T., Gonzalez, M. A., Molino, J. F., Sabatier, D., Savolainen, V. & Chave, J. (2012) Using functional traits and phylogenetic trees to examine the assembly of tropical tree communities. *Journal of Ecology,* **100,** 690-701.

Barton, K. (2015) MuMIn: Multi-Model Inference. R package version 1.15.1. http://CRAN.R-project.org/package=MuMIn.

Blomberg, S. P., Garland, T., Jr. & Ives, A. R. (2003) Testing for Phylogenetic Signal in Comparative Data: Behavioral Traits Are More Labile. *Evolution,* **57,** 717-745.

Borer, E. T., Harpole, W. S., Adler, P. B., Lind, E. M., Orrock, J. L., Seabloom, E. W. & Smith, M. D. (2014) Finding generality in ecology: a model for globally distributed experiments. *Methods in Ecology and Evolution,* **5,** 65-73.

Borer, E. T., Seabloom, E. W., Mitchell, C. E. & Power, A. G. (2010) Local context drives infection of grasses by vector-borne generalist viruses. *Ecology Letters,* **13,** 810-818.

Bouchenak-Khelladi, Y., Salamin, N., Savolainen, V., Forest, F., Bank, M., Chase, M. W. & Hodkinson, T. R. (2008) Large multi-gene phylogenetic trees of the grasses (Poaceae): progress towards complete tribal and generic level sampling. *Mol Phylogenet Evol,* **47,** 488-505.

Burnham, K. P. & Anderson, D. R. (2002) *Model Selection and Multimodel Inference: A Practical Information-Theoretic Approach.* Springer-Verlag, New York.

Clark, J. S. (2010) Individuals and the Variation Needed for High Species Diversity in Forest Trees. *Science,* **327,** 1129-1132.

Corbin, J. D. & D'Antonio, C. M. (2004) Competition between native perennial and exotic annual grasses: Implications for an historical invasion. *Ecology,* **85,** 1273-1283.

Craine, J. M., Tilman, D., Wedin, D., Reich, P., Tjoelker, M. & Knops, J. (2002) Functional traits, productivity and effects on nitrogen cycling of 33 grassland species. *Functional Ecology,* **16,** 563-574.

Cronin, J. P., Rúa, M. A. & Mitchell, C. E. (2014) Why is living fast dangerous? Disentangling the roles of resistance and tolerance of disease. *The American Naturalist,* **184,** 172-187.

Cronin, J. P., Welsh, M. E., Dekkers, M. G., Abercrombie, S. T. & Mitchell, C. E. (2010) Host physiological phenotype explains pathogen reservoir potential. *Ecology Letters,* **13,** 1221-1232.

D'Antonio, C., Malmstrom, C. M., Reynolds, S. A. & Gerlach, J. (2007) Ecology of Invasive Non-native Species in California Grassland. *Ecology and Management of California Grasslands* (eds M. Stromberg, J. Corbin & C. D'Antonio), pp. 67-86. University of California Press, Berkeley.

Diaz, S., Hodgson, J. G., Thompson, K., Cabido, M., Cornelissen, J. H. C., Jalili, A., Montserrat-Marti, G., Grime, J. P., Zarrinkamar, F., Asri, Y., Band, S. R., Basconcelo, S., Castro-Diez, P., Funes, G., Hamzehee, B., Khoshnevi, M., Perez-Harguindeguy, N., Perez-Rontome, M. C., Shirvany, F. A., Vendramini, F., Yazdani, S., Abbas-Azimi, R., Bogaard, A., Boustani, S., Charles, M., Dehghan, M., de Torres-Espuny, L., Falczuk, V., Guerrero-Campo, J., Hynd, A., Jones, G., Kowsary, E., Kazemi-Saeed, F., Maestro-Martinez, M., Romo-Diez, A., Shaw, S., Siavash, B., Villar-Salvador, P. & Zak, M. R. (2004) The plant traits that drive ecosystems: Evidence from three continents. *Journal of Vegetation Science,* **15,** 295-304.

Dobson, F. S. & Oli, M. K. (2007) Fast and slow life histories of mammals. *Ecoscience,* **14,** 292-299.

Donovan, L. A., Maherali, H., Caruso, C. M., Huber, H. & de Kroon, H. (2011) The evolution of the worldwide leaf economics spectrum. *Trends in Ecology & Evolution,* **26,** 88-95.

Donovan, L. A., Mason, C. M., Bowsher, A. W., Goolsby, E. W. & Ishibashi, C. D. A. (2014) Ecological and evolutionary lability of plant traits affecting carbon and nutrient cycling. *Journal of Ecology,* **102,** 302-314.

Funk, J. L. & Cornwell, W. K. (2013) Leaf traits within communities: Context may affect the mapping of traits to function. *Ecology,* **94,** 1893-1897.

Han, B. A., Schmidt, J. P., Bowden, S. E. & Drake, J. M. (2015) Rodent reservoirs of future zoonotic diseases. *Proceedings of the National Academy of Sciences*.

Harpole, W. S., Goldstein, L. & Aicher, R. (2007) Resource Limitation. *Ecology and Management of California Grasslands* (eds C. D'Antonio, J. Corbin & M. Stromberg), pp. 119-130. University of Californis Press, Berkeley.

Harpole, W. S., Tilman, D. & Ellison, A. (2006) Non-neutral patterns of species abundance in grassland communities. *Ecology Letters,* **9,** 15-23.

Hersh, M. H., Tibbetts, M., Strauss, S. Y., Ostfeld, R. & Keesing, F. (2012) Reservoir competence of wildlife host species for *Babesia microti*. *Emerging Infectious Diseases,* **18**.

Huenneke, L. F., Hamburg, S. P., Koide, R., Mooney, H. A. & Vitousek, P. M. (1990) Effects of Soil Resources on Plant Invasion and Community Structure in Californian Serpentine Grassland. *Ecology,* **71,** 478-491.

Ives, A. R., Midford, P. E. & Garland, T. (2007) Within-species variation and measurement error in phylogenetic comparative methods. *Systematic Biology,* **56,** 252-270.

Jackson, S. T. & Sax, D. F. (2010) Balancing biodiversity in a changing environment: extinction debt, immigration credit and species turnover. *Trends in Ecology & Evolution,* **25,** 153-160.

Johnson, P. T. J., de Roode, J. C. & Fenton, A. (2015) Why infectious disease research needs community ecology. *Science,* **349**.

Johnson, P. T. J., Rohr, J. R., Hoverman, J. T., Kellermanns, E., Bowerman, J. & Lunde, K. B. (2012) Living fast and dying of infection: host life history drives interspecific variation in infection and disease risk. *Ecology Letters,* **15,** 235-242.

Keeling, M. J. & Rohani, P. (2008) *Modeling Infectious Diseases in Humans and Animals.* Princeton University Press, Princeton, NJ.

Kraft, N. J. B., Adler, P. B., Godoy, O., James, E. C., Fuller, S. & Levine, J. M. (2014) Community assembly, coexistence and the environmental filtering metaphor. *Functional Ecology***, 29**, 592–599.

Kursar, T. A. & Coley, P. D. (2003) Convergence in defense syndromes of young leaves in tropical rainforests. *Biochemical Systematics and Ecology,* **31,** 929-949.

Laliberte, E., Shipley, B., Norton, D. A. & Scott, D. (2012) Which plant traits determine abundance under long-term shifts in soil resource availability and grazing intensity? *Journal of Ecology,* **100,** 662-677.

Lan, Z. C. & Bai, Y. F. (2012) Testing mechanisms of N-enrichment-induced species loss in a semiarid Inner Mongolia grassland: critical thresholds and implications for long-term ecosystem responses. *Philosophical Transactions of the Royal Society B-Biological Sciences,* **367,** 3125-3134.

Lavorel, S. (2013) Plant functional effects on ecosystem services. *Journal of Ecology,* **101,** 4-8.

Lavorel, S. & Garnier, E. (2002) Predicting changes in community composition and ecosystem functioning from plant traits: revisiting the Holy Grail. *Functional Ecology,* **16,** 545-556.

Lavorel, S. & Grigulis, K. (2012) How fundamental plant functional trait relationships scale-up to trade-offs and synergies in ecosystem services. *Journal of Ecology,* **100,** 128-140.

Leishman, M. R., Haslehurst, T., Ares, A. & Baruch, Z. (2007) Leaf trait relationships of native and invasive plants: community- and global-scale comparisons. *New Phytologist,* **176,** 635-643.

Lloyd-Smith, J. O., Schreiber, S. J., Kopp, P. E. & Getz, W. M. (2005) Superspreading and the effect of individual variation on disease emergence. *Nature,* **438,** 355-359.

Maire, V., Gross, N., Börger, L., Proulx, R., Wirth, C., Pontes, L. d. S., Soussana, J.-F. & Louault, F. (2012) Habitat filtering and niche differentiation jointly explain species

relative abundance within grassland communities along fertility and disturbance gradients. *New Phytologist,* **196,** 497-509.

Mattson, W. J., Jr. (1980) Herbivory in relation to plant nitrogen content. *Annual Review of Ecology and Systematics,* **11,** 119-161.

Messier, J., McGill, B. J. & Lechowicz, M. J. (2010) How do traits vary across ecological scales? A case for trait-based ecology. *Ecology Letters,* **13,** 838-848.

Olden, J. D., Poff, N. L. & Bestgen, K. R. (2008) Trait synergisms and the rarity, extirpation, and extinction risk of desert fishes. *Ecology,* **89,** 847-856.

Pearse, W. D. & Purvis, A. (2013) phyloGenerator: an automated phylogeny generation tool for ecologists. *Methods in Ecology and Evolution,* **4,** 692-698.

Poland, J. A., Balint-Kurti, P. J., Wisser, R. J., Pratt, R. C. & Nelson, R. J. (2009) Shades of gray: the world of quantitative disease resistance. *Trends in Plant Science,* **14,** 21-29.

Poorter, L. & Bongers, F. (2006) Leaf traits are good predictors of plant performance across 53 rain forest species. *Ecology,* **87,** 1733-1743.

R Core Team (2015) R: A language and environment for statistical computing. R Foundation for Statistical Computing, Vienna, Austria. URL https://www.R-project.org/

Reich, P. B. (2014) The world-wide 'fast-slow' plant economics spectrum: a traits manifesto. *Journal of Ecology,* **102,** 275-301.

Reich, P. B., Ellsworth, D. S., Walters, M. B., Vose, J. M., Gresham, C., Volin, J. C. & Bowman, W. D. (1999) Generality of leaf trait relationships: a test across six biomes. *Ecology,* **80,** 1955-1969.

Revell, L. J. (2012) phytools: An R package for phylogenetic comparative biology (and other things). *Methods in Ecology and Evolution,* **3,** 217-223.

Scheiter, S., Langan, L. & Higgins, S. I. (2013) Next-generation dynamic global vegetation models: learning from community ecology. *New Phytologist,* **198,** 957-969.

Seabloom, E. W., Harpole, W. S., Reichman, O. J. & Tilman, D. (2003) Invasion, competitive dominance, and resource use by exotic and native California grassland species. *Proceedings of the National Academy of Sciences of the United States of America,* **100,** 13384-13389.

Smith, M. D., Knapp, A. K. & Collins, S. L. (2009) A framework for assessing ecosystem dynamics in response to chronic resource alterations induced by global change. *Ecology,* **90,** 3279-3289.

Stevens, C. J., Dise, N. B., Mountford, J. O. & Gowing, D. J. (2004) Impact of nitrogen deposition on the species richness of grasslands. *Science* **303,** 1876-1879.

Suding, K. N. & Goldstein, L. J. (2008) Testing the Holy Grail framework: using functional traits to predict ecosystem change. *New Phytologist,* **180,** 559-562.

Suding, K. N., Lavorel, S., Chapin, F. S., Cornelissen, J. H. C., Diaz, S., Garnier, E., Goldberg, D., Hooper, D. U., Jackson, S. T. & Navas, M. L. (2008) Scaling environmental change through the community-level: a trait-based response-and-effect framework for plants. *Global Change Biology,* **14,** 1125-1140.

Taborsky, B. (2006) The influence of juvenile and adult environments on life-history trajectories. *Proceedings of the Royal Society B-Biological Sciences,* **273,** 741-750.

Todesco, M., Balasubramanian, S., Hu, T. T., Traw, M. B., Horton, M., Epple, P., Kuhns, C., Sureshkumar, S., Schwartz, C., Lanz, C., Laitinen, R. A. E., Huang, Y., Chory, J., Lipka, V., Borevitz, J. O., Dangl, J. L., Bergelson, J., Nordborg, M. & Weigel, D. (2010) Natural allelic variation underlying a major fitness trade-off in *Arabidopsis thaliana*. *Nature,* **465,** 632-636.

Violle, C., Enquist, B. J., McGill, B. J., Jiang, L., Albert, C. H., Hulshof, C., Jung, V. & Messier, J. (2012) The return of the variance: intraspecific variability in community ecology. *Trends in Ecology & Evolution,* **27,** 244-252.

Webb, C. T., Hoeting, J. A., Ames, G. M., Pyne, M. I. & Poff, N. L. (2010) A structured and dynamic framework to advance traits-based theory and prediction in ecology. *Ecology Letters,* **13,** 267-283.

Welsh, M.E., Cronin, J.P., Mitchell, C.E. (2016) Data from: The role of habitat filtering in the leaf economics spectrum and plant susceptibility to pathogen infection. *Journal of Ecology* doi:10.5061/dryad.356v3

Weiss, S. B. (2006) Impacts of nitrogen deposition on California ecosystems and biodiversity, CEC-500-2005-165 (ed California Energy Commission). PIER Energy-Related Environmental Research.

Wright, I. J., Reich, P. B., Westoby, M., Ackerly, D. D., Baruch, Z., Bongers, F., Cavender-Bares, J., Chapin, T., Cornelissen, J. H. C., Diemer, M., Flexas, J., Garnier, E., Groom, P. K., Gulias, J., Hikosaka, K., Lamont, B. B., Lee, T., Lee, W., Lusk, C., Midgley, J. J., Navas, M. L., Niinemets, U., Oleksyn, J., Osada, N., Poorter, H., Poot, P., Prior, L., Pyankov, V. I., Roumet, C., Thomas, S. C., Tjoelker, M. G., Veneklaas, E. J. & Villar, R. (2004) The worldwide leaf economics spectrum. *Nature,* **428,** 821-827.

Wright, J. P. & Sutton-Grier, A. (2012) Does the leaf economic spectrum hold within local species pools across varying environmental conditions? *Functional Ecology,* **26,** 1390-1398.

Wright, S. J., Kitajima, K., Kraft, N. J. B., Reich, P. B., Wright, I. J., Bunker, D. E., Condit, R., Dalling, J. W., Davies, S. J., Diaz, S., Engelbrecht, B. M. J., Harms, K. E., Hubbell, S. P., Marks, C. O., Ruiz-Jaen, M. C., Salvador, C. M. & Zanne, A. E. (2010) Functional traits and the growth-mortality trade-off in tropical trees. *Ecology,* **91,** 3664-3674.

Zavaleta, E. S., Shaw, M. R., Chiariello, N. R., Thomas, B. D., Cleland, E. E., Field, C. B. & Mooney, H. A. (2003) Grassland responses to three years of elevated temperature, CO(2), precipitation, and N deposition. *Ecological Monographs,* **73,** 585-604.

CHAPTER 3: A SINGLE AXIS OF PLANT HOST TRAITS EXPLAINS MULTIPLE COMPONENTS OF HOST COMPETENCE

Introduction

One of the most effective means of controlling epidemics is to identify and target the most competent hosts, those most capable of generating new infections (Haydon et al. 2002, Lloyd-Smith et al. 2005, Streicker et al. 2013, Viana et al. 2014). Hosts that readily acquire and/or transmit infection are generally more competent (Huang et al. 2013, Streicker et al. 2013), and we will respectively refer to these qualities as host susceptibility and infectiousness. For vector-borne pathogens, host contribution to vector population size is another important component of host competence (Dobson 2004, Kilpatrick et al. 2006). For many endemic pathogens, available data and models can be used to estimate these parameters and identify competent hosts. When pathogens emerge, however, there is often little scientific basis on which to identify competent hosts—the models and data from other systems may not apply (Restif et al. 2012, Lloyd-Smith et al. 2015). For this reason, disease ecologists are increasingly advocating for less system-specific models of disease dynamics (Cronin et al. 2010, Johnson et al. 2012, Huang et al. 2013, Han et al. 2015). One such approach combines theory from physiological ecology, epidemiology, and evolutionary biology to propose that the traits of hosts can be used to predict *a priori* which hosts will be most competent (Cronin et al. 2010, Han et al. 2015).

Studies of multi-host pathogens infecting plants, mammals, birds, and amphibians have found that fast-growing host species are more susceptible and/or infectious (Cronin et al. 2010, Johnson et al. 2012, Huang et al. 2013, García-Guzmán and Heil 2014, Han et al. 2015, Welsh et

al. 2016), but see (Ostfeld et al. 2014). Fast-growing hosts can also contribute disproportionately to vector populations (Cronin et al. 2010). These relationships between host competence and growth rate are commonly attributed to growth-defense tradeoffs: both within and across host species, growth rate is often negatively correlated with investment in chemical, structural, and immunological defenses (Mattson 1980, Herms and Mattson 1992, Lochmiller and Deerenberg 2000, Lee et al. 2008, Cronin et al. 2010, Todesco et al. 2010, García-Guzmán and Heil 2014). Yet host stoichiometry and metabolic rate also vary with growth rate (Reich 2001, Vrede et al. 2004, Wright et al. 2004), and these traits have equally plausible mechanisms of effect on host-pathogen and host-vector interactions. Pathogen and vector reproduction can be limited by host tissue nutrient concentrations (Mitchell et al. 2003, Throop and Lerdau 2004, Clasen and Elser 2007), vectors may prefer more nutritious hosts (Mattson 1980), and host metabolic rate may constrain the growth of pathogens that rely on metabolic machinery for reproduction or vascular networks for dispersal (Cable et al. 2007, Cronin et al. 2010, Whitaker et al. 2015).

Variation in host competence may be driven by multiple traits, and each component of competence (susceptibility, infectiousness, and contribution to vector population) may be driven by different but potentially overlapping sets of traits. As such, several authors have proposed that trait-based models use multivariate axes of host trait covariation, instead of specific traits, to predict competence (Cronin et al. 2010, Johnson et al. 2012, Han et al. 2015). These axes capture variation in many of the traits expected to influence host-pathogen and host-vector interactions, and host species position along these axes represents the value of several traits simultaneously.

In plants, the Leaf Economic Spectrum (LES) is a global axis of physiological trait covariation that runs from slow- to quick-return trait combinations. Slow-return species are slow growing and have low mass-based photosynthetic rates and low tissue nutrient concentrations,

but high leaf mass per area (LMA, leaf dry mass:leaf area, a metric of structural defense); quick-return species display the opposite combination of traits (Wright et al. 2004, Reich 2014). These traits are relatively easy to measure, and all have a proposed mechanism of effect on host-pathogen or host-vector interactions. In the case of growth rate, this mechanism is indirect, via tradeoffs with chemical or immunological defenses (Coley et al. 1985, Throop and Lerdau 2004, Todesco et al. 2010), which are harder to quantify. To date, only one study has used host position along the LES to predict competence; across six grass species, those that that were more susceptible and infectious to a generalist, vector-borne virus were more quick-return, vector reproduction was greater on quick-return species, and viral titer (within-host virus load) was also greater on quick-return species (Cronin et al. 2010). Host position along axes of trait covariation has also been used to successfully predict interspecific variation in the competence of animal hosts (Johnson et al. 2012, Han et al. 2015),

Competence can vary substantially both within and among species (Hersh et al. 2012, Keesing et al. 2012), and the addition of intraspecific variation to models of pathogen dynamics can significantly alter predictions (Lloyd-Smith et al. 2005, Gervasi et al. 2015). Despite the success of trait-based approaches at the species level, the ability of multivariate trait axes to predict intraspecific variation in competence is largely untested. While we have previously shown that position along the LES can predict individual-level variation in one component of competence, susceptibility (Welsh et al. 2016), the ability of the LES to predict individual-level variation in infectiousness, vector reproduction, and viral titer has yet to be tested. If trait axes like the LES can capture all components of host competence across individuals, they could be used to more specifically target management efforts and to inform more precise and accurate forecasts of epidemics.

Across individuals and species, our goal was to test the hypothesis that host competence and its component parameters increase from slow- to quick-return along the LES. At community to biome scales, the LES is well supported by observational data (Reich et al. 1999, Diaz et al. 2004, Wright et al. 2004, Leishman et al. 2007, Reich 2014), and references therein). However, when plants are experimentally reared in novel conditions, relative to their inhabitance in the field, the trait correlations of the LES can weaken or even invert, and the strength of the LES declines (Wright and Sutton-Grier 2012, Welsh et al. 2016). As such, we focus here on hosts that were experimentally grown in nutrient supply rates that closely mimic those of the areas they typically inhabit in the field.

Using the same host-pathogen system in which the LES predicted competence across six species (Cronin et al. 2010) and susceptibility across individuals (Welsh et al. 2016), we tested whether susceptibility, infectiousness, vector reproduction, and viral titer increase across 23 species as host individuals or species became more quick-return. We also compared the accuracy of LES-based models at the individual and species level, and quantified the importance of specific host traits in explaining variation in each component of competence. Across both individuals and species, susceptibility, infectiousness, and viral titer increased as hosts became more quick-return along the LES, and vector reproduction increased as host species became more quick-return but not host individuals. Models were generally more accurate at the species level, and the traits most important in explaining each component of competence varied by component.

Materials and Methods

Study System

To test the ability of the LES to predict host competence, we used 23 grass hosts from the

Mediterranean grasslands of California, US (Table 3.1). Focal host species were selected from over 90 grass species present at the University of California's Hopland Research and Extension Center (HREC) in Hopland, CA, US to represent a range of several ecological attributes: local abundance at HREC (including all dominant species in a set of observational plots), life history (annual vs. perennial), geographic provenance (native vs. exotic), and frequency across 11 sites in CA and OR, US spanning 15° latitude (the five sites in Borer et al. 2010 plus six Nutrient Network sites: Hastings UCNRS, Mclaughlin UCNRS, Sedgewick Reserve UCNRS, Hopland REC, Sierra Foothills REC, and Finley NWR: http://www.ilternet.edu/content/nutrient-network, Borer et al. 2014). As a model pathogen, we used *Barley Yellow Dwarf Virus-PAV* (BYDV-PAV, family *Luteoviridae*), a generalist, vector-borne virus that is shared by all hosts. BYDV-PAV is a phloem-infecting RNA virus that is obligately and persistently transmitted by certain species of aphids, of which we used *Rhopalosiphum padi* L.

Experimental design and protocol

We quantified inter- and intra-specific variation in host traits and in host epidemiological parameters in two greenhouse experiments at the University of North Carolina, Chapel Hill, NC, USA. Host susceptibility was quantified in the first experiment (the Susceptibility Experiment), which ran from August-November 2010. Host infectiousness, viral titer, and vector reproduction were quantified in the second experiment (the Infectiousness Experiment), which ran from August-November 2012.

Susceptibility Experiment

In a randomized, blocked design (N=6), we factorially manipulated host identity (23 species; Table 3.1) and environment (two levels of nitrogen supply; Table 3.2) for a total of 276 host individuals. On each individual, we measured three traits of the LES: photosynthetic

capacity, LMA, and percent tissue nitrogen, as well as two metrics of growth rate: leaf emergence rate and leaf elongation rate (Table 3.3). At 4.5 weeks post germination, hosts were exposed to infection by caging five *Rhopalosiphum padi* vectors carrying BYDV-PAV on each host. The BYDV-PAV isolate was obtained from a wild *Bromus vulgaris* (Hook.) Shear individual in Oregon, US (Cronin et al. 2010, Cronin et al. 2014). After three days, vectors were removed with horticultural oil. Five weeks after exposure, the infection status of all hosts was determined via Enzyme-Linked Immunosorbent Assays (ELISAs; Agdia Inc., IN, US). See (Welsh et al. 2016) for detailed methods.

Infectiousness Experiment

We factorially manipulated host identity (23 Species; Table 3.1) and environment (two levels of nitrogen supply; Table 3.2) in a randomized block design (N=3), for a total of 138 treatment combinations. In each block, each unique combination of host species and nitrogen supply was represented twice: 1) in an infected individual, used to quantify infectiousness and viral titer, and 2) in a paired, healthy individual, used to quantify host traits and vector reproduction, for 138 pairs total. Each host was grown in a separate 1L Conetainer pot (Stuewe and Sons, Inc., OR, US) filled with a 50:50 mix of soil and sand, with ample phosphorous, potassium, and micronutrients (Table 3.2). Planting was timed to minimize differences in grass host ontogeny, such that all hosts reached the two-leaf stage within a week of each other. One week after germination, all hosts were thinned to one individual per pot.

At the two-leaf stage, about two weeks post-germination, we generated the infected hosts by caging infected aphid vectors on each (5 *Rhopalosiphum padi* aphids/host). Not all hosts become infected when exposed, so to generate the required number of infected hosts we varied the number of inoculated host individuals from 4-12 per host species-nitrogen treatment

combination, depending on the observed susceptibility of each host species in the Susceptibility Experiment. Infected vectors were produced by feeding aphids in dishes on lab-maintained, infected host tissue of the agricultural host *Avena sativa* var. Coast Black Oats for 48 hours. Vectors were propagated from field-collected populations in New York, USA, and the BYDV-PAV isolate was obtained from a wild *Avena sativa* L. individual in New York, US (Rochow et al. 1971, Rua et al. 2013, Whitaker et al. 2015). After three days, vectors were removed with horticultural oil.

Simultaneously with the virus inoculation to generate the infected hosts, paired, healthy host individuals were generated in a mock-inoculation procedure that was identical except that the aphids had been fed on uninfected host tissue, and thus the paired, healthy hosts were exposed to uninfected vectors. Immediately prior to being sprayed with horticultural oil, vectors were counted on each healthy host. Vector reproduction (aphids/aphid/day) was calculated on healthy hosts by dividing the final number of vectors on each host by 3 (days) and 5 (initial vectors). In addition to quantifying vector reproduction, this mock-inoculation procedure controlled for any effects of vector feeding on host traits.

Beginning at the four-leaf stage, about three weeks post-germination, we measured three traits of the LES on healthy hosts: maximum photosynthetic capacity, LMA, and percent tissue nitrogen, as well as two estimates of growth rate, leaf elongation and leaf emergence rate (Table 3.3). Photosynthetic capacity was quantified with an infrared gas analyzer, the CIRAS-2 Portable Photosynthesis System V2.01 (PP Systems).

At five weeks post-germination, after all host traits had been measured, tissue from all host individuals was tested for BYDV-PAV infection using Enzyme-Linked Immunosorbent Assays (ELISA; Agdia Inc., IN, US). Infection status was determined for each host based on

optical density values from a microplate reader (ELx-800; BioTek, VT, USA). All mock-inoculated hosts were determined to be uninfected. As expected, a fraction of virus-inoculated hosts were also determined to be uninfected, and these were not considered further. Of the virus-inoculated hosts that were determined to be infected, one from each species-nitrogen-block combination was selected randomly and paired with the healthy host of the same treatment combination.

Relative viral titer was quantified on each paired, infected host by back-calculating from its optical density value, using a curve of optical density values vs. a standard dilution series of infected tissue on each ELISA plate. The infected tissue used for the dilution series came from a lab-maintained, infected individual of *Avena sativa* var. Coast Black Oats. Prior to fitting standard curves and back-calculating relative titer, all optical density values were corrected for potential species-level effects of plant compounds by subtracting the optical densities of healthy control tissue from the same ELISA plate. R^2 values for standard curves ranged from 0.960-0.987. Building on principals from Copeland (1998), our specific protocol followed that of (Whitaker et al. 2015) with one exception: our standard curve did not include a standard with a relative titer of 0.5 because, in their experiment, this value was often above the range in which optical density values began to saturate in response to increasing viral titer. In all plates, our sample optical density values fell well within the lower (non-asymptotic) range of the optical densities of the standard curve (Fig. 3.1).

At six weeks post-germination, 20-30 uninfected aphid vectors were caged on each infected host. After 48 hours, from each infected host, six haphazardly selected, adult, feeding aphids were each transferred to one of six separate recipient individuals of *Avena sativa* var. Coast Black Oats. Aphids fed for 120 hours on the *Avena sativa* individuals, after which they

were removed with esfenvalerate, a non-systemic insecticide (Asana XL; DuPont, DE, US). To allow time for viral replication, all *Avena sativa* individuals were then grown for five weeks in the greenhouse, after which they were tested for BYDV-PAV infection with ELISA. Under our experimental conditions, *Avena sativa* has a susceptibility approaching 100% (Cronin et al. 2010), so *Avena sativa* infection was used as a proxy for vector infection. Host infectiousness was quantified for each infected host individual as the proportion of the six recipient *Avena sativa* individuals that became infected.

Statistical Analyses

Our goal was to test the hypothesis that host competence and its component parameters increase from slow- to quick-return individuals or species along the LES. Because the strength of the LES can decline when plants are experimentally reared in novel conditions, relative to their inhabitance in the field (Welsh et al. 2016), we limited our analyses to the host-nitrogen combinations that most closely mimicked the typical environments of our hosts in the field: perennial grass hosts at low nitrogen supply and annual grass hosts at high nitrogen supply (Huenneke et al. 1990, Maron and Connors 1996, Maron and Jefferies 1999, Seabloom et al. 2003, Zavaleta et al. 2003, Weiss 2006, Welsh et al. 2016). In both the Susceptibility and Infectiousness Experiments, principal components analyses (PCAs) of host traits showed that the LES was most strongly supported in these conditions, and support for the LES declined when hosts were observed in novel nitrogen supply environments (Table 3.4; Welsh et al. 2016).

Thus, of the 276 total individuals in the Susceptibility Experiment, all subsequent analyses included half of the species-nitrogen treatment combinations: those in which hosts were grown in the nitrogen environments they typically inhabit in the field (perennial hosts at low nitrogen and annual hosts at high nitrogen, for a total of 138 host individuals across 23 species).

Similarly, of the 138 pairs of individuals in the Infectiousness Experiment, our analyses again included half of them (perennial pairs at low nitrogen and annual pairs at high nitrogen, for a total of 69 pairs across 23 species). In analyses of infectiousness and viral titer, 11 pairs were removed due to missing trait data on healthy hosts, and 8 were removed for lack of an infected pair, leaving 50 pairs across 20 species. In analyses of vector reproduction, the same 11 healthy hosts were removed due to missing trait data, leaving 58 individuals across 22 species. Analyses used trait data from the Susceptibility Experiment when the response was susceptibility, and in all other cases they used trait data from the healthy individuals in the Infectiousness experiment. We found no evidence of a block effect in either experiment, so all analyses were conducted across blocks.

In both experiments, we used a PCA of individual host traits to quantify the LES, and the principal component 1 (PC1) scores of host individuals to quantify their position along the LES. At the species level, we used species mean PC1 scores to quantify the position of each species along the LES. In the Infectiousness Experiment, leaf emergence rate was square root transformed to meet assumptions of normality. The PCA from the Susceptibility Experiment has been presented elsewhere, so we present only the Infectiousness Experiment PCA here (Table 3.4; Welsh et al. 2016). At both the individual and species levels, we used logistic regression to test for significant effects of host PC1 score on susceptibility and infectiousness. At the species level, mean PC1 score was used and counts of host or vector infection were combined into a grouped binomial response across all individuals of a species. We used linear regression to test for effects of individual or species mean PC1 score on vector reproduction and viral titer. Viral titer was log transformed to meet assumptions of normality, and species-level analyses used mean vector reproduction and viral titer. The individual-level analysis of host susceptibility on

PC1 has been presented elsewhere, so we omit the details of that analysis here (Welsh et al. 2016). Because hosts with greater pathogen loads are often more infectious (Handel & Rohani 2015), we also used logistic regression to test for an effect of viral titer on infectiousness at both the individual and species levels.

Among individuals or species, when the LES was a significant predictor of susceptibility, infectiousness, viral titer, or vector reproduction, the individual traits most correlated with each response could not be determined using AIC model selection, as several models competed for AIC-best. We therefore used relative variable importance (RVI) to assess which traits of the LES most influenced variation in the response variable. RVI is calculated by summing the Akaike weights of the models that contain each trait across a global model and all nested models. When the best model cannot be determined based on AIC, RVI can be interpreted as the probability (from 0 to 1) that a given trait is included in the best model (Burnham and Anderson 2002). For each significant relationship, we also tested whether it could be driven by shared evolutionary history by testing for a phylogenetic signal in the residuals (Fig. 3.2; Blomberg et al. 2003, Ives et al. 2007, Bouchenak-Khelladi et al. 2008, Pearse and Purvis 2013). Using model residuals allowed us to include intraspecific variation in tests of phylogenetic signal, as there are currently no tests of phylogenetic signal that can incorporate intraspecific variation in a binomial trait like susceptibility (Ives et al. 2007).

All analyses were run in R ver. 3.0.2 (R Core Team 2015). PCA ordinations used the 'prcomp' function, logistic regressions used the 'glm' function, linear regressions used the 'lm' function, RVI analyses used the 'dredge' and 'importance' functions in the 'MuMIn' package (Barton 2015), and tests for phylogenetic signal used the 'phylosig' function in the 'phytools' package (v 0.4-60; randomizations=1,000; Revell 2012).

Results

At both the individual and species levels, host susceptibility, infectiousness, and viral titer increased significantly as hosts became more quick-return along the LES (Fig. 3.3a-c, e-g; Table 3.5a, b; Table 3.6a-c; Welsh et al. 2016). Vector reproduction increased as hosts species became more quick return (Fig. 3.3h; Table 3.6d), but not host individuals (Fig. 3.3d; Table 3.5c). Specifically, the susceptibility models predicted a 248-fold increase in the odds of host infection across 138 individuals (reflecting probabilities that increased from 0.05 to 0.93; Fig. 3.3a; Welsh et al. 2016), and an 86-fold increase in the odds of host infection across 23 species (reflecting probabilities that increased from 0.01 to 0.90; Fig. 3.3e). The infectiousness models predicted a 17-fold increase in the odds of vector infection across 50 individuals (reflecting probabilities that increased from 0.10 to 0.65; Fig. 3.3b), and a 29-fold increase in the odds of vector infection across 20 species (reflecting a probabilities that increased from 0.10 to 0.70; Fig. 3.3f). Model predicted viral titer increased 14-fold across 50 individuals and 18-fold across 20 species (Fig. 3.3c, g). While vector reproduction was unrelated to individual host position along the LES (Fig. 3.3d), species-level models predicted a 3-fold increase in vector reproduction across 22 species (Fig. 3.3h). The LES predicted susceptibility with similar accuracy across individuals and species, but the LES more accurately predicted infectiousness, viral titer, and vector reproduction across species than across individuals (Table 3.7).

Because one potential mechanism of greater infectiousness in quick-return hosts is the maintenance of higher viral titers, we tested for an effect of viral titer on host infectiousness. At both the individual (N=50) and species (N=20) levels, infectiousness was unrelated to viral titer (Table 3.5d; Table 3.6e).

In the RVI analyses, the host traits that were most important in explaining variation in

susceptibility, infectiousness, and viral titer were largely the same across individuals and species. Susceptibility was most influenced by positive effects of percent tissue nitrogen, leaf emergence rate, and photosynthetic capacity (Fig. 3.4a,d; Table 3.8b; Table 3.9b; Welsh et al. 2016), infectiousness was most strongly influenced by positive effects of photosynthetic capacity and leaf emergence rate, and a negative effect of leaf elongation rate (Fig. 3.4b,e; Table 3.8a; Table 3.9a), and viral titer was most influenced by positive effects of leaf elongation rate and photosynthetic capacity (Fig. 3.4c,f; Table 3.8c; Table 3.9d). While the LES did not influence vector reproduction at the individual level, at the species level, vector reproduction was most influenced by positive effects of leaf emergence rate, LMA, and tissue nitrogen (Fig. 3.4g; Table 3.9c). Lastly, we found no evidence that host phylogenetic relationships could explain any of the above relationships (Table 3.10).

Discussion

Our results reinforce a growing body of literature in support of trait-based approaches to disease ecology and eco-immunology (Cable et al. 2007, Cronin et al. 2010, Johnson et al. 2012, Huang et al. 2013, Cronin et al. 2014, Han et al. 2015). We found that a single, global axis of plant trait covariation, the LES, can predict several components of host competence. At the individual level, three of four tested components of competence: susceptibility, infectiousness, and viral titer, all increased significantly as hosts became more quick-return along the LES (Welsh et al. 2016). While capable of capturing individual-level variation, LES-based models were generally more accurate at the species level, and at the species level the LES was also significant predictor of vector reproduction. Particularly at the species level, but also across individuals, our results suggest that the LES could be used to improve forecasts of disease or target surveillance and management efforts when within- and among host contributions to

transmission are poorly understood, which is often the case. Our results also serve as a proof-of-concept from a model system that is easily manipulated: vectors and pathogens likely respond to multiple host traits and variation in susceptibility and infectiousness may be driven by different traits, but trait axes still capture enough variation across host traits to be broadly predictive.

Indeed, we found some overlap in the traits that were most important in explaining variation in susceptibility, infectiousness, viral titer, and (at the species level) vector reproduction, but we also found traits that were uniquely important to some responses. For example, one metric of growth rate, leaf emergence rate, had an important positive effect on susceptibility, infectiousness, and vector reproduction, while tissue nitrogen concentration only had an important positive effect on susceptibility. Photosynthetic capacity had important positive effects on infectiousness and viral titer, while another metric of growth rate, leaf elongation rate, had an important positive effect on viral titer but an important negative effect on infectiousness. While most of these effects were in the directions predicted, a consistent, negative importance of leaf elongation rate on infectiousness was not. This illustrates yet another strength of using trait axes or considering multiple traits as predictors: the predicted effect of a trait in isolation may be different that the predicted effects of traits acting in concert, in the context of a host organism. Only when traits are considered simultaneously can we begin to advance a more mechanistic understanding of host-pathogen and host-vector interactions. While multi-gene control of host-pathogen interactions is well documented (Poland et al. 2009), much remains to be done in terms of scaling these approaches to the use of physiological or life-history traits in trait-based disease ecology.

In our system, host-vector interactions were the primary means through which host traits were expected to affect host susceptibility and infectiousness. We expected vector preference

and feeding duration to increase with host growth rate, via growth-defense tradeoffs, and to increase with host tissue nutrient concentration (Mattson 1980, Gray et al. 1991, Kursar and Coley 2003). While host susceptibility and infectiousness both depend on vector feeding, the traits most important in explaining each response were different. Susceptibility was most influenced by a positive effect of host tissue nitrogen, while infectiousness was most influenced by a positive effect of photosynthetic capacity and a negative effect of leaf elongation rate. This suggests that vector feeding could be responding to different traits in healthy vs. infected hosts. In healthy hosts, vectors may feed preferentially on hosts with high tissue quality. If fast-growing hosts are differentially affected by infection, vectors may prefer to feed on those that are most able to maintain their metabolic processes, that is, hosts that have a high photosynthetic capacity relative to their growth rate.

In agreement with previous work in our system (Cronin et al. 2010, Whitaker et al. 2015), viral titer and host infectiousness both increased as individuals or species became more quick-return. In contrast to previous work in BYDV-infected crop hosts (Gray et al. 1991), however, infectiousness was unrelated to viral titer across our wild hosts, and our results did not support increased titer as a primary mechanism of greater infectiousness. Infectiousness is often assumed to increase with within-host pathogen load in epidemiological models that incorporate both within- and among-host dynamics. While there are some human and animal pathogens for which this assumption has been tested (ex., dengue, malaria; Handel and Rohani 2015), and references therein), it remains largely untested, and our results advise caution in its application. In some cases, other hots traits or disease-induced changes in host traits may be more important determinants of infectiousness.

In addition to their use as predictive tools and in generating new hypotheses in disease

ecology, axes of trait covariation could be used to synthesize disease models with other trait-based models of organism-environment interaction. For example, a large body of literature documents predictable changes in LES trait values along environmental gradients, and convergence of community trait distributions in similar abiotic conditions (Diaz et al. 2004, Poorter and Bongers 2006, Leishman et al. 2007, Jung et al. 2010, Lebrija-Trejos et al. 2010, Baraloto et al. 2012, Krober et al. 2012, Laliberte et al. 2012, Fortunel et al. 2014). Even though our disease models were generally more accurate at the species than individual level, quantifying and preserving intraspecific host trait information may be an essential component of successful synthesis across models. Particularly in the context of predicting host community response to global change, several recent studies emphasize the importance of considering intraspecific trait variation. Models of community assembly are often more accurate when intraspecific trait information is included (Clark 2010, Laughlin et al. 2012, Violle et al. 2012), and the local abundance of a given species may depend on the relative breadth of its trait variation (Umaña et al. 2015). To date, the available data on trait-environment relationships suggests that one component of global change, increased resource availability, will likely act to increase the abundance of quick-return individuals and species (Stevens et al. 2004, Fynn et al. 2005, Leishman et al. 2007, Laliberte et al. 2012, Fortunel et al. 2014). Our results suggest that these individuals and species will be more competent, and thus increase the frequency and severity of epidemics.

Table 3.1. Host identities, life history (A=annual, P=perennial), and seed source.

Host Species	Life History	Seed Source
Aegilops triuncialis L.	A	Field collected: Basket Butte, OR, US
Aira caryophyllea L.	A	Field collected: Basket Butte, OR, US
Arrhenatherum elatius (L.) P. Beauv. ex J. Presl & C. Presl	P	Field collected: Basket Butte, OR, US
Avena barbata Pott ex Link	A	Field collected: Hopland, CA, US
Avena fatua L.	A	Azlin Seed Service, Leland, MS, US
Briza maxima L.	A	Field collected: Basket Butte, OR, US
Bromus carinatus Hook. & Arn.	P	Field collected: Basket Butte, OR, US
Bromus diandrus Roth	A	Field collected: Basket Butte, OR, US
Bromus hordeaceus L.	A	Field collected: Basket Butte, OR, US
Cynosurus echinatus L.	A	Field collected: Basket Butte, OR, US
Elymus glaucus Buckley	P	Field collected: Basket Butte, OR, US
Elymus multisetus M.E. Jones	P	Field collected: Basket Butte, OR, US
Koeleria macrantha (Ledeb.) Schult.	P	Field collected: Basket Butte, OR, US
Lolium multiflorum Lam.	A	Field collected: Basket Butte, OR, US
Melica californica Scribn.	P	Hedgerow Farms, Winters, CA, US
Nassella lepida (Hitchc.) Barkworth	P	Field collected: Basket Butte, OR, US
Nassella pulchra (Hitchc.) Barkworth	P	Field collected: Basket Butte, OR, US
Poa secunda J. Presl	P	Field collected: Basket Butte, OR, US
Schedonorus arundinaceus (Schreb.) Dumort., nom. cons.	P	Field collected: Basket Butte, OR, US
Taeniatherum caput-medusae (L.) Nevski	A	Field collected: Basket Butte, OR, US
Vulpia microstachys (Nutt.) Munro	A	Field collected: Basket Butte, OR, US
Vulpia myuros (L.) C.C. Gmel.	A	Field collected: Basket Butte, OR, US
Avena sativa L. 'Coast Black'	A	National Small Grains Collection, Aberdeen, ID, USA

Table 3.2. Potting medium and nitrogen treatment. On a per area basis, nutrient and high nitrogen addition rates reflect those of the Nutrient Network, a world-wide fertilization experiment in grasslands (Borer *et al.* 2014).

Soil Component	Description	Ammount per Individual
Sand	Pasteurized	0.5 L
LC1 Soil	Low-nutrient soil, SunGro Horticulture, Agawam, MA, US	0.5 L
Phosphorous	Triple Phosphate, 45% P_2O_5, Espoma, NJ, US	0.196 g
Potassium	Potash, 50% K_2O, Winston Weaver Co., Inc., NC, US	0.093 g
Micronutrients	Micromax, Scotts, OH, US	0.385 g
Nitrogen	>98% NH_4NO_3, Fisher Scientific, NY, US	low N: 0.005 g *
		high N: 0.110 g *

* Applied in equal parts over 5 weeks and dissolved in 10mL H_20 per week

Table 3.3. List of host traits, abbreviations, units, and measurement methods. Traits included three leaf traits and two metrics of growth rate.

Host Trait	Abbr	Units	Timing of Measurement(s)	Method
Maximum Photosynthetic Capacity	Photo.	umol/ mg/s	~4 wks post-germination on youngest, fully expanded leaf	Maximum CO_2 flux: CIRAS-2 infrared gas analyzer, PP Systems, MA, US
Leaf Mass per Area	LMA	mg/cm^2	~4 wks post-germination on youngest, fully expanded leaf	Dry mass/scanned leaf section area: WinFOLIA, Regent Instruments, QC, CA
% Tissue Nitrogen	%N	100*mg/ mg	~4 wks post-germination on youngest, fully expanded leaf	Combustion analysis: Duke Environmental Stable Isotope Laboratory, NC, US
Growth: leaf elongation rate	Lf. Elong	cm/day	~2 wks post-germination on 3rd-4th emergent leaf	length increase over 4 days
Growth: leaf emergence rate	Lf. Emerge	leaves/ day	~2 wks post-germination, beginning with 3rd-4th emergent leaf	Number of new leaves over 10 days

Table 3.4. Principal Components Analyses of host traits in two environmental contexts: the nitrogen supply rates they typically inhabit in the field, and novel nitrogen supply rates. Host traits are as in Table 3.3. Loadings are for each trait onto principal component 1 (PC1). 'Corr.' is the correlation coefficient between each trait and PC1. The LES was most evident when individuals were grown in the conditions they typically inhabit.

Scenario	Variance Captured by PC1	Trait	Loading	Corr.
Typical conditions: Annuals +N, Perennials -N (N=58)	53.1%	LMA	-0.255	-0.415
		Photo	0.554	0.903
		%N	0.489	0.796
		Lf. Elong	0.403	0.657
		sqrt (Lf. Emerge)	0.476	0.775
Novel conditions: Annuals -N, Perennials +N (N=62)	32.4%	LMA	0.346	0.441
		Photo	0.628	0.799
		%N	0.515	0.655
		Lf. Elong	0.086	0.11
		sqrt (Lf. Emerge)	0.462	0.589

Table 3.5. (a-c): Coefficients and model performance for individual-level models of (a) infectiousness, (b) viral titer, and (c) aphid reproduction based on host PC1 score, which represents a host individual's position along the LES. Hosts become more quick-return as PC1 increases. (d): Coefficients and model performance for the individual-level model of infectiousness on viral titer. The likelihood ratio tests for a significant improvement over a null model, based on null and residual deviances ($p<0.05$=improvement). Pearson's Chi-squared tests model fit to the data, based on observed and predicted values ($p<0.05$=evidence for a lack of fit).

(a) *Infectiousness, logistic (N=50)*						
Predictor	β	SE β	Wald's X^2	*df*	*p*	e^{β} (odds ratio)
Constant	-0.553	0.131	17.8	1	*<0.001*	NA
PC1	0.501	0.092	29.8	1	<0.001	1.65
Test			X2	*df*	*p*	
Model						
Liklihood ratio			35.8	1	<0.001	
Goodness-of-fit						
Pearson's chi-squared			130.5	47	<0.001	
(b) *Relative Viral Titer, linear (N=50)*						
Predictor	β	SE β	Wald's X^2	*df*	*p*	
Constant	-6.141	0.254	583.1	1	*<0.001*	
PC1	0.485	0.162	9	1	0.003	
Test			R^2	*df*	*F*	p
Model Evaluation			0.158	48	9.015	0.004
(c) *Aphid reproduction (aphids/aphid/day), linear (N=58)*						
Predictor	β	SE β	Wald's X^2	*df*	*p*	
Constant	1.176	0.122	93	1	*<0.001*	
PC1	0.111	0.076	2.2	1	0.14	
Test			R^2	*df*	*F*	p
Model			0.037	56	2.152	0.148
(d) *Infectiousness, logistic (N=50)*						
Predictor	β	SE β	Wald's X^2	*df*	*p*	e^{β} (odds ratio)
Constant	-0.102	0.394	0.067	1	*0.800*	NA
Rel. Viral Titer	0.054	0.062	0.77	1	0.38	NA
Test			X2	*df*	*p*	
Model Evaluation						
Liklihood ratio			0.8	1	0.379	
Goodness-of-fit						
Pearson's chi-squared			154.9	48	<0.001	

Table 3.6. (a-d): coefficients and model performance for species-level models of (a) susceptibility, (b) infectiousness, (c) viral titer, and (d) vector reproduction based on host species mean PC1 score, which represents a species position along the LES. (e): coefficients and model performance for the species-level model of infectiousness on viral titer.

(a) Susceptibility, logistic (N=23)						
Predictor	β	SE β	Wald's X^2	*df*	*p*	e^{β} (odds ratio)
Constant	-0.218	0.210	1.1	1	*0.300*	NA
PC1	0.872	0.149	34.3	1	<0.001	2.391
Test			X^2	*df*	*p*	
Model Evaluation						
Liklihood ratio			47.5	1	<0.001	
Goodness-of-fit						
Pearson's chi-squared			55.4	21	<0.001	
(b) *Infectiousness, logistic (N=20)*						
Predictor	β	SE β	Wald's X^2	*df*	*p*	e^{β} (odds ratio)
Constant	-0.608	0.138	19.4	1	<0.001	NA
PC1	0.636	0.109	34.1	1	<0.001	1.889
Test			X^2	*df*	*p*	
Model Evaluation						
Liklihood ratio			45.6	1	<0.001	
Goodness-of-fit						
Pearson's chi-squared			105.1	18	<0.001	
(c) *Relative Viral Titer, linear (N=20)*						
Predictor	β	SE β	Wald's X^2	*df*	*p*	
Constant	-6.357	0.4	252.4	1	*<0.001*	
PC1	0.536	0.246	4.7	1	0.029	
Test			R^2	*df*	*F*	p
Model Evaluation			0.208	18	4.7	0.043
(d) Vector *reproduction (aphids/aphid/day), linear (N=22)*						
Predictor	β	SE β	Wald's X^2	*df*	*p*	
Constant	1.140	0.12	89.7	1	*<0.001*	
PC1	0.188	0.074	6.5	1	0.011	
Test			R^2	*df*	*F*	p
Model Evaluation			0.245	20	6.5	0.019
(e) *Infectiousness, logistic (N=20)*						
Predictor	β	SE β	Wald's X^2	*df*	*p*	e^{β} (odds ratio)
Constant	-0.111	0.412	0.073	1	0.790	NA
Rel. Viral Titer	0.053	0.065	0.66	1	0.42	N.S.
Test			X^2	*df*	*p*	
Model Evaluation						
Liklihood ratio			0.7	1	0.415	
Goodness-of-fit						
Pearson's chi-squared			138.1	18	0.000	

Table 3.7. Performance of either (a) logistic or (b) linear models of susceptibility, infectiousness, viral titer, and vector reproduction on host individual or species position along the LES (PC1 score). For logistic models, Sensitivity (True Negative Rate) and Specificity (True Positive Rate) give the proportion of correct model predictions of uninfected or infected hosts, respectfully. Predictive Positive and Negative values give the proportion of predicted infections that were true infections, and the proportion of predicted healthy hosts that were actually uninfected.

	Response	Level	N	Sensitivity (TNR)	Specificity (TPR)	Predictive Value Positive	Predictive Value Negative	Average Accuracy
(a)	Susceptibility*	Individual	138 indiv.	79.2%	78.5%	77.3%	80.3%	78.8%
	Susceptibility	Species	23 spp.	80.8%	75.4%	77.8%	78.7%	78.2%
	Infectiousness	Individual	50 indiv.	78.0%	65.3%	65.8%	77.6%	71.7%
	Infectiousness	Species	20 spp.	80.8%	72.0%	70.8%	81.7%	76.3%
(b)				R2	p			
	Viral Titer	Individual	50 indiv.	0.158	0.004			
	Viral Titer	Species	20 spp.	0.208	0.043			
	Aphid Reproduction	Individual	58 indiv.	0.037	0.148			
	Aphid Reproduction	Species	23 spp.	0.245	0.019			

**reprinted from Welsh et al. (2016)*

Table 3.8. Individual-level AICc model selection table used to calculate the relative variable importance of specific host traits in explaining (a) infectiousness, (b) susceptibility, and (c) viral titer. Host traits are: leaf emergence rate (Lf. Emerge), leaf elongation rate (Lf. Long), leaf mass per area (LMA), mass-based photosynthetic capacity (Photo), and percent tissue nitrogen (%N). For all responses, the global model was a significant improvement over a null model (infectiousness: χ^2=77.6, df=5, p<0.001; susceptibility: χ^2=47.9, df=5, p<0.001; viral titer: F=4.5, df=5, p=0.002).

(a) *Infectiousness, individual level*

Intercept	Lf. Long	LMA	Photo	sqrt (Lf. Emerge)	%N	df	logLik	AICc	delta
-3.637	-0.613	NA	0.542	1.204	NA	4	-91.320	191.528	0.000
-3.789	-0.546	NA	0.431	1.137	0.163	5	-90.585	192.534	1.006
-3.247	-0.609	-0.149	0.538	1.184	NA	5	-91.230	193.824	2.295
-3.616	-0.547	-0.064	0.432	1.129	0.158	6	-90.569	195.092	3.564
-3.201	-0.284	NA	NA	1.245	0.449	4	-95.839	200.568	9.039
-3.335	-0.284	0.048	NA	1.253	0.452	5	-95.830	203.024	11.495
-3.359	-0.489	NA	0.456	NA	0.276	4	-98.449	205.786	14.258
-3.408	NA	NA	NA	1.047	0.428	3	-100.254	207.031	15.502
-2.839	-0.491	-0.196	0.459	NA	0.259	5	-98.282	207.927	16.399
-3.078	-0.601	NA	0.661	NA	NA	3	-100.792	208.106	16.578
-3.530	NA	NA	0.063	1.012	0.383	4	-100.038	208.964	17.436
-3.526	NA	0.042	NA	1.053	0.431	4	-100.247	209.384	17.855
-2.243	-0.590	-0.327	0.645	NA	NA	4	-100.297	209.483	17.954
-3.592	NA	0.022	0.063	1.016	0.385	5	-100.036	211.435	19.906
-2.757	-0.190	NA	NA	NA	0.596	3	-104.950	216.421	24.893
-2.970	NA	NA	0.240	1.169	NA	3	-105.307	217.135	25.606
-2.914	NA	NA	NA	NA	0.561	2	-107.146	218.547	27.019
-2.406	-0.191	-0.127	NA	NA	0.585	4	-104.876	218.641	27.112
-2.339	NA	-0.244	0.237	1.130	NA	4	-105.044	218.976	27.447
-3.143	NA	NA	0.120	NA	0.461	3	-106.260	219.042	27.514
-1.717	-0.265	NA	NA	1.754	NA	3	-106.331	219.185	27.656
-0.933	-0.266	-0.306	NA	1.689	NA	4	-105.876	220.641	29.112
-2.610	NA	-0.110	NA	NA	0.551	3	-107.092	220.706	29.177
-2.791	NA	-0.130	0.122	NA	0.448	4	-106.187	221.263	29.735
-1.928	NA	NA	NA	1.496	NA	2	-110.201	224.658	33.130
-1.159	NA	-0.302	NA	1.434	NA	3	-109.763	226.048	34.519
-2.405	NA	NA	0.356	NA	NA	2	-114.472	233.200	41.671
-1.286	NA	-0.451	0.344	NA	NA	3	-113.461	233.444	41.916
1.106	NA	-0.655	NA	NA	NA	2	-126.795	257.845	66.316
1.257	-0.072	-0.670	NA	NA	NA	3	-126.435	259.391	67.863
-0.433	NA	NA	NA	NA	NA	1	-129.421	260.926	69.397
-0.341	-0.057	NA	NA	NA	NA	2	-129.189	262.632	71.104

(b) *Susceptibility, individual level**

Intercept	Lf. Emerge	Lf. Long	LMA	Photo	%N	df	logLik	AICc	delta
-4.376	1.302	NA	NA	NA	0.858	3	-72.490	151.158	0.000
-4.991	1.254	NA	NA	0.275	0.597	4	-71.684	151.668	0.510
-4.268	NA	NA	NA	NA	1.028	2	-74.089	152.266	1.108
-4.921	NA	NA	NA	0.293	0.742	3	-73.152	152.484	1.325
-2.799	1.241	NA	-0.444	NA	0.773	4	-72.172	152.645	1.487
-4.273	1.398	-0.098	NA	NA	0.881	4	-72.346	152.992	1.834
-2.334	NA	NA	-0.548	NA	0.914	3	-73.584	153.348	2.190
-4.893	1.345	-0.107	NA	0.283	0.615	5	-71.508	153.470	2.312
-4.282	1.235	NA	-0.180	0.246	0.589	5	-71.641	153.736	2.578
-4.883	1.719	NA	NA	0.608	NA	3	-73.958	154.094	2.936
-4.238	NA	-0.025	NA	NA	1.037	3	-74.078	154.336	3.177
-3.821	NA	NA	-0.281	0.246	0.729	4	-73.045	154.391	3.233
-4.878	NA	-0.047	NA	0.298	0.753	4	-73.117	154.535	3.377
-2.894	1.312	-0.070	-0.395	NA	0.798	5	-72.103	154.660	3.501
-2.331	NA	0.003	-0.550	NA	0.913	4	-73.584	155.469	4.311
-4.533	1.328	-0.100	-0.093	0.267	0.610	6	-71.497	155.635	4.477
-3.670	1.680	NA	-0.312	0.551	NA	4	-73.824	155.949	4.791
-4.828	1.772	-0.063	NA	0.621	NA	4	-73.892	156.085	4.927
-3.884	NA	-0.031	-0.257	0.253	0.737	5	-73.031	156.517	5.358
-3.776	1.721	-0.044	-0.274	0.567	NA	5	-73.794	158.043	6.885
-4.759	NA	NA	NA	0.759	NA	2	-77.041	158.171	7.013
-2.980	NA	NA	-0.456	0.670	NA	3	-76.744	159.667	8.509
-4.790	NA	0.031	NA	0.751	NA	3	-77.025	160.228	9.070
-2.891	NA	0.056	-0.494	0.647	NA	4	-76.691	161.684	10.525
2.302	2.271	NA	-1.404	NA	NA	3	-78.635	163.449	12.291
2.147	2.097	0.137	-1.440	NA	NA	4	-78.303	164.906	13.748
-1.862	2.947	NA	NA	NA	NA	2	-83.060	170.210	19.051
-2.063	2.818	0.108	NA	NA	NA	3	-82.849	171.876	20.718
4.365	NA	0.293	-1.945	NA	NA	3	-83.009	172.196	21.038
5.161	NA	NA	-1.957	NA	NA	2	-84.777	173.644	22.485
-0.947	NA	0.322	NA	NA	NA	2	-92.975	190.038	38.880
-0.116	NA	NA	NA	NA	NA	1	-95.422	192.874	41.716

*reprinted from Welsh et al. (2016)

(c) *Viral titer, individual level*

Intercept	Lf. Long	LMA	Photo	sqrt (Lf. Emerge)	%N	df	logLik	AICc	delta
-10.794	0.417	0.968	0.321	NA	NA	5	-93.324	198.011	0.000
-8.258	0.439	NA	0.268	NA	NA	4	-94.917	198.723	0.712
-7.191	0.664	NA	NA	NA	NA	3	-96.530	199.583	1.572
-11.283	NA	1.037	0.508	NA	NA	4	-95.488	199.866	1.855
-8.942	0.681	0.729	NA	NA	NA	4	-95.659	200.207	2.196
-10.477	0.632	0.971	NA	NA	0.244	5	-94.484	200.331	2.320
-10.695	0.419	0.943	0.340	-0.155	NA	6	-93.271	200.495	2.484
-10.798	0.417	0.968	0.320	NA	0.002	6	-93.324	200.601	2.590
-7.844	0.626	NA	NA	NA	0.167	4	-95.959	200.808	2.797
-8.581	NA	NA	0.462	NA	NA	3	-97.172	200.866	2.854
-8.197	0.441	NA	0.304	-0.271	NA	5	-94.762	200.887	2.876
-8.174	0.411	NA	0.321	NA	-0.076	5	-94.859	201.082	3.070
-10.837	NA	0.950	0.590	NA	-0.159	5	-95.210	201.785	3.773
-7.267	0.651	NA	NA	0.101	NA	4	-96.506	201.901	3.890
-8.260	NA	NA	0.587	NA	-0.233	4	-96.586	202.061	4.050
-11.207	NA	1.018	0.524	-0.122	NA	5	-95.458	202.280	4.269
-9.262	0.654	0.788	NA	0.236	NA	5	-95.528	202.420	4.409
-10.444	0.639	0.963	NA	-0.082	0.257	6	-94.470	202.894	4.883
-8.527	NA	NA	0.496	-0.246	NA	4	-97.054	202.998	4.986
-7.822	0.640	NA	NA	-0.159	0.193	5	-95.911	203.186	5.175
-10.738	0.426	0.952	0.327	-0.166	0.021	7	-93.267	203.200	5.189
-8.152	0.424	NA	0.332	-0.244	-0.046	6	-94.742	203.437	5.426
-10.822	NA	0.946	0.594	-0.043	-0.155	6	-95.207	204.367	6.356
-8.251	NA	NA	0.597	-0.121	-0.220	5	-96.559	204.481	6.470
-7.340	NA	NA	NA	NA	0.289	3	-102.138	210.799	12.787
-9.855	NA	0.929	NA	NA	0.364	4	-101.093	211.074	13.063
-6.104	NA	NA	NA	NA	NA	2	-103.512	211.279	13.268
-6.725	NA	NA	NA	0.649	NA	3	-102.654	211.830	13.819
-8.668	NA	0.768	NA	0.782	NA	4	-101.930	212.750	14.739
-7.400	NA	0.548	NA	NA	NA	3	-103.140	212.802	14.791
-7.406	NA	NA	NA	0.323	0.233	4	-101.972	212.833	14.822
-10.052	NA	0.972	NA	0.400	0.297	5	-100.828	213.019	15.008

Table 3.9. Species-level AICc model selection table used to calculate the relative variable importance of specific host traits in explaining (a) infectiousness, (b) susceptibility, and (c) vector reproduction, and (d) viral titer. Host traits are: leaf emergence rate (Lf. Emerge), leaf elongation rate (Lf. Long), leaf mass per area (LMA), mass-based photosynthetic capacity (Photo), and percent tissue nitrogen (%N). For all responses except viral titer, the global model was a significant improvement over a null model (infectiousness: χ^2=100.3, df=5, p<0.001; susceptibility: χ^2=53.0, df=5, p<0.001; vector reproduction: F=3.0, df=5, p=0.044; viral titer: F=1.9, df=5, p=0.156).

(a) *Infectiousness, species level*

Intercept	%N	Lf. Long	LMA	Photo	sqrt (Lf. Emerge)	df	logLik	AICc	delta
-4.810	NA	-0.959	NA	0.902	0.945	4	-53.646	117.958	0.000
-2.626	NA	-0.953	-0.851	0.905	0.729	5	-52.067	118.420	0.462
-1.651	NA	-1.017	-1.135	1.009	NA	4	-54.024	118.714	0.756
-2.170	0.398	-0.775	-0.954	0.634	NA	5	-52.918	120.122	2.164
-4.657	0.548	-0.711	NA	0.541	NA	4	-54.898	120.464	2.505
-4.785	0.183	-0.861	NA	0.753	0.781	5	-53.504	121.295	3.336
-4.512	NA	-1.059	NA	1.060	NA	3	-57.129	121.757	3.799
-4.470	1.042	-0.349	NA	NA	NA	3	-57.211	121.922	3.964
-2.638	0.121	-0.889	-0.835	0.805	0.627	6	-52.005	122.472	4.514
-2.403	0.981	-0.363	-0.756	NA	NA	4	-55.911	122.489	4.530
-4.442	0.977	-0.358	NA	NA	0.271	4	-57.000	124.666	6.708
-2.491	0.955	-0.366	-0.720	NA	0.122	5	-55.867	126.021	8.062
-4.808	0.978	NA	NA	NA	NA	2	-62.112	128.929	10.971
-2.937	0.923	NA	-0.692	NA	NA	3	-61.131	129.762	11.804
-4.652	1.157	NA	NA	-0.169	NA	3	-61.336	130.172	12.214
-2.915	1.092	NA	-0.639	-0.159	NA	4	-60.472	131.610	13.652
-4.808	0.948	NA	NA	NA	0.128	3	-62.062	131.623	13.665
-2.943	0.921	NA	-0.690	NA	0.008	4	-61.131	132.929	14.970
-4.652	1.145	NA	NA	-0.167	0.037	4	-61.332	133.331	15.372
-2.856	1.114	NA	-0.660	-0.164	-0.078	5	-60.454	135.193	17.235
-1.595	NA	NA	-0.848	0.372	1.008	4	-73.759	158.184	40.226
-3.737	NA	NA	NA	0.359	1.230	3	-75.373	158.247	40.288
0.085	NA	NA	-1.306	0.454	NA	3	-77.916	163.333	45.375
-1.905	NA	-0.292	NA	NA	1.962	3	-79.654	166.807	48.849
-0.153	NA	-0.294	-0.647	NA	1.739	4	-78.424	167.515	49.557
-3.062	NA	NA	NA	0.471	NA	2	-82.325	169.355	51.397
-2.152	NA	NA	NA	NA	1.696	2	-83.440	171.585	53.627
-0.378	NA	NA	-0.663	NA	1.488	3	-82.200	171.899	53.941
2.969	NA	NA	-1.442	NA	NA	2	-94.703	194.112	76.154
3.292	NA	-0.129	-1.489	NA	NA	3	-93.821	195.143	77.184
-0.433	NA	NA	NA	NA	NA	1	-102.481	207.183	89.225
-0.314	NA	-0.073	NA	NA	NA	2	-102.165	209.037	91.078

(b) *Susceptibility, species level*

Intercept	%N	Lf. Emerge	Lf. Long	LMA	Photo	df	logLik	AICc	delta
-5.180	1.250	NA	NA	NA	NA	2	-42.308	89.216	0.000
-5.090	1.061	1.092	NA	NA	NA	3	-41.699	90.661	1.446
-5.893	0.920	NA	NA	NA	0.331	3	-41.755	90.773	1.557
-4.111	1.184	NA	NA	-0.296	NA	3	-42.222	91.708	2.492
-5.131	1.275	NA	-0.057	NA	NA	3	-42.264	91.791	2.576
-5.784	0.770	1.004	NA	NA	0.311	4	-41.225	92.673	3.457
-5.000	1.092	1.208	-0.108	NA	NA	4	-41.556	93.334	4.118
-5.906	0.921	NA	-0.111	NA	0.379	4	-41.597	93.417	4.201
-4.569	1.036	1.052	NA	-0.146	NA	4	-41.679	93.580	4.365
-6.168	0.922	NA	NA	0.068	0.344	4	-41.751	93.725	4.509
-5.994	NA	1.662	NA	NA	0.789	3	-43.243	93.750	4.534
-6.301	NA	NA	NA	NA	1.007	2	-44.945	94.490	5.274
-4.211	1.209	NA	-0.040	-0.259	NA	4	-42.203	94.627	5.411
-5.784	0.767	1.108	-0.144	NA	0.363	5	-40.965	95.459	6.243
-6.703	0.770	1.053	NA	0.229	0.354	5	-41.188	95.904	6.689
-6.040	NA	1.720	-0.150	NA	0.854	4	-42.954	96.129	6.913
-7.098	0.932	NA	-0.138	0.293	0.448	5	-41.542	96.614	7.398
-4.900	1.086	1.197	-0.106	-0.029	NA	5	-41.555	96.639	7.424
-6.746	NA	1.704	NA	0.192	0.824	4	-43.216	96.654	7.438
-6.339	NA	NA	-0.112	NA	1.062	3	-44.784	96.831	7.615
-5.966	NA	NA	NA	-0.084	0.990	3	-44.939	97.142	7.926
-8.060	0.771	1.259	-0.199	0.564	0.490	6	-40.767	98.784	9.568
-8.034	NA	1.855	-0.196	0.503	0.964	5	-42.790	99.109	9.893
-6.642	NA	NA	-0.118	0.076	1.080	4	-44.780	99.782	10.566
1.782	NA	2.865	NA	-1.343	NA	3	-48.920	105.104	15.888
-2.379	NA	3.805	NA	NA	NA	2	-51.145	106.890	17.674
1.785	NA	2.538	0.174	-1.441	NA	4	-48.488	107.198	17.982
-2.569	NA	3.617	0.117	NA	NA	3	-50.947	109.157	19.941
5.642	NA	NA	0.374	-2.498	NA	3	-52.581	112.424	23.208
6.829	NA	NA	NA	-2.572	NA	2	-55.073	114.745	25.529
-1.256	NA	NA	0.440	NA	NA	2	-63.298	131.196	41.980
-0.116	NA	NA	NA	NA	NA	1	-67.260	136.711	47.495

(c) *Vector reproduction, species level*

Intercept	%N	Lf. Long	LMA	Photo	sqrt (Lf. Emerge)	df	logLik	AICc	delta
-1.121	NA	NA	0.646	NA	0.803	4	-14.626	39.605	0.000
0.559	NA	NA	NA	NA	0.618	3	-16.642	40.617	1.011
0.181	0.229	NA	NA	NA	NA	3	-17.051	41.434	1.829
-1.257	0.091	NA	0.614	NA	0.624	5	-14.246	42.242	2.636
0.283	0.116	NA	NA	NA	0.402	4	-16.120	42.593	2.988
-1.231	NA	NA	0.638	0.044	0.696	5	-14.425	42.601	2.995
-1.155	NA	0.039	0.650	NA	0.764	5	-14.537	42.823	3.218
-0.757	0.251	NA	0.361	NA	NA	4	-16.390	43.133	3.528
0.412	NA	NA	NA	0.050	0.500	4	-16.427	43.207	3.601
0.381	NA	NA	NA	0.144	NA	3	-18.017	43.367	3.762
0.540	NA	0.032	NA	NA	0.585	4	-16.591	43.535	3.930
0.178	0.210	0.054	NA	NA	NA	4	-16.901	44.154	4.549
0.178	0.219	NA	NA	0.009	NA	4	-17.047	44.448	4.842
-0.533	NA	NA	0.352	0.162	NA	4	-17.450	45.253	5.647
1.100	NA	NA	NA	NA	NA	2	-20.494	45.620	6.014
0.278	0.113	0.020	NA	NA	0.385	5	-16.099	45.947	6.342
-0.848	0.228	0.072	0.395	NA	NA	5	-16.113	45.976	6.371
0.287	0.128	NA	NA	-0.012	0.406	5	-16.115	45.979	6.374
-1.277	0.087	0.030	0.619	NA	0.602	6	-14.192	45.984	6.379
-1.258	0.090	NA	0.615	0.001	0.624	6	-14.246	46.091	6.486
0.878	NA	0.149	NA	NA	NA	3	-19.460	46.253	6.648
0.364	NA	-0.020	NA	0.154	NA	4	-18.005	46.364	6.758
-1.230	NA	0.005	0.639	0.042	0.697	6	-14.424	46.449	6.843
-0.782	0.225	NA	0.368	0.023	NA	5	-16.368	46.486	6.880
0.401	NA	-0.013	NA	0.057	0.499	5	-16.421	46.593	6.987
0.201	0.297	0.118	NA	-0.094	NA	5	-16.754	47.257	7.652
0.791	NA	NA	0.132	NA	NA	3	-20.428	48.189	8.583
-0.538	NA	-0.012	0.350	0.167	NA	5	-17.446	48.641	9.036
0.244	NA	0.166	0.259	NA	NA	4	-19.190	48.733	9.128
-0.826	0.315	0.136	0.395	-0.095	NA	6	-15.953	49.506	9.901
0.292	0.182	0.070	NA	-0.071	0.371	6	-16.011	49.622	10.016
-1.254	0.144	0.070	0.615	-0.058	0.589	7	-14.123	50.246	10.640

(d) *Viral titer, species level*

Intercept	%N	Lf. Long	LMA	Photo	sqrt (Lf. Emerge)	df	logLik	AICc	delta
-7.686	NA	0.828	NA	NA	NA	3	-37.747	82.994	0.000
-9.076	NA	NA	NA	0.521	NA	3	-37.978	83.456	0.462
-8.659	NA	0.518	NA	0.284	NA	4	-37.143	84.953	1.958
-12.254	NA	NA	1.213	0.584	NA	4	-37.305	85.277	2.283
-8.580	-0.537	NA	NA	0.855	NA	4	-37.351	85.369	2.375
-9.790	NA	0.872	0.865	NA	NA	4	-37.385	85.437	2.443
-8.338	0.192	0.740	NA	NA	NA	4	-37.504	85.675	2.680
-7.819	NA	0.793	NA	NA	0.201	4	-37.710	86.087	3.093
-9.066	NA	NA	NA	0.600	-0.447	4	-37.853	86.372	3.377
-11.739	NA	0.503	1.171	0.350	NA	5	-36.462	87.209	4.215
-6.399	NA	NA	NA	NA	NA	2	-41.276	87.257	4.263
-8.293	0.460	NA	NA	NA	NA	3	-40.036	87.572	4.577
-11.453	-0.470	NA	1.074	0.869	NA	5	-36.804	87.894	4.900
-11.355	0.272	0.760	1.128	NA	NA	5	-36.909	88.104	5.109
-8.493	-0.293	0.388	NA	0.525	NA	5	-37.001	88.287	5.292
-8.662	NA	0.503	NA	0.351	-0.348	5	-37.061	88.408	5.414
-7.303	NA	NA	NA	NA	0.974	3	-40.518	88.537	5.542
-10.822	NA	0.795	1.147	NA	0.524	5	-37.163	88.611	5.617
-12.124	NA	NA	1.165	0.603	-0.125	5	-37.296	88.878	5.883
-8.568	-0.550	NA	NA	0.855	0.051	5	-37.350	88.986	5.991
-8.407	0.271	0.756	NA	NA	-0.303	5	-37.460	89.205	6.211
-7.140	NA	NA	0.315	NA	NA	3	-41.241	89.983	6.988
-10.894	0.535	NA	0.973	NA	NA	4	-39.695	90.057	7.063
-8.266	0.426	NA	NA	NA	0.122	4	-40.030	90.727	7.732
-10.261	NA	NA	1.130	NA	1.294	4	-40.120	90.906	7.912
-11.478	-0.208	0.411	1.117	0.519	NA	6	-36.386	91.234	8.240
-11.711	NA	0.502	1.161	0.355	-0.027	6	-36.461	91.384	8.390
-11.702	-0.569	NA	1.200	0.866	0.400	6	-36.727	91.915	8.921
-11.371	0.265	0.758	1.136	NA	0.026	6	-36.909	92.279	9.284
-8.522	-0.243	0.404	NA	0.513	-0.148	6	-36.990	92.441	9.447
-11.174	0.421	NA	1.115	NA	0.447	5	-39.623	93.531	10.537
-11.602	-0.271	0.391	1.179	0.535	0.201	7	-36.367	96.067	13.073

Table 3.10. Blomberg's K tests for effects of host phylogeny in all significant models of infectiousness, susceptibility, vector reproduction, and viral titer at the (a) individual or (b) species level (Blomberg *et al.*, 2003).

	Response	*N*	*Blomberg's K*	*p*
(a)	Infectiousness	50 indiv.	0.340	0.218
	Susceptibility*	138 indiv.	0.045	0.895
	Vector Reproduction	58 indiv.	N/A	N/A
	Viral Titer	50 indiv.	0.108	0.563
(b)	Infectiousness	20 spp.	0.367	0.166
	Susceptibility	23 spp.	0.045	0.872
	Vector	22 spp.	0.376	0.134
	Viral Titer	20 spp.	0.109	0.570

**reprinted from Welsh et al. (2016)*

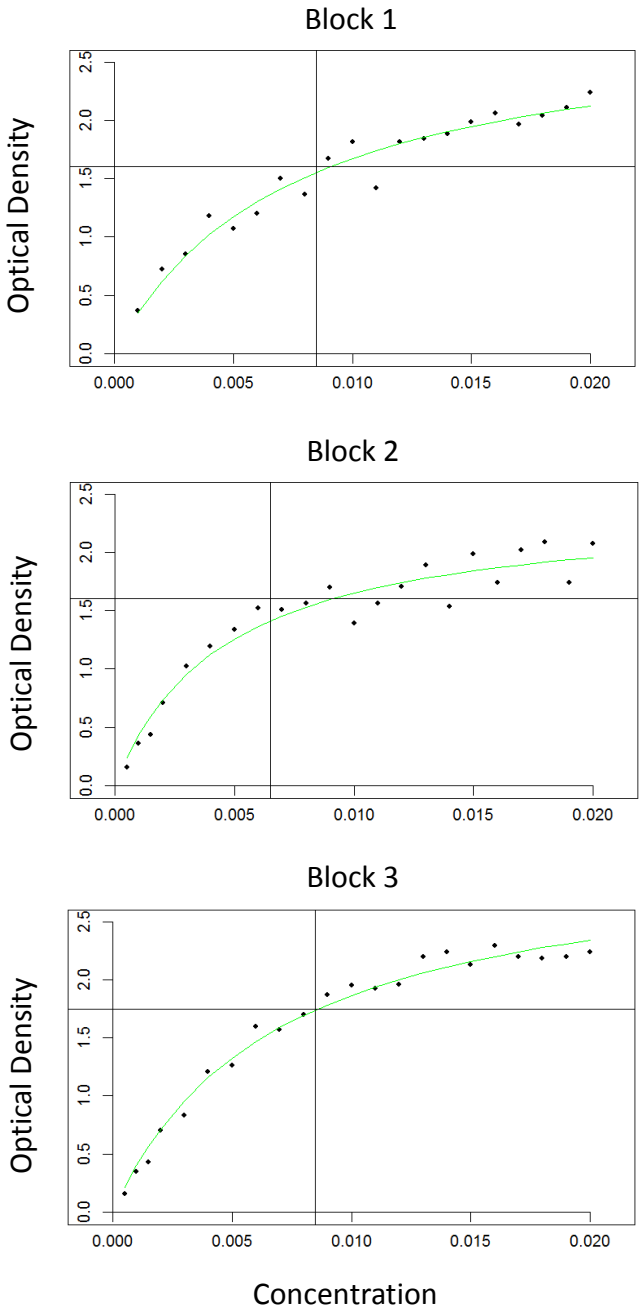

Figure 3.1. Standard curves used to calculate relative viral titer (concentration) from the optical density of each experimental sample in each of three ELISA plates by experimental block. Experimental optical density values ranged from 0 to the horizontal line in each graph, and thus the bottom left quadrat of each graph delineates the segment of each standard curve that was used to calculate relative viral titer.

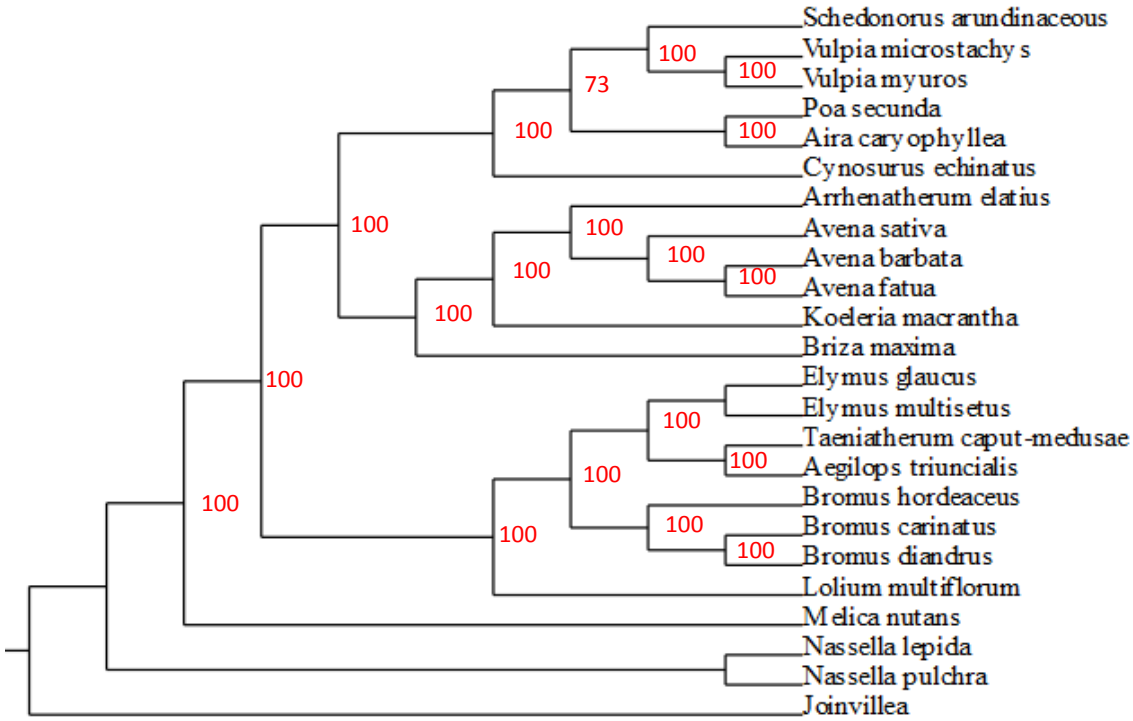

Figure 3.2. Phylogeny used in the phylogenetic analyses. Node labels indicate bootstrap support. Created using phyloGenerator (Pearse and Purvis, 2013) with options '-gene *rbcL*, *matK* –alignment muscle –phylogen RAxML –integrated Bootstrap 1000', and constraint tree topology following Bouchenak-Khelladi et al. (2008). Sequence data was not available for *Elymus multisetus*, *Nassella pulchra*, and *Melica californica*, so polytomies were created for *Elymus* and *Nassella*, and *Melica californica* was replaced with the congener *Melica nutans*. Joinvillea (monocot, Joinvilleaceae) was used as an outgroup.

Figure 3.3. (Next page) Individual-level (a-d) and species level (e-h) models of susceptibility (a, e), infectiousness (b, f), viral titer (c, g), and vector reproduction (d, h). Black lines and shaded regions are linear model predictions and 95% confidence intervals, respectively; points are observed values. At both the individual and species levels, susceptibility, viral titer, and infectiousness increased significantly with PC1, as hosts became more quick-return along the LES. Vector reproduction was unrelated to PC1 at the individual level but increased significantly with PC1 at the species level. Individual-level susceptibility (a) is reprinted from analyses in Welsh et al. (2016). At both levels, viral titer had no effect on host infectiousness (not shown). For (b-d), see Table 3.5 for model specifics, for (a) see Welsh et al. (2016), and for (e-f) see Table 3.6.

Figure 3.3

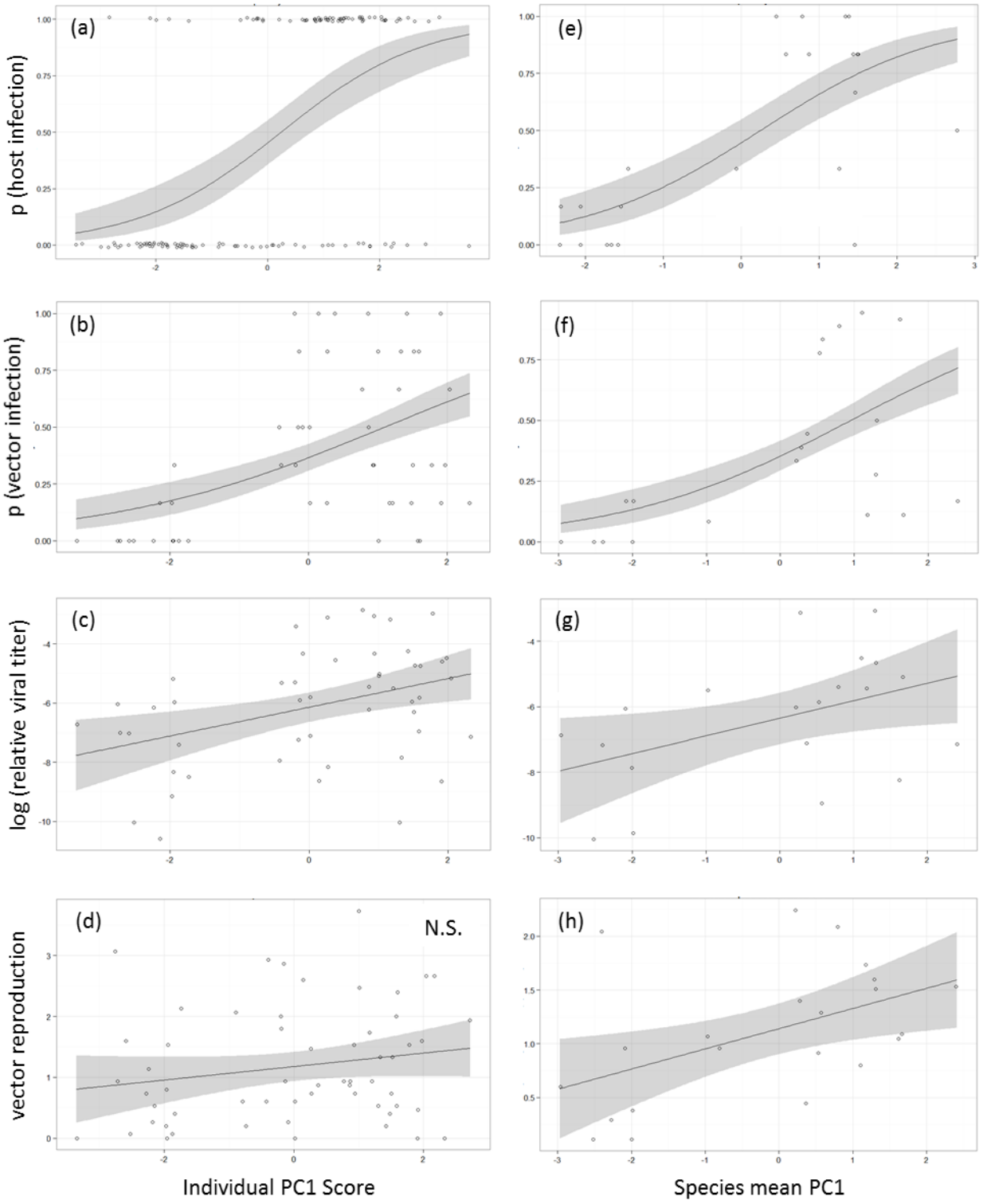
(a)
(b)
(c)
(d)
(e)
(f)
(g)
(h)
p (host infection)
p (vector infection)
log (relative viral titer)
vector reproduction
N.S.
Individual PC1 Score
Species mean PC1

Figure 3.4. (Next page) Relative variable importance (RVI) of each host trait in individual-level (a-c) and species-level (d-g) models of susceptibility (a, d), infectiousness (b, e), viral titer (c, f), and vector reproduction (g). At the individual level, the response of vector reproduction is omitted because it did not vary significantly with individual host PC1 score. (+) or (-) symbols indicate the direction of each effect. N=138 individuals for susceptibility (a), and 50 individuals for viral titer (b) and infectiousness (c). N=32 species for susceptibility (d), 20 species for viral titer (e) and infectiousness (f), and 22 species for vector reproduction (g). Individual-level susceptibility (a) is reprinted from analyses in Welsh et al. (2016). See Tables 3.8 and 3.9 for model AICc values used to calculate RVI.

Figure 3.4

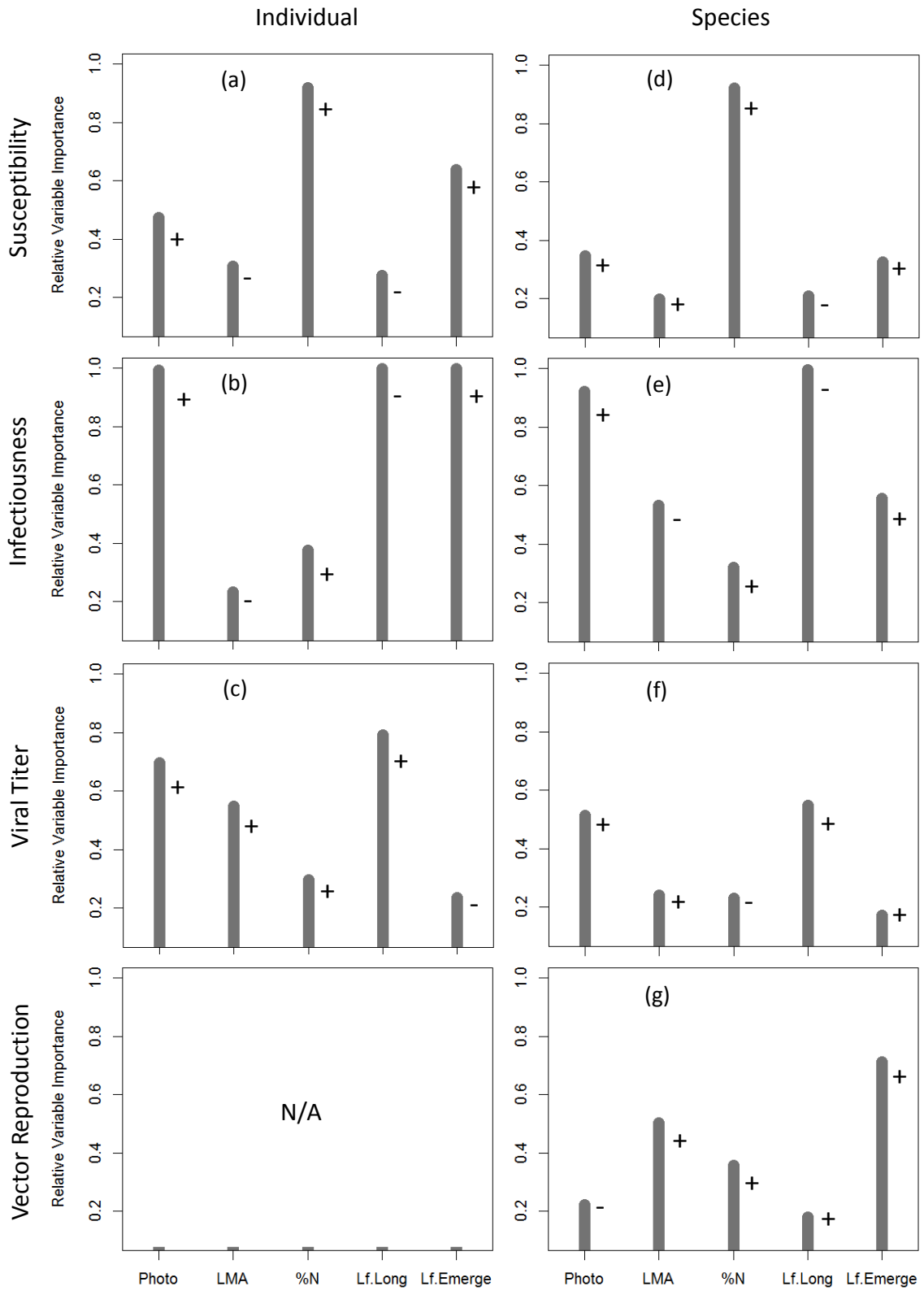
Individual
Species
Susceptibility
Infectiousness
Viral Titer
Vector Reproduction
Relative Variable Importance
(a)
(b)
(c)
(d)
(e)
(f)
(g)
N/A
Photo
LMA
%N
Lf.Long
Lf.Emerge

REFERENCES

Baraloto, C., O. J. Hardy, C. E. T. Paine, K. G. Dexter, C. Cruaud, L. T. Dunning, M. A. Gonzalez, J. F. Molino, D. Sabatier, V. Savolainen, and J. Chave. 2012. Using functional traits and phylogenetic trees to examine the assembly of tropical tree communities. Journal of Ecology **100**:690-701.

Barton, K. 2015. MuMIn: Multi-Model Inference. R package version 1.15.1. http://CRAN.R-project.org/package=MuMIn.

Blomberg, S. P., T. Garland, Jr., and A. R. Ives. 2003. Testing for Phylogenetic Signal in Comparative Data: Behavioral Traits Are More Labile. Evolution **57**:717-745.

Borer, E. T., W. S. Harpole, P. B. Adler, E. M. Lind, J. L. Orrock, E. W. Seabloom, and M. D. Smith. 2014. Finding generality in ecology: a model for globally distributed experiments. Methods in Ecology and Evolution **5**:65-73.

Borer, E. T., E. W. Seabloom, C. E. Mitchell, and A. G. Power. 2010. Local context drives infection of grasses by vector-borne generalist viruses. Ecology Letters **13**:810-818.

Bouchenak-Khelladi, Y., N. Salamin, V. Savolainen, F. Forest, M. Bank, M. W. Chase, and T. R. Hodkinson. 2008. Large multi-gene phylogenetic trees of the grasses (Poaceae): progress towards complete tribal and generic level sampling. Mol Phylogenet Evol **47**:488-505.

Burnham, K. P., and D. R. Anderson. 2002. Model Selection and Multimodel Inference: A Practical Information-Theoretic Approach. 2 edition. Springer-Verlag, New York.

Cable, J. M., B. J. Enquist, and M. E. Moses. 2007. The Allometry of Host-Pathogen Interactions. PLoS ONE **2**:e1130.

Clark, J. S. 2010. Individuals and the Variation Needed for High Species Diversity in Forest Trees. Science **327**:1129-1132.

Clasen, J. L., and J. J. Elser. 2007. The effect of host Chlorella NC64A carbon : phosphorus ratio on the production of Paramecium bursaria Chlorella Virus-1. Freshwater Biology **52**:112-122.

Coley, P. D., J. P. Bryant, and F. S. Chapin, III. 1985. Resource availability and plant antiherbivore defense. Science **230**:895-899.

Copeland, R. 1998. Assaying levels of plant virus by ELISA. Pages 455-460 *in* G. D. Foster and S. C. Taylor, editors. Plant Virology protocols. Humana Press, Clifton, NJ, USA.

Cronin, J. P., M. A. Rúa, and C. E. Mitchell. 2014. Why Is Living Fast Dangerous? Disentangling the Roles of Resistance and Tolerance of Disease. The American Naturalist **184**:172-187.

Cronin, J. P., M. E. Welsh, M. G. Dekkers, S. T. Abercrombie, and C. E. Mitchell. 2010. Host physiological phenotype explains pathogen reservoir potential. Ecology Letters **13**:1221-1232.

Diaz, S., J. G. Hodgson, K. Thompson, M. Cabido, J. H. C. Cornelissen, A. Jalili, G. Montserrat-Marti, J. P. Grime, F. Zarrinkamar, Y. Asri, S. R. Band, S. Basconcelo, P. Castro-Diez, G. Funes, B. Hamzehee, M. Khoshnevi, N. Perez-Harguindeguy, M. C. Perez-Rontome, F. A. Shirvany, F. Vendramini, S. Yazdani, R. Abbas-Azimi, A. Bogaard, S. Boustani, M. Charles, M. Dehghan, L. de Torres-Espuny, V. Falczuk, J. Guerrero-Campo, A. Hynd, G. Jones, E. Kowsary, F. Kazemi-Saeed, M. Maestro-Martinez, A. Romo-Diez, S. Shaw, B. Siavash, P. Villar-Salvador, and M. R. Zak. 2004. The plant traits that drive ecosystems: Evidence from three continents. Journal of Vegetation Science **15**:295-304.

Dobson, A. 2004. Population dynamics of pathogens with multiple host species. American Naturalist **164**:S64-S78.

Fortunel, C., C. E. T. Paine, P. V. A. Fine, N. J. B. Kraft, and C. Baraloto. 2014. Environmental factors predict community functional composition in Amazonian forests. Journal of Ecology **102**:145-155.

Fynn, R. W. S., C. D. Morris, and K. P. Kirkman. 2005. Plant strategies and trait trade-offs influence trends in competitive ability along gradients of soil fertility and disturbance. . Journal of Ecology **93**:384-394.

García-Guzmán, G., and M. Heil. 2014. Life histories of hosts and pathogens predict patterns in tropical fungal plant diseases. New Phytologist **201**:1106-1120.

Gervasi, S. S., D. J. Civitello, H. J. Kilvitis, and L. B. Martin. 2015. The context of host competence: a role for plasticity in host–parasite dynamics. Trends in Parasitology.

Gray, S. M., A. G. Power, D. M. Smith, A. J. Seaman, and N. S. Altman. 1991. Aphid transmission of Barley Yellow Dwarf Virus - acquisition access periods and virus concentration requirements. Phytopathology **81**:539-545.

Han, B. A., J. P. Schmidt, S. E. Bowden, and J. M. Drake. 2015. Rodent reservoirs of future zoonotic diseases. Proceedings of the National Academy of Sciences.

Handel, A., and P. Rohani. 2015. Crossing the scale from within-host infection dynamics to between-host transmission fitness: a discussion of current assumptions and knowledge. Philosophical Transactions of the Royal Society B-Biological Sciences **370**.

Haydon, D. T., S. Cleaveland, L. H. Taylor, and M. K. Laurenson. 2002. Identifying reservoirs of infection: a conceptual and practical challenge. Emerging Infectious Diseases **Dec 2002**.

Herms, D. A., and W. J. Mattson. 1992. The dilemma of plants: to grow or defend. Quarterly Review of Biology **67**:283-335.

Hersh, M. H., M. Tibbetts, S. Y. Strauss, R. Ostfeld, and F. Keesing. 2012. Reservoir competence of wildlife host species for *Babesia microti*. Emerging Infectious Diseases **18**.

Huang, Z. Y. X., W. F. de Boer, F. van Langevelde, V. Olson, T. M. Blackburn, and H. H. T. Prins. 2013. Species' Life-History Traits Explain Interspecific Variation in Reservoir Competence: A Possible Mechanism Underlying the Dilution Effect. PLoS ONE **8**:e54341.

Huenneke, L. F., S. P. Hamburg, R. Koide, H. A. Mooney, and P. M. Vitousek. 1990. Effects of Soil Resources on Plant Invasion and Community Structure in Californian Serpentine Grassland. Ecology **71**:478-491.

Ives, A. R., P. E. Midford, and T. Garland. 2007. Within-species variation and measurement error in phylogenetic comparative methods. Systematic Biology **56**:252-270.

Johnson, P. T. J., J. R. Rohr, J. T. Hoverman, E. Kellermanns, J. Bowerman, and K. B. Lunde. 2012. Living fast and dying of infection: host life history drives interspecific variation in infection and disease risk. Ecology Letters **15**:235-242.

Jung, V., C. Violle, C. Mondy, L. Hoffmann, and S. Muller. 2010. Intraspecific variability and trait-based community assembly. Journal of Ecology **98**:1134-1140.

Keesing, F., M. H. Hersh, M. Tibbetts, D. J. McHenry, S. Duerr, J. Brunner, M. Killilea, K. LoGiudice, K. A. Schmidt, and R. S. Ostfeld. 2012. Reservoir Competence of Vertebrate Hosts for Anaplasma phagocytophilum. Emerging Infectious Diseases **18**:2013-2016.

Kilpatrick, A. M., P. Daszak, M. J. Jones, P. P. Marra, and L. D. Kramer. 2006. Host heterogeneity dominates West Nile virus transmission. Proceedings of the Royal Society B-Biological Sciences **273**:2327-2333.

Krober, W., M. Bohnke, E. Welk, C. Wirth, and H. Bruelheide. 2012. Leaf Trait-Environment Relationships in a Subtropical Broadleaved Forest in South-East China. PLoS ONE **7**:e35742.

Kursar, T. A., and P. D. Coley. 2003. Convergence in defense syndromes of young leaves in tropical rainforests. Biochemical Systematics and Ecology **31**:929-949.

Laliberte, E., B. Shipley, D. A. Norton, and D. Scott. 2012. Which plant traits determine abundance under long-term shifts in soil resource availability and grazing intensity? Journal of Ecology **100**:662-677.

Laughlin, D. C., C. Joshi, P. M. van Bodegom, Z. A. Bastow, and P. Z. Fule. 2012. A predictive model of community assembly that incorporates intraspecific trait variation. Ecology Letters **15**:1291-1299.

Lebrija-Trejos, E., E. A. Perez-Garcia, J. A. Meave, F. Bongers, and L. Poorter. 2010. Functional traits and environmental filtering drive community assembly in a species-rich tropical system. Ecology **91**:386-398.

Lee, K. A., M. Wikelski, W. D. Robinson, T. R. Robinson, and K. C. Klasing. 2008. Constitutive immune defences correlate with life-history variables in tropical birds. Journal of Animal Ecology **77**:356-363.

Leishman, M. R., T. Haslehurst, A. Ares, and Z. Baruch. 2007. Leaf trait relationships of native and invasive plants: community- and global-scale comparisons. New Phytologist **176**:635-643.

Lloyd-Smith, J. O., S. Funk, A. R. McLean, S. Riley, and J. L. N. Wood. 2015. Nine challenges in modelling the emergence of novel pathogens. Epidemics **10**:35-39.

Lloyd-Smith, J. O., S. J. Schreiber, P. E. Kopp, and W. M. Getz. 2005. Superspreading and the effect of individual variation on disease emergence. Nature **438**:355-359.

Lochmiller, R. L., and C. Deerenberg. 2000. Trade-offs in evolutionary immunology: just what is the cost of immunity? Oikos **88**:87-98.

Maron, J. L., and P. G. Connors. 1996. A native nitrogen-fixing shrub facilitates weed invasion. Oecologia **105**:302-312.

Maron, J. L., and R. L. Jefferies. 1999. Bush lupine mortality, altered resource availability, and alternative vegetation states. Ecology **80**:443-454.

Mattson, W. J., Jr. 1980. Herbivory in relation to plant nitrogen content. Annual Review of Ecology and Systematics **11**:119-161.

Mitchell, C. E., P. B. Reich, D. Tilman, and J. V. Groth. 2003. Effects of elevated CO_2, nitrogen deposition, and decreased species diversity on foliar fungal plant disease. Global Change Biology **9**:438-451.

Ostfeld, R. S., T. Levi, A. E. Jolles, L. B. Martin, P. R. Hosseini, and F. Keesing. 2014. Life History and Demographic Drivers of Reservoir Competence for Three Tick-Borne Zoonotic Pathogens. PLoS ONE **9**:e107387.

Pearse, W. D., and A. Purvis. 2013. phyloGenerator: an automated phylogeny generation tool for ecologists. Methods in Ecology and Evolution **4**:692-698.

Poland, J. A., P. J. Balint-Kurti, R. J. Wisser, R. C. Pratt, and R. J. Nelson. 2009. Shades of gray: the world of quantitative disease resistance. Trends in Plant Science **14**:21-29.

Poorter, L., and F. Bongers. 2006. Leaf traits are good predictors of plant performance across 53 rain forest species. Ecology **87**:1733-1743.

R Core Team. 2015. R: A language and environment for statistical computing. R Foundation for Statistical Computing, Vienna, Austria. URL https://www.R-project.org/

Reich, P. B. 2001. Body size, geometry, longevity and metabolism: do plant leaves behave like animal bodies? Trends in Ecology & Evolution **16**:674-680.

Reich, P. B. 2014. The world-wide 'fast-slow' plant economics spectrum: a traits manifesto. Journal of Ecology **102**:275-301.

Reich, P. B., D. S. Ellsworth, M. B. Walters, J. M. Vose, C. Gresham, J. C. Volin, and W. D. Bowman. 1999. Generality of leaf trait relationships: a test across six biomes. Ecology **80**:1955-1969.

Restif, O., D. T. S. Hayman, J. R. C. Pulliam, R. K. Plowright, D. B. George, A. D. Luis, A. A. Cunningham, R. A. Bowen, A. R. Fooks, T. J. O'Shea, J. L. N. Wood, and C. T. Webb. 2012. Model-guided fieldwork: practical guidelines for multidisciplinary research on wildlife ecological and epidemiological dynamics. Ecology Letters **15**:1083-1094.

Revell, L. J. 2012. phytools: An R package for phylogenetic comparative biology (and other things). Methods in Ecology and Evolution **3**:217-223.

Rochow, W. F., A. I. E. Aapola, M. K. Brakke, and L. E. Carmichael. 1971. Purification and antigenicity of three isolates of barley yellow dwarf virus. Virology **46**:117-126.

Rua, M. A., J. Umbanhowar, S. J. Hu, K. O. Burkey, and C. E. Mitchell. 2013. Elevated CO2 spurs reciprocal positive effects between a plant virus and an arbuscular mycorrhizal fungus. New Phytologist **199**:541-549.

Seabloom, E. W., W. S. Harpole, O. J. Reichman, and D. Tilman. 2003. Invasion, competitive dominance, and resource use by exotic and native California grassland species. Proceedings Of The National Academy Of Sciences Of The United States Of America **100**:13384-13389.

Stevens, C. J., N. B. Dise, J. O. Mountford, and D. J. Gowing. 2004. Impact of nitrogen deposition on the species richness of grasslands. Science **303**:1876-1879.

Streicker, D. G., A. Fenton, and A. B. Pedersen. 2013. Differential sources of host species heterogeneity influence the transmission and control of multihost parasites. Ecology Letters **16**:975-984.

Throop, H. L., and M. T. Lerdau. 2004. Effects of nitrogen deposition on insect herbivory: implications for community and ecosystem processes. Ecosystems **7**:109-133.

Todesco, M., S. Balasubramanian, T. T. Hu, M. B. Traw, M. Horton, P. Epple, C. Kuhns, S. Sureshkumar, C. Schwartz, C. Lanz, R. A. E. Laitinen, Y. Huang, J. Chory, V. Lipka, J. O. Borevitz, J. L. Dangl, J. Bergelson, M. Nordborg, and D. Weigel. 2010. Natural allelic variation underlying a major fitness trade-off in Arabidopsis thaliana. Nature **465**:632-636.

Umaña, M. N., C. Zhang, M. Cao, L. Lin, and N. G. Swenson. 2015. Commonness, rarity, and intraspecific variation in traits and performance in tropical tree seedlings. Ecology Letters **18**:1329-1337.

Viana, M., R. Mancy, R. Biek, S. Cleaveland, P. C. Cross, J. O. Lloyd-Smith, and D. T. Haydon. 2014. Assembling evidence for identifying reservoirs of infection. Trends in Ecology & Evolution **29**:270-279.

Violle, C., B. J. Enquist, B. J. McGill, L. Jiang, C. H. Albert, C. Hulshof, V. Jung, and J. Messier. 2012. The return of the variance: intraspecific variability in community ecology. Trends in Ecology & Evolution **27**:244-252.

Vrede, T., D. R. Dobberfuhl, S. Kooijman, and J. J. Elser. 2004. Fundamental connections among organism C : N : P stoichiometry, macromolecular composition, and growth. Ecology **85**:1217-1229.

Weiss, S. B. 2006. Impacts of nitrogen deposition on California ecosystems and biodiversity, CEC-500-2005-165.*in* California Energy Commission, editor. PIER Energy-Related Environmental Research.

Welsh, M. E., J. P. Cronin, and C. E. Mitchell. 2016. The role of habitat filtering in the leaf economics spectrum and plant susceptibility to pathogen infection. Journal of Ecology.

Whitaker, B. K., M. A. Rua, and C. E. Mitchell. 2015. Viral pathogen production in a wild grass host driven by host growth and soil nitrogen. New Phytologist **207**:760-768.

Wright, I. J., P. B. Reich, M. Westoby, D. D. Ackerly, Z. Baruch, F. Bongers, J. Cavender-Bares, T. Chapin, J. H. C. Cornelissen, M. Diemer, J. Flexas, E. Garnier, P. K. Groom, J. Gulias, K. Hikosaka, B. B. Lamont, T. Lee, W. Lee, C. Lusk, J. J. Midgley, M. L. Navas, U. Niinemets, J. Oleksyn, N. Osada, H. Poorter, P. Poot, L. Prior, V. I. Pyankov, C. Roumet, S. C. Thomas, M. G. Tjoelker, E. J. Veneklaas, and R. Villar. 2004. The worldwide leaf economics spectrum. Nature **428**:821-827.

Wright, J. P., and A. Sutton-Grier. 2012. Does the leaf economic spectrum hold within local species pools across varying environmental conditions? Functional Ecology **26**:1390-1398.

Zavaleta, E. S., M. R. Shaw, N. R. Chiariello, B. D. Thomas, E. E. Cleland, C. B. Field, and H. A. Mooney. 2003. Grassland responses to three years of elevated temperature, CO(2), precipitation, and N deposition. Ecological Monographs **73**:585-604.

CHAPTER 4: TRAIT-BASED VARIATION IN PATHOGEN IMPACT ACROSS HOSTS AND ENVIRONMENTS

Introduction

To counter the effect of enemies on fitness, host plants have evolved a diversity of defense strategies, which are broadly grouped into means avoiding attack (resistance) vs. means of tolerating it. Tolerance is defined as the ability to minimize the fitness impacts of enemy damage, as quantified by the slope of the relationship between relative fitness and proportional damage (Strauss and Agrawal 1999; Stowe et al. 2000; Wise et al. 2008). While the concept of tolerance as a form of defense has mostly been applied to plant-herbivore interactions, there is growing recognition of the importance of tolerance as a form of defense against pathogens and parasites (Baucom and de Roode 2011; Raberg et al. 2009; Schneider and Ayres 2008). Tolerance varies widely both within and among host species (Agrawal and Fishbein 2008; Leimu and Koricheva 2006; Hawkes and Sullivan 2001), and variation in tolerance is expected to influence the outcome of species interactions, the dynamics of host-pathogen coevolution, and the course of epidemics (Chase et al. 2000; Boots 2008; Gervasi et al. 2015). Despite its ecological and evolutionary significance, variation in tolerance—particularly tolerance of pathogen damage—remains poorly explained, both within and among host species. Within species across resource supply gradients, host growth traits and resource economics are hypothesized to drive variation in tolerance (Wise and Abrahamson 2007; Herms and Mattson 1992). Across species, traits related to host growth, plasticity, and resistance are hypothesized to drive variation in tolerance (Strauss and Agrawal 1999; Fornoni and Nunez-Farfan 2003). Of

these potential drivers, empirical work has yet to produce a consensus set of the processes and traits most responsible for intra- and interspecific variation in tolerance (Hawkes and Sullivan 2001; Agrawal 2011; Tiffin 2000). To address this, we experimentally tested multiple hypotheses explaining intraspecific variation in tolerance across resource supply gradients and trait-based variation in tolerance across host species.

Across resource supply gradients, host species' tolerance is predicted to increase, decrease, or both, depending on the hypothesis. Table 4.1 summarizes four key hypotheses of intraspecific variation in tolerance with resource supply: the Growth Rate Model (GRM: Hilbert et al. 1981; Wise and Abrahamson 2007), the Compensatory Continuum Hypothesis (CCH: Maschinski and Whitham 1989; Wise and Abrahamson 2007), the Limiting Resource Hypothesis (LRH: Wise and Abrahamson 2005; Wise and Abrahamson 2007), and growth-defense tradeoffs (GDTs: Coley et al. 1985; Herms and Mattson 1992). Moving from low to high resource supply, the GRM predicts that tolerance will decrease, the CCH and GDTs predict that tolerance will increase, and the LRH predicts that tolerance will either increase or decrease. All hypotheses agree that tolerance is related to the relative growth rate of hosts and that growth is resource limited. They differ in the specifics of how growth rate influences tolerance and the number of resources considered. Only the LRM explicitly considers more than one resource, and this allows its predictions to be contingent. For example, if enemy damage disproportionately affects carbon acquisition, the LRM predicts that tolerance will increase with carbon supply, as hosts become less carbon-limited, but decrease with nitrogen supply, as hosts shift from being nitrogen- to carbon-limited. Because the LRM predicts variable responses of tolerance to resource supply, its predictions are better supported by empirical data than those of the GRM, the CCH, or GDTs (Hawkes and Sullivan 2001; Wise and Abrahamson 2007; Banta et al. 2010). However, few

studies have simultaneously investigated support for both the mechanisms and predictions of the LRM (Wise and Abrahamson 2005; Banta et al. 2010).

Across host species, empirical and theoretical work has generated a set of species traits hypothesized to influence tolerance and thus explain interspecific variation in tolerance (Table 4.2). These traits can be grouped into: 1) traits that influence or estimate growth rate 2) storage traits, 3) traits that influence or estimate plasticity in response to damage, and 4) traits that represent alternate allocation strategies and may trade off with tolerance. Tolerance is predicted to increase with host growth rate; therefore, it is predicted to increase with traits that confer greater rates of resource acquisition or utilization, and to decrease with traits that impose a high cost of tissue construction. Hosts with greater below-ground carbon stores are also predicted to be more tolerant, as are hosts with greater physiological or morphological plasticity in response to damage (Fornoni and Nunez-Farfan 2003; van der Meijden et al. 1988; Rosenthal and Kotanen 1994; Strauss and Agrawal 1999; Stowe et al. 2000; Cronin et al. 2014). In addition, tolerance and resistance are often considered redundant strategies of reducing enemy impact, and tolerance is predicted to increase as investment in resistance decreases (Fornoni and Nunez-Farfan 2003; van der Meijden et al. 1988; Rosenthal and Kotanen 1994; Strauss and Agrawal 1999). Empirical support for a role of growth traits, storage traits, or plasticity in generating variation in tolerance has been equivocal. While tolerance increased with these traits in some studies (van der Meijden et al. 1988; Bilbrough and Richards 1993; Kursar and Coley 2003), these associations are not consistent across studies (Rosenthal and Welter 1995; Bilbrough and Richards 1993; Agrawal and Fishbein 2008). Resistance-tolerance tradeoffs have garnered similarly mixed support (Leimu and Koricheva 2006).

Across host species and resource supply rates, variation in tolerance can be driven by

suites of covarying traits (Agrawal and Fishbein 2006; Tiffin 2000; Cronin et al. 2010), and, furthermore, the strength of resistance-tolerance tradeoffs can vary with resource supply (Fornoni et al. 2003; Valverde et al. 2003). In an effort to synthesize and operationalize these ideas, one recent hypothesis suggests that tolerance constitutes one of several pathways through which a set of covarying host traits can influence the ultimate fitness consequences of enemy attack (Cronin et al. 2014). Because host traits respond to resource supply, this hypothesis also argues that measuring and using trait values as they are expressed in a given context, rather than species means, could eliminate the need to consider resource supply explicitly. In the one test of this hypothesis to date, several covarying host traits (representing "Host Developmental Tempo", or "HDT") determined the impact of pathogen infection on the biomass of six host species. Structural equation modeling indicated that HDT influenced the impact of infection on biomass via 1) a host resource economics pathway, and 2) a post-infection, within-host resistance pathway. Variation in the impact of infection on biomass was mostly driven by the within-host resistance pathway, and hosts with a slow developmental tempo were more resistant and lost proportionally less biomass to infection. While the resource economics pathway indicated that hosts with a fast developmental tempo were better able to upregulate photosynthesis or reallocate carbon in response to infection, these responses were not strongly associated with a reduced impact of infection.

In the most comprehensive test of tolerance mechanisms to date, we used 23 hosts of a generalist pathogen and a resource supply treatment to test: 1) the mechanisms and predictions of four key hypotheses of the effect of resource supply on intraspecific variation in tolerance (Table 4.1), 2) whether specific host traits were consistently associated with interspecific variation in tolerance (Table 4.2), and 3) across host species and resource supply rates, whether HDT can

predict the impact of infection via a resource economics pathway, a post-infection resistance pathway, or both.

Materials and Methods

Study system

To experimentally test several theoretical explanations of variation in tolerance both within and among species and environments, we used 23 grass species from the Mediterranean grasslands of California as a model hosts (Table 4.3). These grasses all share a generalist, vector-borne pathogen, *Barley yellow dwarf virus PAV* (BYDV-PAV, family *Luteoviridae*), which we used as a model natural enemy. BYDV-PAV is a phloem-infecting RNA virus that is obligately and persistently transmitted by certain species of aphids. Focal host species were selected from over 90 grass species present at the University of California's Hopland Research and Extension Center (HREC) in Hopland, CA, USA. To capture a diversity of locally and regionally co-occurring ecological strategies, focal hosts were selected based on life history (annual vs. perennial), local abundance at HREC (including all perennial and common annual species in a set of observational plots), and geographic frequency across 11 sites spanning 15° latitude (Borer et al. 2010; Borer et al. 2014: CA and OR, US sites).

Experimental design and protocol

We quantified variation in host tolerance and host traits in two separate greenhouse experiments at the University of North Carolina, Chapel Hill, NC, USA. Host tolerance and all host physiological traits were quantified in the first experiment (the Tolerance Experiment), which ran from July – October 2011. Variation in host resistance to BYDV-PAV was quantified in an earlier experiment (the Resistance Experiment), which ran from August – November 2010 (Welsh et al. 2016).

Tolerance experiment

We factorially manipulated host identity (23 Species; Table 4.3) and environment (two levels of nitrogen supply; Table 4.4) in a randomized block design (N=3), for a total of 138 treatment-block combinations (i.e., 138 replicates). Each replicate integrated data from up to three individuals: 1) an infected individual 2) a paired, healthy individual, and 3) a biomass control individual, which was harvested at the time of infection, for a total of 414 experimental individuals. For an observation to be complete, all three individuals (infected, healthy, biomass control) had to be represented, and incomplete observations were excluded from the analyses, which reduced the sample size to different degrees for different analyses (see *Statistical analyses* for details). Infected individuals were used to quantify infected biomass and pathogen load (relative viral titer), healthy individuals were used to quantify host traits and healthy biomass, biomass control individuals were used to control for any pre-infection differences in biomass, and the biomass of healthy and biomass control individuals was used to quantify relative growth rate (RGR over 35 days). All individuals were grown in a separate 1L Conetainer pot (Stuewe and Sons, Inc., OR, US) filled with a 50:50 mix of soil and sand, with ample phosphorous, potassium, and micronutrients (Table 4.4). Planting was timed to minimize differences in grass host ontogeny, such that all hosts reached the two-leaf stage within a week of each other. At one week post-germination, all hosts were thinned to one individual per pot.

At the two-leaf stage, about two weeks post-germination, we generated the infected hosts by caging infected aphid vectors on each (5 *Rhopalosiphum padi* aphids/host). To generate the required number of infected hosts, we varied the number of inoculated host individuals from 6-18 per host species-nitrogen treatment combination, depending on the observed resistance of each host species in the Resistance Experiment. Infected vectors were produced by feeding

aphids in dishes on lab-maintained, infected host tissue of the agricultural host *Avena sativa* var. Coast Black Oats for 48 hours. Vectors were propagated from field-collected populations in New York, USA, and the virus isolate was obtained from a wild *Avena sativa* L. individual in New York, US (Rochow et al. 1971; Whitaker et al. 2015; Rua et al. 2013). After three days, vectors were removed with the insecticide Asana XL (DuPont, DE, USA). Simultaneously with the virus inoculation to generate the infected hosts, paired, healthy host individuals were generated in a mock-inoculation procedure that was identical except that the aphids had been fed on uninfected host tissue, and thus the paired, healthy hosts were exposed to uninfected vectors. Also simultaneous with the virus inoculation to generate infected hosts, all biomass control individuals were harvested and their above- and below-ground biomass was separated, washed, dried, and weighed (Table 4.5).

Beginning at the four-leaf stage, about three weeks post-germination, we measured four physiological traits on all healthy host individuals: maximum photosynthetic capacity, leaf mass per area (LMA), percent tissue carbon, and percent tissue nitrogen (Table 4.5). Photosynthetic capacity was quantified with an infrared gas analyzer, the CIRAS-2 Portable Photosynthesis System V2.01 (PP Systems). After all host traits had been measured, at 7 weeks post-germination and 35 days after the inoculations, all hosts were harvested. At harvest, we counted the number of tillers on each host and separated their above- and below-ground biomass. The belowground biomass of each host was washed, dried, and weighed. Of the above-ground biomass, a fresh sample of about 0.5g was clipped, weighed, and prepped to be tested for viral infection. The remaining above-ground biomass was weighed, dried, and then weighed again. For each host, its above-ground wet to dry biomass weight ratio was used to back-calculate the dry weight of the fresh sample that was tested for virus infection. This back-calculated dry

weight was included in the total above-ground biomass weight.

The fresh above-ground tissue samples from all host individuals were tested for BYDV-PAV infection using Enzyme-Linked Immunosorbent Assays (ELISA; Agdia Inc., IN, US). Infection status was determined for each host based on optical density values from a microplate reader (ELx-800; BioTek, VT, USA). All mock-inoculated hosts were determined to be uninfected. As expected, a fraction of virus-inoculated hosts were also determined to be uninfected, and these were not considered further. Of the virus-inoculated hosts that were determined to be infected, one from each species-nitrogen-block combination was selected randomly and paired with the healthy and biomass control hosts of the same treatment combination.

On each paired, infected host, relative viral titer was quantified by back-calculating from its optical density value using a curve of optical density values vs. a standard dilution series of infected tissue within each ELISA plate. The infected tissue used for the dilution series came from a lab-maintained, infected individual of *Avena sativa* var. Coast Black Oats. Prior to fitting standard curves and back-calculating relative titer, all optical density values were corrected for potential species-level effects of plant compounds by subtracting the optical densities of healthy control tissue from the same ELISA plate. R^2 values for standard curves ranged from 0.962-0.999. Building on principles from Copeland (1998), our specific protocol followed that of (Whitaker et al. 2015) with one exception: our standard curve did not include a standard with a relative titer of 0.5 because, in their experiment, this value was often above the range in which optical density values began to saturate in response to increasing viral titer. In all plates, our sample optical density values fell well within the lower (non-asymptotic) range of the optical densities of the standard curve (Fig. 4.1).

We quantified tolerance by dividing the proportional effect of infection on total host biomass by relative viral titer. Prior to quantifying tolerance, we controlled for any pre-infection differences in biomass across observations by subtracting the biomass of the biomass control individual from that of both healthy and infected individuals. We calculated the relative growth rate (RGR) of healthy and infected individuals by subtracting the biomass of the paired, biomass control individual from their biomass and then dividing by 35 days, the length of time between harvests. Root mass fraction (RMF) of healthy and infected individuals was calculated by dividing their root biomass by their total biomass. To quantify the response of tolerance and tissue carbon:nitrogen (C:N) ratio to increased nitrogen supply, we calculated the absolute difference in value between low and high nitrogen treatments for each combination of host species and experimental block. We used proportional differences between infected and healthy individuals to quantify the effect of infection on RMF, tiller number, RGR, and total biomass (for all calculations, see Table 4.6 for specifics).

Resistance Experiment

In a randomized, blocked design (N=6), we factorially manipulated host identity (23 species; Table 4.3) and environment (two levels of nitrogen supply; Table 4.4) for a total of 276 host individuals. At 4.5 weeks post germination, all hosts were exposed to infection by caging five *Rhopalosiphum padi* vectors carrying BYDV-PAV on each host. The virus isolate was obtained from a wild *Bromus vulgaris* (Hook.) Shear individual in Oregon, US (Cronin et al. 2010; Cronin et al. 2014). After three days, vectors were removed with horticultural oil. Five weeks after exposure, the infection status of all hosts was determined via Enzyme-Linked Immunosorbent Assays (ELISAs; Agdia Inc., IN, US). For each combination of host species and nitrogen treatment, resistance was calculated by dividing the number of uninfected individuals

by the total number (six) of individuals that were exposed to infected vectors (Table 4.6). See Welsh et al. (2016) for detailed methods.

Statistical analyses

Effects of resource supply on tolerance. To test the predictions of the GRM, we used linear regression to test for a positive effect of nitrogen supply on species mean RGR and a negative effect of nitrogen supply on species mean tolerance. To test the predictions of the CCH, we used linear regression to test for a positive effect of nitrogen supply on species mean RGR and a positive effect of nitrogen supply on species mean tolerance. Because growth-defense tradeoffs are a potential mechanism of the CCH, we also used phylogenetic generalized least squares (PGLS) regression to test for a negative relationship between the response of species mean tolerance to increased nitrogen supply and the response of species mean resistance to increased nitrogen supply (Δ Tolerance and Δ Resistance in Table 4.6). In testing for growth-defense tradeoffs, PGLS was used to control for the possibility of phylogenetic autocorrelation in species plasticity. To test the predictions of the LRM, we again used PGLS regression to test for a positive relationship between the response of species mean tolerance to increased nitrogen supply and the response of species mean tissue C:N ratios to increased nitrogen supply (Δ Tolerance and Δ C:N in Table 4.6).

All analyses were run in R v 3.2.2 (R Core Team 2015). Linear regressions used the *lm* and ANOVA functions in the base package. PGLS regressions used the *gls* function in the *nlme* package with the correlation argument set to "corBrownian" and the phylogeny in Fig. 4.2 (Pinheiro et al. 2015; Pearse and Purvis 2013; Bouchenak-Khelladi et al. 2008). Of 23 species, eight were excluded from the analyses due to missing tolerance data (when inoculations failed to generate infected pairs); if a species was excluded from either nitrogen treatment it was removed

from the dataset entirely (Table 4.7).

Variation in tolerance across species. Across species within each nitrogen treatment, we used PGLS regression to test for significant, phylogenetically controlled relationships between species mean tolerance and each of nine other species mean traits hypothesized to effect tolerance. To test for effects of growth traits on tolerance, we tested for positive relationships between tolerance and species mean RGR, species mean photosynthetic capacity (Photo), and species mean tissue nitrogen concentration (%N), and we tested for negative relationships between tolerance and species mean C:N and LMA. To test whether species with greater below-ground carbon stores were more tolerant, we tested for a positive relationship between species mean RMF and tolerance. To test whether tolerance is affected by trait plasticity, we tested for a negative relationship between tolerance and the response of RMF to infection (ΔRMF), and a positive relationship between tolerance and the response of tiller number to infection (Δ Tillers; see Tables 4.5 and 4.6 for variable descriptions and calculations). To test for a resistance-tolerance tradeoff, we tested for a negative relationship between species mean resistance and species mean tolerance.

Again, all analyses were run in R v 3.2.2 and PGLS regressions used the *gls* function in the *nlme* package with the correlation argument set to "corBrownian" and the phylogeny in Fig. 4.2 (R Core Team 2015; Pinheiro et al. 2015). Because these analyses were conducted within each nitrogen treatment, species with missing data within a nitrogen treatment were excluded from the analysis of that nitrogen treatment. Of 23 species, eight were excluded from the analyses at low nitrogen and six were excluded from the analyses at high nitrogen (Table 4.7). Lastly, as the traits in these analyses have been hypothesized to affect variation in tolerance across species independent of resource supply, we focus our results and discussion on the host

traits that had a consistent effect on tolerance across nitrogen treatments.

The impact of infection across species and resource supply rates. Across host species and nitrogen treatments, and using observations at the individual level, we used structural equation modeling (SEM) to test whether a suite of covarying host traits determined the fitness impact of pathogen infection. Specifically, we used the metamodel of Cronin et al. (2014) to design a causal model (SEM) that mimicked theirs as closely as possible with our data. Their metamodel hypothesizes that 1) a suite of covarying host traits will be good indicators of the latent variable Host Developmental Tempo (HDT), and 2) HDT can drive variation in the impact of infection via a post-infection resistance pathway, a host resource economics pathway, or both. The resource economics pathway is mediated by host plasticity, specifically the responses of RMF and photosynthetic rate to infection. Relative to Cronin et al. (2014), our causal model differed in two ways. First, we did not have photosynthetic data on infected individuals, so we instead used the effect of infection on tiller number to estimate the plasticity of carbon acquisition in response to infection. Second, our model used three of the same host traits as indicators of HDT (LMA, RMF, and %N), but lacked the trait of tissue phosphorous concentration and used two additional traits (Photo and RGR; Fig. 4.3).

All analyses were run in R v 3.2.2 (R Core Team 2015). To fit the measurement component of the SEM, we conducted confirmatory factor analyses (CFAs) in the *lavaan* package to test for an axis of host developmental tempo (HDT) among healthy host individuals (Fig. 4.3 measurement; Rosseel 2012). To begin, we ran two 'full' CFAs: the first included five mock-inoculated host traits as indicator variables (Photo, %N, RGR, RMF, and LMA; Tables 4.5 and 4.6), and the second included all the same traits except the RMF of biomass control individuals was substituted for that of mock-inoculated individuals. For each full CFA, non-

significant indicators were removed sequentially and the fit of each reduced CFA was evaluated. We considered HDT well measured when all indicators were significant and the CFA was a good fit to the data ($\chi 2$ $P>0.05$, comparative fit index (CFI)> 0.90, and Tucker-Lewis index (TLI)>0.90). Prior to analyses, three variables were $\log_{10}$-transformed to meet assumptions of normality: mock-inoculated %N, mock-inoculated LMA, and the RMF of biomass control individuals.

Prior to analyzing the structural component of the SEM, we controlled for any pre-infection differences in biomass by subtracting the root, shoot, or total biomass of biomass control individuals from that of paired infected and healthy individuals. We then calculated Δ RMF and Δ biomass by dividing the RMF of infected individuals by that of paired, healthy individuals (Table 4.6). Because we neglected to count tillers on biomass control individuals, we were unable to control for any pre-inoculation differences in the calculation of Δ tillers. However, in our experimental timeline, the planting of each species was staggered such that all individuals were inoculated around the 2-leaf stage, so large, pre-infection differences in tiller number are unlikely.

To control for phylogenetic relationships among host individuals, we used a piecewise approach to fit the structural component of the SEM (Fig. 4.3 structural). As piecewise methods cannot yet incorporate latent variables (Lefcheck 2015), we used the predicted values of HDT from the final CFA measurement model as an independent variable in the structural model. We then used the *gls* function in the *nlme* package to fit relationships between structural variables with the model correlation matrix fixed to the expected genetic distances between individuals (Pinheiro et al. 2015). For individuals of the same species, an expected correlation of 0.99 was used, and for individuals of different species their expected correlation was extracted from the

phylogeny in Fig. 4.2 using the *vcv* function of the *ape* package (Paradis et al. 2004; Lefcheck 2015). Piecewise SEMs were run and evaluated using the *sem.fit*, *sem.coefs*, and *sem.model.fits* functions in the piecewiseSEM package (Lefcheck 2015).

In our structural model, we expected Δ RMF and Δ tillers to covary. This is generally implemented by adding correlated errors to the model structure (Lefcheck 2015), but we wanted to test for a correlation after controlling for phylogenetic relatedness, which fixes error correlations. As such, we ran the full structural model twice: once with a path from Δ RMF to Δ tillers, and again with a path from Δ tillers to ΔRMF. Model fit, the sign and significance of path coefficients, and the form of the best-supported structural model were not qualitatively affected by the direction of the path between Δ RMF and Δ tillers, so we present only one full model in the results. After the full models were fit, we reduced them by omitting all non-significant structural variables and then tested the omitted structural variables for conditional independence using the *add.vars* argument of the *sem.fit* function. Structural model fit was evaluated using tests of directed separation with Fisher's C ($P>0.05$), and the p-values of individual path coefficients were used to determine the significance of relationships between structural variables ($P<0.05$). Of 138 possible observations (complete triplets of an infected, healthy, and biomass control individual), 73 observations were missing data for one or more variables and were thus excluded from the CFA and SEM analyses. Across nitrogen treatments, 21 species remained and the number of observations per species ranged from 1-6 (Table 4.7).

Results

Effects of resource supply on tolerance

Increased nitrogen supply increased RGR across species ($R^2 = 0.37$, $F_{1, 28} = 16.27$, $P<0.001$; Fig. 4.4a), as predicted by the GRM and CCH. Counter to the predictions of the GRM

and CCH, however, nitrogen supply did not significantly affect tolerance across species ($F_{1, 28}$ = 2.20, P=0.150), perhaps reflecting idiosyncratic responses among species (Fig. 4.4b). After controlling for the phylogenetic structure of the data, the plastic response of tolerance to increased nitrogen supply, Δ tolerance, was unrelated to the plastic response of resistance, Δ resistance, but was positively correlated with the plastic response of tissue C:N ratios, Δ C:N (Δ resistance: Estimate = -2.580, 95% CI = -5.766 – 0.605, $t_{2, 15}$ = -1.750, P = 0.104; Δ C:N: Estimate = 0.186, 95% CI = 0.047 – 0.324, $t_{2, 15}$ = 2.897, P = 0.013, Fig. 4.5).

Variation in tolerance across species

After controlling for the phylogenetic structure of the data, only host resistance had a consistent relationship to tolerance across nitrogen treatments; tolerance decreased with host resistance (Table 4.8). While host tissue nitrogen had a consistent, negative effect on tolerance across nitrogen treatments when all species were used, this relationship was not robust to the removal of an outlier at high nitrogen supply (Table 4.8; Fig. 4.6). Several other traits had significant influences on tolerance at low nitrogen supply, but their effects did not persist at high nitrogen supply (Table 4.8).

The impact of infection across species and resource supply rates

The best-supported measurement model of HDT contained mock-inoculated host maximum photosynthetic capacity (Photo), percent tissue nitrogen (%N), root mass fraction (RMF), and relative growth rate (RGR). This model fit the data ($\chi 2$ = 3.92, df = 2, P = 0.141; CFI = 0.976; TLI = 0.929; n : p = 65 : 8) and all path coefficients were significant (Fig. 4.7). While the full hypothesized measurement model also included leaf mass per area (LMA) as an indicator, its path coefficient was not significant (P=0.169). In addition, when the RMF of biomass control individuals was substituted for that of mock-inoculated individuals in the full

measurement model, neither its path coefficient nor that of LMA was significant (biomass control RMF P = 0.265; LMA P=0.149).

When the full structural model was run, all paths except those from HDT to Δ tillers, Δ tillers to Δ biomass, and Δ tillers to Δ RMF were non-significant (Table 4.9). The model was not a good fit to the data (Fisher's C = 8.95, k = 2, P = 0.011 n : p = 65 : 16), and model output suggested that this was because a direct path from HDT to Δ biomass was missing. This path could represent either an additional, direct causal effect of HDT on Δ biomass, or an effect of HDT mediated by other, unmeasured variables including resource acquisition traits (ex., Δ photosynthetic rate as in Cronin et al. 2014). Because the full structural model was not a good fit, we reduced it by retaining only variables with significant direct or indirect effects on Δ biomass. This model reduction procedure yielded two candidate models. In one candidate model, the effect of HDT on Δ biomass was fully mediated by Δ tillers, and in the other it was partially mediated by Δ tillers. In both models, all path coefficients were significant and the model fit the data (fully mediated model: Fisher's C = 11.6, k = 6, P = 0.085, n = 65, p = 5; partially mediated model: Fisher's C = 1.17, k = 4, P = 0.883, n = 65, p = 6). However, the fit of the fully mediated model was marginal ($0.05 < P < 0.10$) and it had a substantially higher AIC_C value than the partially mediated model (24.56 vs. 17.14). Thus, the partially mediated model was the best supported model. In this model, the direct path between HDT and Δ biomass was significant (P = 0.009), so our data do not support reducing the model further. Furthermore, tests of conditional independence did not support adding either ΔRMF or viral titer to the reduced model (ΔRMF P = 0.649, titer P = 0.858).

The final structural model of biomass loss to infection included only HDT and Δ tillers, with the effect of HDT on Δ biomass partially mediated by Δ tillers (Fig. 4.8). This model

indicated that hosts with a slow developmental tempo lost proportionally less biomass to infection, in part because, when infected, they were able to maintain or upregulate the production of above-ground biomass modules (tillers). The final model did not support a path mediated by viral titer, which indicates that the effect of HDT on biomass loss to infection was primarily mediated by host resource economics and not post-infection resistance.

Discussion

In previous studies, the effect of resource supply on tolerance has varied among host species (Hawkes and Sullivan 2001; Wise and Abrahamson 2007). Similarly here, nitrogen supply increased tolerance in some hosts, decreased it in others, and in some hosts tolerance remained unchanged. To our knowledge, however, ours is the first empirical demonstration of a specific mechanism underlying these idiosyncratic responses across species, namely, species-specific differences in the response of resource ratios (C:N) to increased nitrogen supply (Wise and Abrahamson 2005; Banta et al. 2010). Our study virus disproportionately affects phloem vessels and thus the translocation and utilization of fixed carbon (Schultz et al. 2013; D'Arcy and Burnett 1995). As predicted by the LRM, the more host growth shifted from being nitrogen- to carbon-limited with increased nitrogen supply (as indicated by decreasing C:N), the more tolerance decreased in response to increased nitrogen supply. As such, our results support both the predictions and mechanism of the LRM, and suggest that resource economics play an important role in determining the response of host tolerance to changing environments.

Of the many traits hypothesized to drive interspecific variation in tolerance, only one of them, resistance, predicted species-level variation in tolerance regardless of resource supply. At both low and high nitrogen, species that were more resistant to pathogen infection were less tolerant. At low nitrogen supply, many other species-level traits were correlated with tolerance,

but their effects did not persist at high nitrogen. In addition, correlations at low nitrogen were in the hypothesized direction for some traits (LMA, tissue C:N, and Δ Tillers) but in the opposite direction for others (RGR, %N). This indicates that species traits mattered more at low resource supply, consistent with the idea that tolerance is more challenging to achieve when resources are limited and allocation tradeoffs are stronger (Valverde et al. 2003). This interpretation is further supported by the observation that tolerance varied less across species at high nitrogen supply, and by the observation that the slope of all relationships between traits and tolerance decreased at high nitrogen supply. While the resistance-tolerance tradeoff also relaxed at high nitrogen supply, it was the only relationship that remained significant, which suggests that our hosts face a strong, fundamental tradeoff between avoiding infection and tolerating it.

Across host species and resource supply rates, we found that HDT, an axis integrating multiple covarying host traits, was a strong predictor of the impact of infection on host biomass. This supports the general hypothesis that host traits modulate the effects of resource supply on host-enemy interactions, and more specifically that hosts with a slow developmental tempo are less impacted by infection (Cronin et al. 2014). Also like Cronin et al. (2014), our results suggest that measuring traits as they are expressed at each level of resource supply may make the explicit consideration of resource supply unnecessary. In contrast with Cronin et al. (2014), however, we did not find that HDT chiefly affected enemy impact via a post-infection resistance pathway. This contrasting result may stem from differences in the data used to model host resource economics, specifically carbon acquisition. While we modeled it using an aquisitional unit, tillers, Cronin et al. (2014) modeled it using an aquisitional process, photosynthesis. The activation of dormant meristems and the upregulation of photosynthesis are both well-documented responses to damage (Fornoni and Nunez-Farfan 2003; Strauss and Agrawal 1999),

but photosynthetic upregulation may be more common in response to leaf removal than in response to other types of damage (Welter 1989). When the pathways of modular plasticity and post-infection resistance were considered simultaneously in response to pathogen damage, our model suggested that the effect of HDT on the impact of infection was primarily mediated by modular plasticity. In models where these two pathways are not considered simultaneously, or in taxa where modular plasticity is constrained, the post-infection resistance pathway may be relatively more important. Regardless of its specific mechanism of effect, enemy impact increased with HDT across both studies, which supports its utility as a general predictor.

Enemy impact and tolerance are not equivalent response variables. To be consistent with the hypotheses tested, we have considered both, but their interpretations differ. Impact is the effect of infection on fitness, regardless of pathogen load, and tolerance is the effect of a one-unit increase in pathogen load on fitness. Across host species, we found support for a resistance-tolerance tradeoff, and we have previously shown that hosts with a fast developmental tempo are less resistant (Welsh et al. 2016; Cronin et al. 2010). Combined, this suggests that hosts with a fast developmental tempo are less resistant and more tolerant. Yet hosts with a fast developmental were more impacted by infection in our SEM. Pathogen load was unrelated to impact in our SEM, and two previous experiments in our study system found that pathogen load increased with HDT (Cronin et al. 2014; Whitaker et al. 2015). Mathematically, this scenario leads to a decoupling of tolerance and impact. Hosts with a fast developmental tempo may be more tolerant, but if they also harbor greater pathogen loads, they lose the same amount of biomass to infection as hosts with a slow developmental tempo. Consequently, differences in biomass loss to infection result not from differences in tolerance but from differences in other host characteristics, and our model suggests that this characteristic is the ability of hosts with a

slow developmental tempo to upregulate tillering in response to infection. If we had only considered tolerance, we may have concluded that hosts with a fast developmental tempo were less impacted by infection. This illustrates an important caveat: in systems where impact is unrelated to pathogen load, impact may be a more biologically meaningful response than tolerance when it comes to estimating the fitness consequences of infection and a host's potential contribution to pathogen transmission.

We have shown here that a single axis of trait covariation, HDT, holds across species and resource supply rates and can therefore predict the impact of infection across individuals. As indicators of HDT, we used three leaf-level traits and two whole-plant traits: RGR and RMF. In a previous study, we used the same three leaf-level traits and two estimates of growth rate to place hosts along the Leaf Economics Spectrum, a plant-specific analogue of HDT. In contrast to HDT, the strength of the LES was sensitive to the resource supply rates in which it was quantified, and its accuracy as a predictor of individual host susceptibility, the inverse of resistance, declined as its constituent trait correlations weakened (Welsh et al. 2016). While we measured many of the same traits in both studies, the difference lies in the specific traits that were most associated with impact vs. susceptibility, and in how these traits responded to resource supply. In the case of impact, our CFA did not support LMA as a strong indicator of HDT, and, as evidenced by the SEM results, LMA was not an important driver of variation in impact. In contrast, LMA was associated with variation in susceptibility. In response to nitrogen supply, all of the traits associated with impact shifted in parallel along the axis of HDT. In contrast, LMA respond to nitrogen supply by shifting orthogonal to the LES, causing the LES to weaken and become a less accurate predictor of susceptibility in some cases. The difference in predictive generality between the trait-based model of impact presented here and the trait-based model of

susceptibility in Welsh et al. (2016) exemplifies the importance of crafting specific, *a priori* hypotheses of trait effects in the design of trait-based models. If the traits most associated with a particular response do not respond to the environment in a coordinated fashion, they could be weeded out of consideration by approaches that use all available traits to quantify axes of trait covariation. If these axes are then used for prediction, the importance of their constituent traits could be inflated or one might erroneously conclude that a particular process is not trait-based.

Table 4.1. Hypotheses of intraspecific variation in tolerance along resource supply gradients. RGR = relative growth rate.

Hypothesis	Predicted effect of increased resource supply	Rationale	Refs
Growth Rate Model (GRM)	Decreased tolerance	RGR increases with resource supply; regrowth potential increases with the difference between current and maximum RGR	Hilbert et al. 1981; Wise and Abrahamson 2007
Compensatory Continuum Hypothesis (CCH)	Increased tolerance	RGR increases with resource supply; rate and extent of regrowth increase with RGR	Maschinski and Whitham 1989; Wise and Abrahamson 2007
Limiting Resource Model (LRM)	Decreased or increased tolerance	Outcome depends on focal resource identity and effects of damage on resource economics	Wise and Abrahamson 2005; Wise and Abrahamson 2007
Growth-defense tradeoffs (GDTs)	Increased tolerance and decreased resistance	RGR increases with resource supply; relative costs of resistance increase with RGR	Coley 1985; Herms and Mattson 1992

Table 4.2. Species traits with the potential to influence interspecific variation in tolerance, their mechanism of effect, specific traits, and the predicted effects of increasing each trait on tolerance. Of the traits that have been considered elsewhere, we limit the list of specific traits to those that are also considered in the present study (except Δ Photo). Table summarized from Rosenthal and Kotanen (1994), Strauss and Agrawal (1999), Stowe (2000), and Fornoni and Nunez-Farfan (2003).

Category	Mechanism	Specific Traits	Predicted effect on tolerance
Growth traits	Indicate or affect rates of resource acquisition and utilization as well as the cost of replacing lost tissue	Relative growth rate (RGR) Photosynthetic capacity (Photo) Tissue nutrient concentrations (%N, C:N ratio) Leaf mass per area (LMA)	Positive Positive %N Positive C:N Negative Negative
Storage traits	Indicate pre-existing reserves that can be allocated to regrowth or repair	Root : total biomass (Root mass fraction, RMF)	Positive
Trait plasticity	Affects rate and extent of physiological response to damage	Photosynthetic plasticity (Δ Photo) Allocational plasticity (Δ RMF) Modular plasticity (Δ Tillers)	Positive Positive Positive
Resistance traits	Trade-off with growth traits; constitute an alternate allocation strategy	Resistance to enemy damage	Negative

Table 4.3. Host identities, life history (A=annual, P=perennial), and seed source.

Host Species	Life History	Seed Source
Aegilops triuncialis L.	A	Field collected: Hopland, CA, USA
Aira caryophyllea L.	A	Field collected: Hopland, CA, USA
Arrhenatherum elatius (L.) P. Beauv. ex J. Presl & C. Presl	P	Field collected: Basket Butte, OR, USA
Avena barbata Pott ex Link	A	Field collected: Hopland, CA, USA
Avena fatua L.	A	Azlin Seed Service, Leland, MS, USA
Briza maxima L.	A	Field collected: Hopland, CA, USA
Bromus carinatus Hook. & Arn.	P	Field collected: Hopland, CA, USA
Bromus diandrus Roth	A	Field collected: Hopland, CA, USA
Bromus hordeaceus L.	A	Field collected: Hopland, CA, USA
Cynosurus echinatus L.	A	Field collected: Hopland, CA, USA
Elymus glaucus Buckley	P	Field collected: Hopland, CA, USA
Elymus multisetus M.E. Jones	P	Field collected: Hopland, CA, USA
Koeleria macrantha (Ledeb.) Schult.	P	Hedgerow Farms, Winters, CA, USA
Lolium multiflorum Lam.	A	Field collected: Hopland, CA, USA
Melica californica Scribn.	P	Hedgerow Farms, Winters, CA, USA
Nassella lepida (Hitchc.) Barkworth	P	Hedgerow Farms, Winters, CA, USA
Nassella pulchra (Hitchc.) Barkworth	P	Hedgerow Farms, Winters, CA, USA
Poa secunda J. Presl	P	Hedgerow Farms, Winters, CA, USA
Schedonorus arundinaceus (Schreb.) Dumort., nom. cons.	P	Field collected: Basket Butte, OR, USA
Taeniatherum caput-medusae (L.) Nevski	A	Field collected: Hopland, CA, USA
Vulpia microstachys (Nutt.) Munro	A	Hedgerow Farms, Winters, CA, USA
Vulpia myuros (L.) C.C. Gmel.	A	Field collected: Hopland, CA, USA
Avena sativa L. 'Coast Black'	A	National Small Grains Collection, Aberdeen, ID, USA

Table 4.4. Potting medium and nitrogen treatment. On a per area basis, nutrient and high nitrogen addition rates reflect those of the Nutrient Network, a world-wide fertilization experiment in grasslands (Borer et al., 2014).

Soil Component	Form and Source	Ammount per Individual
Pasteurized Sand	Pasteurized	0.5 L
Low-nutrient soil	LC1 soil, SunGro Horticulture, Agawam, MA, USA	0.5 L
Phosphorous	Triple Phosphate, 45% P_2O_5, Espoma, NJ, USA	0.196 g
Potassium	Potash, 50% K_2O, Winston Weaver Co., Inc., NC, USA	0.093 g
Micronutrients	Micromax, Scotts, OH, USA	0.385 g
Nitrogen	>98% NH_4NO_3, Fisher Scientific, NY, USA	low N: 0.005 g *
		high N: 0.110 g *

* Applied in equal parts over 5 weeks and dissolved in 10mL H_20 per week

Table 4.5. Host characteristics and measurement methods.

Host Characteristic	**Abbr**	**Units**	**Timing of Measurement(s)**	**Method**
Maximum Photo-synthetic Capacity	Photo	µmol/ mg/s	~4 wks post-germination on youngest, fully expanded leaf	Maximum CO_2 flux: CIRAS-2 infrared gas analyzer, PP Systems, MA, US
Leaf Mass per Area	LMA	mg/cm^2	~4 wks post-germination on youngest, fully expanded leaf	Dry mass/scanned leaf section area: WinFOLIA, Regent Instruments, QC, CA
% Tissue Carbon and Nitrogen	%C %N	100*mg/mg	~4 wks post-germination on youngest, fully expanded leaf	Combustion analysis: Univ. of Georgia Stable Isotope Ecology Laboratory, GA, US
Biomass	NA	g dry weight	2 weeks (biomass control) or 7 weeks (healthy and infected) post-germination	Biomass dried for >1 week at 50°C

Table 4.6. Calculated variables, method of calculation, and units.

Variable	Calculation	Units
Tolerance	((((Infected biomass – Biomass control biomass) / (Healthy biomass – Biomass control biomass)) - 1) / Relative titer) * 0.01	Post-infection % biomass increase or decrease per 0.01 increase in relative titer
Relative Growth Rate (RGR)	(ln(Healthy or Infected biomass) – ln(Biomass control biomass)) / 35 days	g/g/day
Resistance	# Uninfected individuals / 6 Exposed individuals	% uninfected
Δ Tolerance	(Tolerance at +N) – (Tolerance at –N)	Absolute difference in tolerance between N treatments
Δ Resistance	(Resistance at +N) – (Resistance at –N)	Absolute difference in % uninfected between N treatments
Δ C:N %Tissue Carbon / %Tissue Nitrogen	(Healthy C:N at +N) – (Healthy C:N at –N)	Absolute difference in %Carbon / %Nitrogen between N treatments
Root Mass Fraction (RMF)	Healthy root biomass / Healthy total biomass	g Root/g Total
Δ RMF	Infected RMF / Healthy RMF (- Biomass control root and total biomass prior to RMF calculation)	Proportional change in RMF when infected
Δ Tillers	Infected # Tillers / Healthy # Tillers	Proportional change in tiller number when infected
Δ RGR	Infected RGR / Healthy RGR	Proportional change in RGR when infected
Δ Biomass	(Infected biomass – Biomass control biomass) / (Healthy Biomass – Biomass control biomass)	Proportional change in biomass when infected

Table 4.7. (Continued on next page) Number of individuals included in each analysis by species and nitrogen treatment. Means by species and nitrogen treatment were used for analyses contained in the *Effects of resource supply on tolerance* and *Variation in tolerance across species* sections. Analyses described in *The impact of infection across species and resource supply rate* section used individual values.

		Analysis group		
Host Species	Nitrogen Treatment	*Effects of resource supply on tolerance*	*Variation in tolerance across species*	*The impact of infection across species and resource supply rate*
Aegilops triuncialis L.	-	1	1	1
	+	2	2	2
Aira caryophyllea L.	-	3	3	2
	+	3	3	3
Arrhenatherum elatius (L.) P. Beauv. ex J. Presl & C. Presl	-	0	1	1
	+	0	0	0
Avena barbata Pott ex Link	-	2	2	2
	+	2	2	2
Avena fatua L.	-	1	1	1
	+	2	2	2
Briza maxima L.	-	3	3	3
	+	3	3	2
Bromus carinatus Hook. & Arn.	-	0	0	0
	+	0	2	2
Bromus diandrus Roth	-	3	3	3
	+	2	2	2
Bromus hordeaceus L.	-	2	2	2
	+	2	2	2
Cynosurus echinatus L.	-	3	3	3
	+	1	1	1
Elymus glaucus Buckley	-	1	1	1
	+	1	1	1
Elymus multisetus M.E. Jones	-	3	3	3
	+	1	1	1
Koeleria macrantha (Ledeb.) Schult.	-	0	2	2
	+	0	0	0
Lolium multiflorum Lam.	-	0	0	0
	+	0	1	1
Melica californica Scribn.	-	0	0	0
	+	0	0	0
Nassella lepida (Hitchc.) Barkworth	-	2	2	2
	+	3	3	3

Nassella pulchra (Hitchc.) Barkworth	-	0	0	0
	+	0	1	1
Poa secunda J. Presl	-	0	0	0
	+	0	1	1
Schedonorus arundinaceus (Schreb.) Dumort., nom. cons.	-	0	0	0
	+	0	0	0
Taeniatherum caput-medusae (L.) Nevski	-	1	1	1
	+	1	1	1
Vulpia microstachys (Nutt.) Munro	-	1	1	1
	+	3	3	3
Vulpia myuros (L.) C.C. Gmel.	-	1	1	1
	+	1	1	1
Avena sativa L. 'Coast Black'	-	3	3	2
	+	3	3	3

Table 4.8. Host traits, their predicted effects on tolerance, and phylogenetic generalized least squares regressions showing the effect of species mean trait values on tolerance in the low and high nitrogen treatments. P-values of significant relationships are in bold. To meet assumptions of normality, Δ RMF was log-10 transformed in both nitrogen treatments and Δ Tillers was log-10 transformed in the low nitrogen treatment.

Host Trait	**Predicted effect on tolerance**	**Tolerance ~ Host trait**							
		Low **N (N=17 species)**				**High N (N = 19 species)**			
		Estimate	95% CI	t value	p	Estimate	95% CI	t value	p
Resistance	-	-1.510	(-2.848, -0.172)	-2.405	**0.030**	-0.952	(-1.895, -0.009)	-2.130	**0.048**
RGR	+	-13.250	(-25.43, -1.070)	-2.318	**0.035**	-3.531	(-59.92, 52.86)	0.132	0.896
Photo	+	-1.209	(-2.783, 0.364)	-1.639	0.122	-0.287	(-0.725, 0.150)	-1.387	0.183
RMF (mock)	+	-7.796	(-19.02, 3.427)	-1.481	0.159	0.994	(-0.940, 2.827)	1.057	0.305
LMA	-	-0.378	(-0.755, -0.002)	-2.142	**0.049**	-0.045	(-0.313, 0.223)	-0.355	0.727
%N	+	-2.437	(-4.152, -0.721)	-3.027	**0.002**	-1.329	(-2.216, -0.441)	9.970	**0.006**
%N [-outlier*]	+	-2.138	(-3.928, -0.348)	-2.562	**0.023**	-0.400	(-1.761, 0.961)	-0.623	0.542
C:N	+	0.234	(0.052, 0.415)	2.746	**0.015**	0.079	(-0.042, 0.200)	1.381	0.185
Δ RMF	-	-2.677	(-6.240, 0.886)	-1.601	0.130	-0.063	(-0.395, 0.269)	-0.401	0.693
Δ Tillers	+	0.911	(0.361, 1.461)	3.529	**0.003**	0.167	(-0.366, 0.699)	0.660	0.158

* Outliers were *Vulpia myuros* at low N (so N=16 species) and *Poa secunda* at high N (so N=18 species).

Table 4.9. Coefficients and significance of all paths in the full structural model, which was not a good fit to the data. Abbreviations are as in Fig. 4.3.

Path	Standardized Coefficient	Unstandardized Coefficient	P-value
HDT → Viral Titer	0.082	0.047	0.295
HDT → Δ RMF	-0.040	-0.009	0.674
HDT → Δ Tillers	**-0.540**	**-0.216**	**<0.001**
Viral Titer → Δ RMF	-0.118	-0.045	0.360
Viral Titer → Δ Tillers	0.156	0.108	0.360
Viral Titer → Δ Biomass	-0.019	-0.012	0.848
Δ Tillers → Δ RMF	**-0.376**	**-0.207**	**<0.001**
Δ Tillers → Δ Biomass	**0.825**	**0.775**	**<0.001**
Δ RMF → Δ Biomass	0.059	0.101	0.556

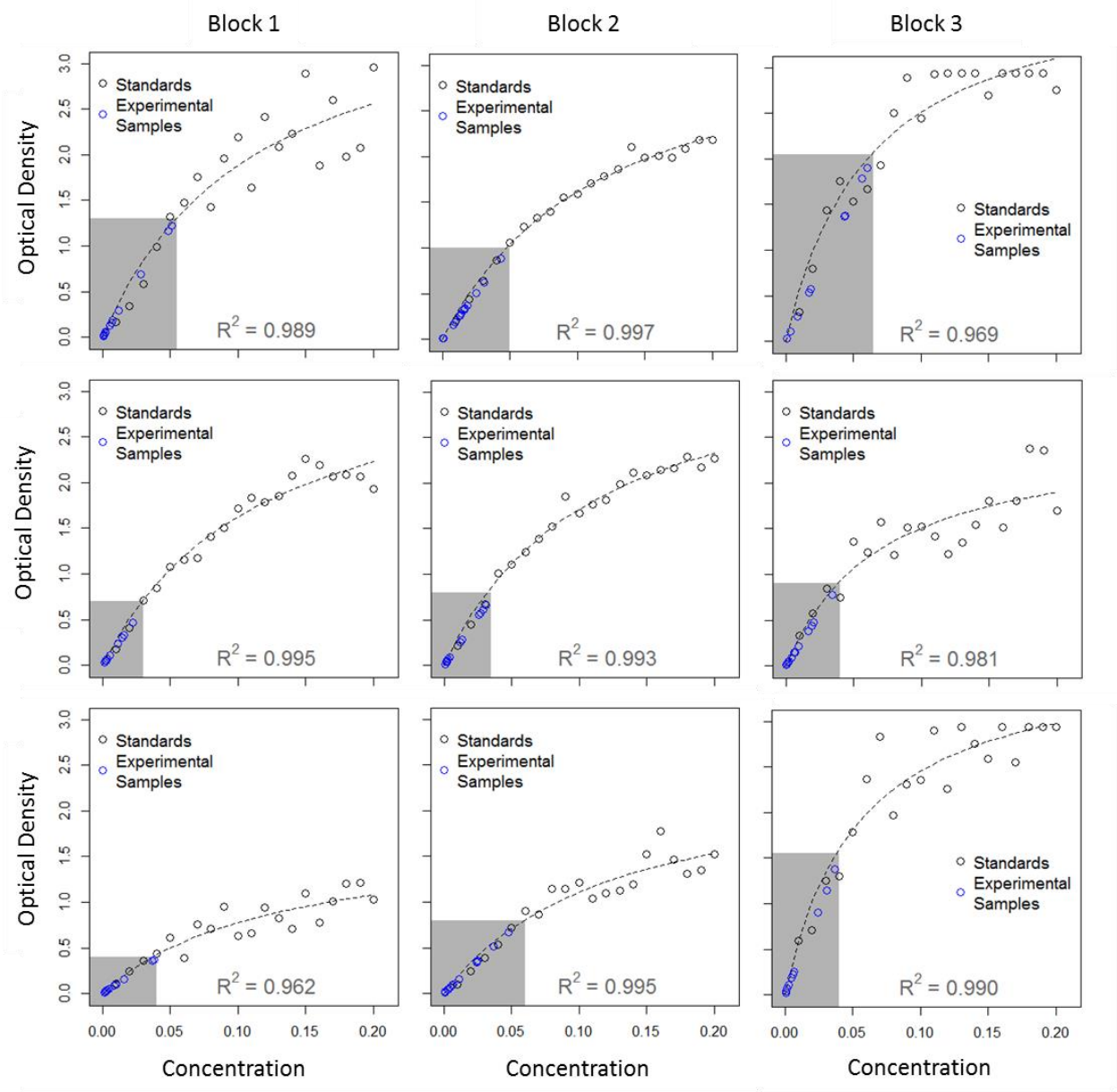

Figure 4.1. Standard curves (dashed lines and black circles) used to calculate relative viral titer (concentration) from the optical density of each experimental sample (blue circles) in each of nine ELISA plates, three per experimental block. Gray squares indicate the range of each standard curve that encompassed all experimental OD values, and R^2 values indicate the fit of the standard curve in that range.

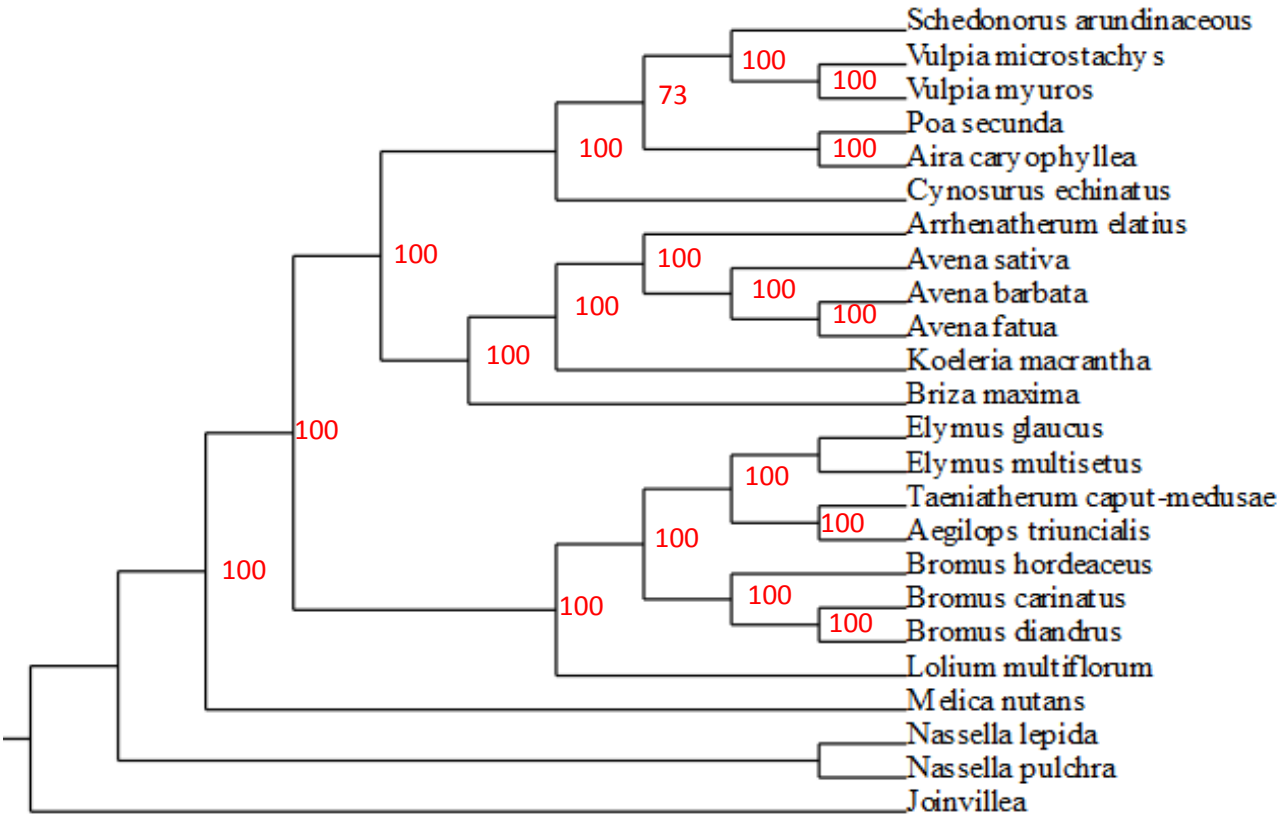

Figure 4.2. Phylogeny used for all phylogenetic analyses. Node labels indicate bootstrap support. Created using phyloGenerator (Pearse and Purvis, 2013) with options '-gene *rbcL*, *matK* –alignment muscle –phylogen RAxML –integrated Bootstrap 1000', and constraint tree topology following Bouchenak-Khelladi et al. (2008). Sequence data was not available for *Elymus multisetus*, *Nassella pulchra*, and *Melica californica*, so polytomies were created for *Elymus* and *Nassella*, and *Melica californica* was replaced with the congener *Melica nutans*. Joinvillea (monocot, Joinvilleaceae) was used as an outgroup.

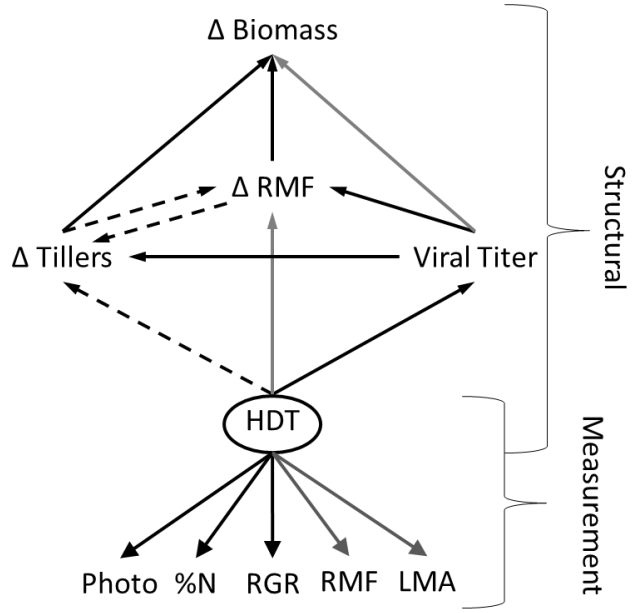

Figure 4.3. Structural and measurement components of the SEM and expected relationships between variables. Black arrows indicate positive relationships, gray arrows indicate negative relationships, and dashed arrows indicate relationships for which either a positive or negative relationship was expected. HDT= host developmental temop, Photo = maximum photosynthetic capacity, %N = percent tissue nitrogen, RGR = relative growth rate, RMF = root mass fraction, and LMA = leaf mass per area. Except for paths involving Δ tillers, see Cronin etal (2014) Table 2 for hypothesized mecahnism(s) for each relationship. See Cronin etal. (2014) Figure 1a for the corresponding metamodel.

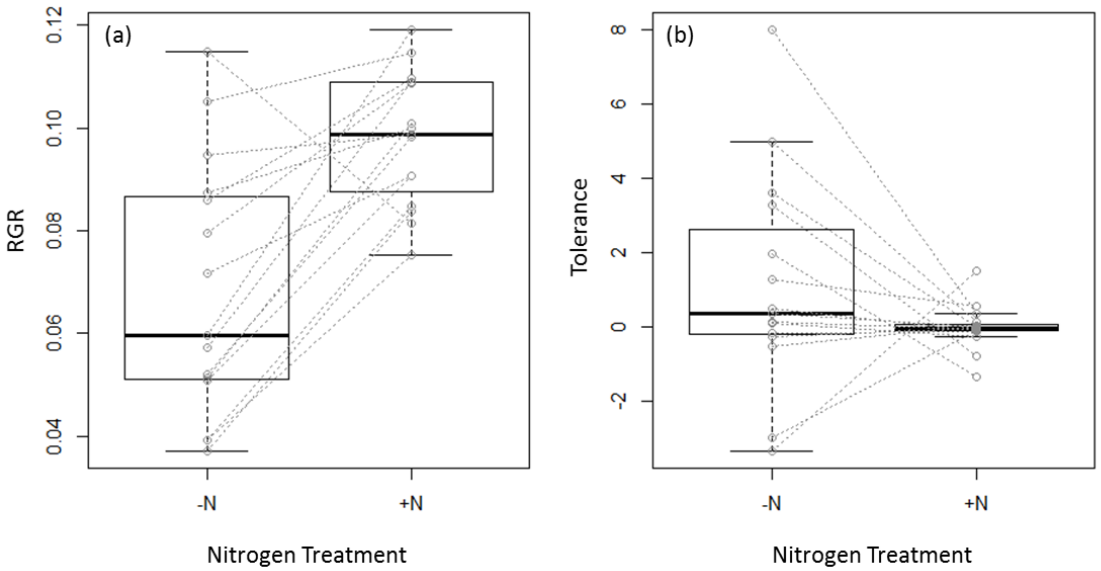

Figure 4.4. Nitrogen supply treatment increased (a) RGR but did not affect (b) tolerance. Box and whisker diagrams represent the observed distribution of RGR and tolerance: medians (black bars), first quartiles (box edges), and third quartiles (whisker edges). Gray points and lines represent the responses of individual species.

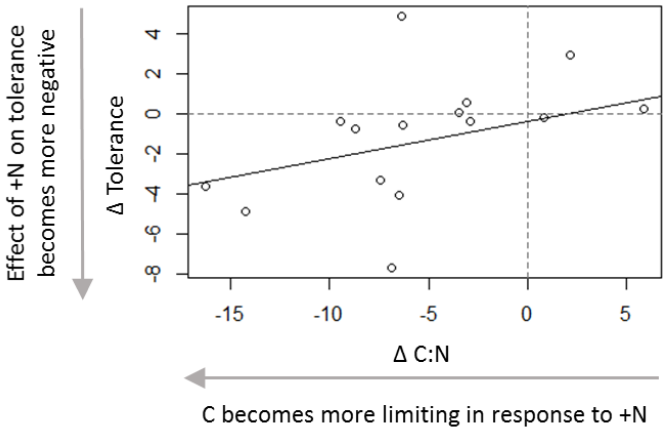

Figure 4.5. Fitted, phylogenetic generalized least squares relationship between the response of tissue C:N ratio and the response of tolerance to increasing nitrogen supply, which the LRM predicts should intersect (0,0). Open circles are observed values. See text for model specifics.

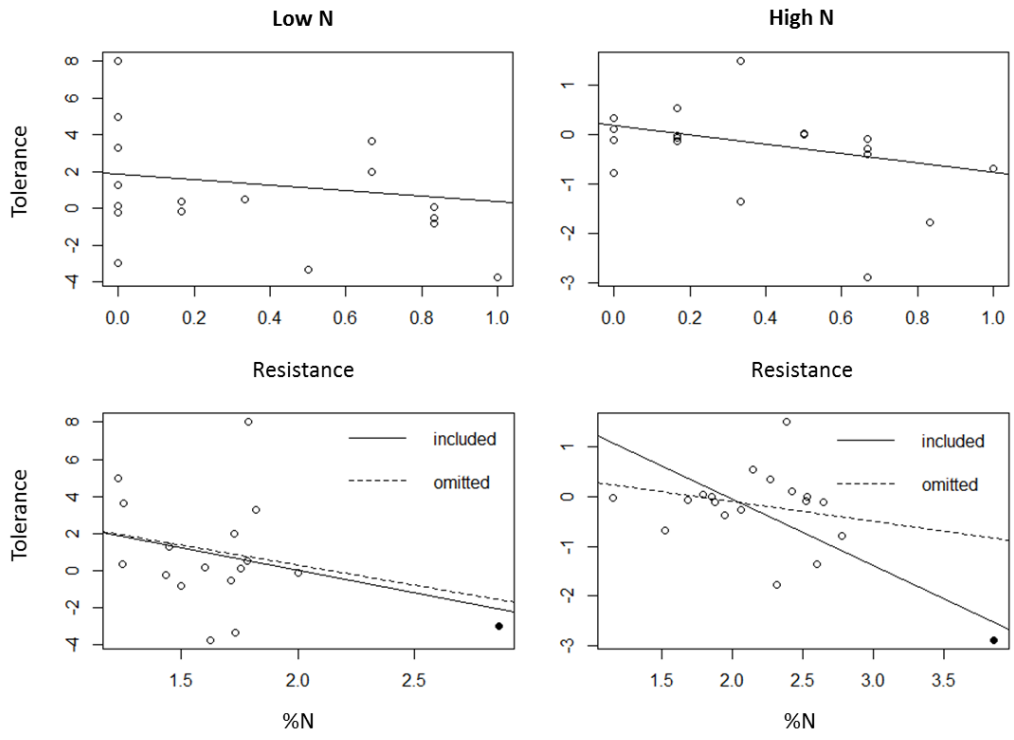

Figure 4.6. Fitted, phylogenetic generalized least squares relationships between host tolerance and either host resistance (top row) or host tissue nitrogen concentration (%N, bottom row) at both low and high nitrogen supply (left and right columns, respectively). Circles are observed values. At low nitrogen, the relationship between tolerance and %N was robust to the omission of an outlier (filled circle), but this was not the case at high nitrogen. See Table 4.8 for model specifics.

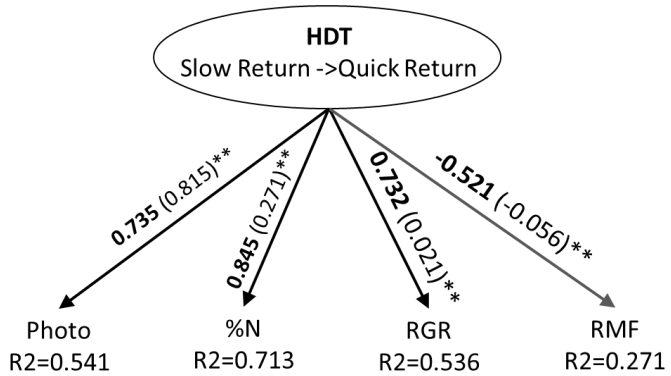

Figure 4.7. Final CFA results for the measurement model of host developmental tempo. Abbreviations are as in Fig. 4.3. Bold path coefficients are standardized and those in parentheses are unstandardized. **P<0.001

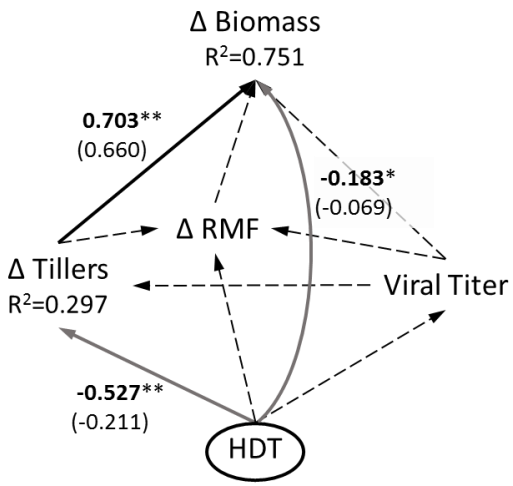

Figure 4.8. The best supported structural model of host biomass loss to infection (Fisher's C = 1.17, k = 4, P = 0.883, n : p = 65 : 6). Abbreviations are as in Fig. 4.3. Dashed arrows are hypothesized paths that were removed because they were not significant, solid gray arrows are negative paths, and black arrows are positive paths. Bold path coefficients are standardized and those in parentheses are unstandardized. *P<0.01, **P<0.001

REFERENCES

Agrawal, A. A. (2011) Current trends in the evolutionary ecology of plant defence. *Functional Ecology,* **25,** 420-432.

Agrawal, A. A. & Fishbein, M. (2006) Plant Defense Syndromes. *Ecology,* **87,** S132-S149.

Agrawal, A. A. & Fishbein, M. (2008) Phylogenetic escalation and decline of plant defense strategies. *Proceedings of the National Academy of Sciences,* **105,** 10057-10060.

Banta, J. A., Stevens, M. H. H. & Pigliucci, M. (2010) A comprehensive test of the 'limiting resources' framework applied to plant tolerance to apical meristem damage. *Oikos,* **119,** 359-369.

Baucom, R. S. & de Roode, J. C. (2011) Ecological immunology and tolerance in plants and animals. *Functional Ecology,* **25,** 18-28.

Bilbrough, C. J. & Richards, J. H. (1993) Growth of Sagebrush and Bitterbrush Following Simulated Winter Browsing: Mechanisms of Tolerance. *Ecology,* **74,** 481-492.

Boots, M. (2008) Fight or learn to live with the consequences? *Trends in Ecology and Evolution,* **23,** 248-250.

Borer, E. T., Harpole, W. S., Adler, P. B., Lind, E. M., Orrock, J. L., Seabloom, E. W. & Smith, M. D. (2014) Finding generality in ecology: a model for globally distributed experiments. *Methods in Ecology and Evolution,* **5,** 65-73.

Borer, E. T., Seabloom, E. W., Mitchell, C. E. & Power, A. G. (2010) Local context drives infection of grasses by vector-borne generalist viruses. *Ecology Letters,* **13,** 810-818.

Bouchenak-Khelladi, Y., Salamin, N., Savolainen, V., Forest, F., Bank, M., Chase, M. W. & Hodkinson, T. R. (2008) Large multi-gene phylogenetic trees of the grasses (Poaceae): progress towards complete tribal and generic level sampling. *Mol Phylogenet Evol,* **47,** 488-505.

Chase, J. M., Leibold, M. A. & Simms, E. L. (2000) Plant tolerance and resistance in food webs: Community-level predictions and evolutionary implications. *Evolutionary Ecology,* **14,** 289-314.

Coley, P. D., Bryant, J. P. & Chapin, F. S., III (1985) Resource availability and plant antiherbivore defense. *Science,* **230,** 895-899.

Copeland, R. (1998) Assaying levels of plant virus by ELISA. *Plant Virology protocols* (eds G. D. Foster & S. C. Taylor), pp. 455-460. Humana Press, Clifton, NJ, USA.

Cronin, J. P., Rúa, M. A. & Mitchell, C. E. (2014) Why Is Living Fast Dangerous? Disentangling the Roles of Resistance and Tolerance of Disease. *The American Naturalist,* **184,** 172-187.

Cronin, J. P., Welsh, M. E., Dekkers, M. G., Abercrombie, S. T. & Mitchell, C. E. (2010) Host physiological phenotype explains pathogen reservoir potential. *Ecology Letters,* **13,** 1221-1232.

D'Arcy, C. J. & Burnett, P. A. (1995) *Barley Yellow Dwarf: 40 Years of Progress.* APS Press, St. Paul.

Fornoni, J. & Nunez-Farfan, J. (2003) Evolutionary ecology of tolerance to herbivory: advances and perspectives. *Comments on Theoretical Biology,* **8,** 643-663.

Fornoni, J., Valverde, P. L. & Nunez-Farfan, J. (2003) Quantitative genetics of plant tolerance and resistance against natural enemies of two natural populations of Datura stramonium. *Evolutionary Ecology Research,* **5,** 1049-1065.

Gervasi, S. S., Civitello, D. J., Kilvitis, H. J. & Martin, L. B. (2015) The context of host competence: a role for plasticity in host–parasite dynamics. *Trends in Parasitology*.

Hawkes, C. V. & Sullivan, J. J. (2001) The impact of herbivory on plants in different resource conditions: a meta-analysis. *Ecology,* **82,** 2045-2058.

Herms, D. A. & Mattson, W. J. (1992) The dilemma of plants: to grow or defend. *Quarterly Review of Biology,* **67,** 283-335.

Hilbert, D. W., Swift, D. M., Detling, J. K. & Dyer, M. I. (1981) Relative growth rates and the grazing optimization hypothesis. *Oecologia,* **51,** 14-18.

Kursar, T. A. & Coley, P. D. (2003) Convergence in defense syndromes of young leaves in tropical rainforests. *Biochemical Systematics and Ecology,* **31,** 929-949.

Lefcheck, J. S. (2015) piecewiseSEM: Piecewise structural equation modelling in r for ecology, evolution, and systematics. *Methods in Ecology and Evolution,* n/a-n/a.

Leimu, R. & Koricheva, J. (2006) A meta-analysis of tradeoffs between plant tolerance and resistance to herbivores: combining the evidence from ecological and agricultural studies. *Oikos,* **112,** 1-9.

Maschinski, J. & Whitham, T. G. (1989) The Continuum of Plant Responses to Herbivory: The Influence of Plant Association, Nutrient Availability, and Timing. *The American Naturalist,* **134,** 1-19.

Paradis, E., Claude, J. & Strimmer, K. (2004) APE: analyses of phylogenetics and evolution in R language. *Bioinformatics,* **20,** 289-290.

Pearse, W. D. & Purvis, A. (2013) phyloGenerator: an automated phylogeny generation tool for ecologists. *Methods in Ecology and Evolution,* **4,** 692-698.

Pinheiro, J., Bates, D., DebRoy, S., Sarkar, D. & Team, R. C. (2015) nlme: Linear and Nonlinear Mixed Effects Models. R package version 3.1-121.

R Core Team (2015) R: A language and environment for statistical computing. R Foundation for Statistical Computing, Vienna, Austria. URL https://www.R-project.org/

Raberg, L., Graham, A. L. & Read, A. F. (2009) Decomposing health: tolerance and resistance to parasites in animals. *Phil. Trans. R. Soc. B,* **364,** 37-49.

Rochow, W. F., Aapola, A. I. E., Brakke, M. K. & Carmichael, L. E. (1971) Purification and antigenicity of three isolates of barley yellow dwarf virus. *Virology,* **46,** 117-126.

Rosenthal, J. P. & Kotanen, P. M. (1994) Terrestrial plant tolerance to herbivory. *Trends in Ecology & Evolution,* **9,** 145-148.

Rosenthal, J. P. & Welter, S. C. (1995) Tolerance to herbivory by a stemboring caterpillar in architecturally distinct maizes and wild relatives. *Oecologia,* **102,** 146-155.

Rosseel, Y. (2012) lavaan: An R Package for Structural Equation Modeling. *Journal of Statistical Software,* **42,** 1-36.

Rua, M. A., Umbanhowar, J., Hu, S. J., Burkey, K. O. & Mitchell, C. E. (2013) Elevated CO2 spurs reciprocal positive effects between a plant virus and an arbuscular mycorrhizal fungus. *New Phytologist,* **199,** 541-549.

Schneider, D. S. & Ayres, J. S. (2008) Two ways to survive infection: what resistance and tolerance can teach us about treating infectious diseases. *Nature Reviews: Immunology,* **8,** 889-895.

Schultz, J. C., Appel, H. M., Ferrieri, A. P. & Arnold, T. M. (2013) Flexible resource allocation during plant defense responses. *Frontiers in Plant Science,* **4,** 324.

Stowe, K. A., Marquis, R. J., Hochwender, C. G. & Simms, E. L. (2000) The evolutionary ecology of tolerance to consumer damage. *Annual Review of Ecology and Systematics,* **31,** 565-595.

Strauss, S. Y. & Agrawal, A. A. (1999) The ecology and evolution of plant tolerance to herbivory. *Trends in Ecology and Evolution,* **14,** 179-185.

Tiffin, P. (2000) Mechanisms of tolerance to herbivore damage: What do we know? *Evolutionary Ecology,* **14,** 523-536.

Valverde, P. L., Fornoni, J. & Núñez-Farfán, J. (2003) Evolutionary ecology of Datura stramonium: equal plant fitness benefits of growth and resistance against herbivory. *Journal of Evolutionary Biology,* **16,** 127-137.

van der Meijden, E., Wijn, M. & Verkaar, H. J. (1988) Defense and regrowth, alternate plant strategies in the struggle against herbivores. *Oikos,* **51,** 355-363.

Welsh, M. E., Cronin, J. P. & Mitchell, C. E. (2016) The role of habitat filtering in the leaf economics spectrum and plant susceptibility to pathogen infection. *Journal of Ecology*.

Welter, S. C. (1989) Arthropod impact on plant gass exchange. *Insect-plant interactions* (ed E. A. Bernays), pp. 135-150. CRC, Boca Raton, FL.

Whitaker, B. K., Rua, M. A. & Mitchell, C. E. (2015) Viral pathogen production in a wild grass host driven by host growth and soil nitrogen. *New Phytologist,* **207,** 760-768.

Wise, M. J. & Abrahamson, W. G. (2005) Beyond the compensatory continuum: environmental resource levels and plant tolerance of herbivory. *Oikos,* **109,** 417-428.

Wise, M. J. & Abrahamson, W. G. (2007) Effects of resource availability on tolerance of herbivory: A review and assessment of three opposing models. *American Naturalist,* **169,** 443-454.

Wise, M. J., Carr, D. E. & Juenger, T. (2008) On Quantifying Tolerance of Herbivory for Comparative Analyses. *Evolution,* **62,** 2429-2434.